DEPOSITED LOOPS COUPLING MAGNETIC FILMS AS FAST COMPUTER ELEMENTS

Thesis by

Bernard Charles Reardon

In Partial Fulfillment of the Requirements

For the Degree of

Doctor of Philosophy

California Institute of Technology

Pasadena, California

1964

(Submitted April 2, 1964)

ACKNOWLEDGEMENTS

I wish to thank my advisors, Dr. Gilbert D. Mc Cann and Dr. Floyd B. Humphrey, for their constructive advice and criticism during the preparation of this thesis. In addition, I wish to acknowledge the assistance of many members of the Faculty of the California Institute of Technology who contributed useful ideas and information on some particular aspects of this work. The assistance of Richard Carrouche, who designed and operated the deposition equipment, James R. Campbell, who assisted in the construction of the test equipment, Mrs. Rosalie Pruss, who devoted much care to the typing of the manuscript, and all those who helped in any way the final production of this thesis, is also acknowledged.

I also wish to thank the California Institute of Technology for financial support during my stay at the Institute and the Office of Naval Research, which, under Contract NONR 220(39), financed part of this work.

ABSTRACT

An experimental study of the fast switching properties of the film-loop assemblies indicated that a line charge model for a rectangular magnetic film represents the external flux distribution of the film with good (≈10%) accuracy. The flux linkage of a deposited loop equals 100% of the film flux. A 20% decrease in film flux was measured at both ends of the film easy axis and a quadratic flux distribution is consistent with the experimental results. Eddy current and circulating loop current fields affect the nanosecond range switching of magnetic films. Eddy current fields increase rapidly with the fraction of magnetic film perimeter covered by the loop conductors. Capacitive loop current fields cause a small increase in film switching time. Resistive loop loading can slow film switching significantly. The bias and drive field properties of deposited loops can be predicted from the loop dimensions. The deposition of complete film assemblies was effected without opening the vacuum of the system. The film switching test equipment incorporated a new method for the integration of fast switching signals and had a response time of 0.8 nsec. A theoretical study of the coupling loop circuitry indicated that the loop attenuation and the spatial distribution of loop induced voltage distort the film output signal. These effects are small, but not negligible, for a loop with conductor separation of 50,000 A and conductor thicknesses of 4000 A, enclosing a 1 cm^2 film switching in 1 nsec.

The use of integrated deposited circuitry containing magnetic films is feasible for fast computers. A set of logic elements suitable

for a deposited configuration has reasonable fan-in and fan-out potentialities. Theoretical miniaturization limits for deposited film logic circuitry depend chiefly on the resistivity of the coupling loops. Operation of such circuitry at low temperature reduces the limit of film size to about 14 microns. Miniaturization alleviates the effect of loop currents and attenuation on film switching signals, leading to low power, short switching time circuitry.

TABLE OF CONTENTS

TABLE OF CONTENTS (Con't.)

TABLE OF CONTENTS (Con't.)

I. INTRODUCTION

Much of the recent interest in magnetic thin films has been motivated by a general trend in computer design towards machines with large memory and logic circuit arrays and having short operating times. These computers are further characterized by the use of miniaturized circuitry with low power dissipation. Circuit miniaturization serves the dual purpose of limiting the physical size of large computers to reasonable dimensions and of reducing the signal transit time between various circuit components. This latter factor becomes of increasing importance as the operating speed increases. The large size of memory and logic arrays necessitates low power dissipation per switching element so that the total power requirements are not excessive and heat dissipation remains within tolerable limits.

The high switching speed of magnetic films with moderate drive requirements, the ease and potential low cost of fabrication of large film arrays by a deposition procedure, and the circuit miniaturization possible by use of small film elements, are features which indicate the great potentiality of circuitry containing magnetic films for future computer devices. To realize the full potential of thin films, future developments in this field will involve the use of integrated deposited circuitry, i.e., the deposition of magnetic films and associated electrical circuitry, such as conductors, resistors, capacitors and inductors on the same substrate.

A number of memory and logic schemes [1-4] have been proposed for use in deposited circuit configurations. Some features of these schemes have been investigated by a number of authors [5-7] and some useful information obtained. However, it was felt that, since all these schemes involve close coupling between magnetic films and conductors, a study of the effects of this common factor should prove useful for the future development of integrated deposited circuitry.

A basic configuration of deposited circuitry consists of a magnetic thin film element, closely coupled by, but insulated from a deposited coupling loop. The work of this thesis consists of an investigation of the properties of this film assembly, which may be of significance in the design of a complete deposited circuit.

A general model is presented for the film assembly. This model serves to delineate the various factors, which determine the characteristics of the complete assembly and is used as a guide to the study which follows.

The diagram of Fig. 1. 1a is used to aid in the presentation of the model. This diagram is a representation of a magnetic film, uniformly acted upon over all its surface by a number of magnetic fields $H_1, H_2, \ldots, H_n$, which may be a mixture of steady and pulse fields. When the initial condition of the film magnetization is known, application of these fields results in a definite state of the magnetization. The state of the film magnetization is represented at any instant of time by the flux vector $\bar{\phi}$ and the corresponding flux derivative $\dot{\bar{\phi}}$.

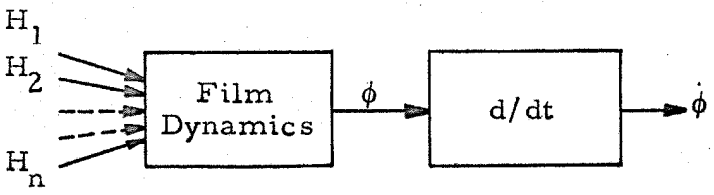

Fig. 1.1a. Magnetic Film Model

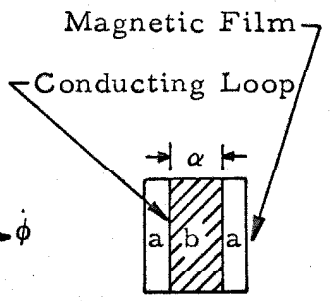

Fig. 1.1c. Film Assembly

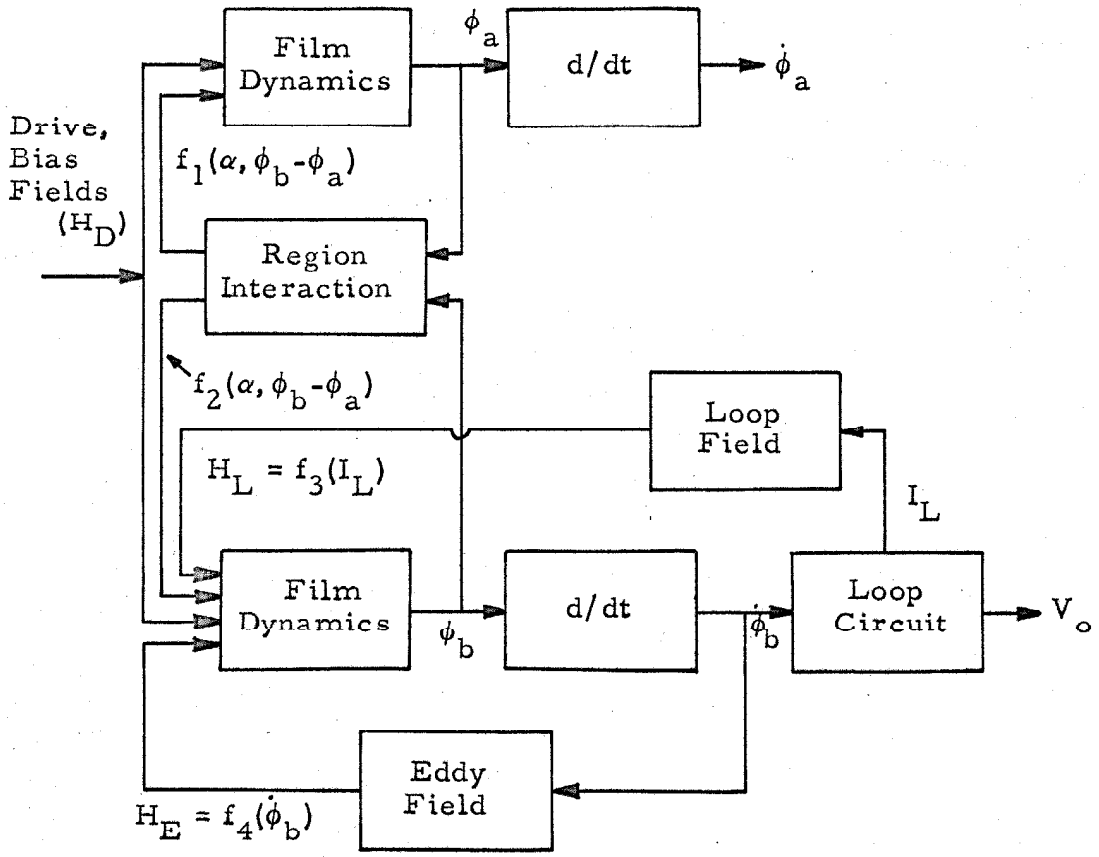

Fig. 1.1b. Film Assembly Model

The general film assembly model, illustrated in Fig. 1.1b, is presented for a rectangular magnetic film, covered over a fraction α of its width by a conducting loop, as shown in Fig. 1.1c. Deposited layer construction of the film assembly is assumed so that the coupling between the magnetic film and the conducting loop is very close. The effect of this close coupling is to localize any fields due to the loop conductor, to the region of the magnetic film directly beneath the conductor. Accordingly, the film magnetization may be considered separately in the two regions a and b, indicated in Fig. 1.1c. Using Fig. 1.1a, regions a and b of the magnetic film are represented by the upper and lower forward paths of Fig. 1.1b. The fields acting on region a of the film consist of externally applied drive and bias fields, and a field f_1, which arises from interaction of the two film regions. This interaction is caused by demagnetizing fields appearing at the region boundaries when the magnetization in the two regions begins to switch differently, and tends to preserve the alignment of the magnetization in the two regions. The quantity f_1 depends on the fractional film coverage α and on the difference of the fluxes $\overline{\phi}_a$ and $\overline{\phi}_b$. Clearly, when $\overline{\phi}_a = \overline{\phi}_b$, the interaction field is zero.

Region b of the film is acted on by the same external fields and by a corresponding interaction field f_2. In addition, two other fields arise due to the presence of the conducting loop and are represented by appropriate feedback loops. The motion of the film magnetization in region b induces eddy currents in the loop conductors and these currents produce a field which reacts on the film magnetization. This

eddy current field, H_E, is assumed to be a function of the flux derivative $\dot{\phi}_b$. The component of $\dot{\phi}_b$, along the deposited loop axis, excites the passive deposited loop circuit. The circulating loop currents produce the other field, H_L, which affects the motion of the film magnetization.

The voltage observed at the deposited loop output is related to the input voltage by the transfer function of the loop and its terminating impedance. When a number of films are associated in a deposited circuit, the terminating impedance of the deposited loop circuit of one film may consist of the deposited loop circuit of another film. The flow of energy between these circuits produces bias and/or drive fields acting on the magnetic films.

The utility of the model just presented lies in its representation of the film assembly in the form of a block diagram. This diagram illustrates the interaction of the various factors which determine the properties of the film assembly.

It will be shown that topics such as film-loop flux linkage, loop circuitry and loop magnetic fields are important to the characterization of this assembly as a circuit element. The general feasibility of integrated deposited circuitry for future computer devices will be demonstrated and some general design features of this circuitry indicated. Suitable equipment was developed to fabricate the film assemblies and to measure their high speed switching characteristics. The complete deposition of a film assembly was accomplished without breaking the vacuum of the fabrication equipment. The measuring equipment

featured a system for studying flux signals, with rise times in the nanosecond range.

II. MAGNETIC FILM FLUX LINKAGE WITH A COUPLING LOOP

When a magnetic film changes the direction of its magnetization, the voltage induced in a coupling loop equals the rate of change of film flux linking the loop. This voltage excites the loop circuitry and, as indicated in Fig. 1. 1, plays a part in the transfer of energy between the film and the loop. The total time integral of the induced voltage represents the total driving effect of the film into a loop, which senses the flux change or the total reaction of the film on a loop, which is used to provide a field for the film. Since this voltage-time integral equals the change of flux linkage with the loop, the importance of determining the flux linkage of a magnetic film with a coupling loop is apparent.

A model of film flux was proposed and applied to predict the flux linkage of various film and coupling loop configurations. By comparing with flux switching measurements, it was shown that the model is quite a good representation of the actual situation, and that, due to the small spacing between a magnetic film and a deposited loop, virtually all the film flux links such loops. The effect of the coupling loop circuit parameters on the time-integral of the loop output voltage was shown to be dependent only on the series resistances of the loop and associated termination impedance. A 20% decrease in film flux was measured at the ends of the easy axis dimension and a quadratic flux variation was found to be consistent with the flux switching measurements. A refined model of film flux, based on the above flux variation, was shown to represent the flux linkage of loosely coupled loops with

improved accuracy.

External Flux Distribution Model for Rectangular Magnetic Thin Film

Consider a single domain rectangular magnetic film which is distant from other magnetic material and has its magnetization M directed parallel to one edge of the film. A model for the external flux distribution of this film is obtained by representing the film magnetization by two uniform magnetic line charges of opposite polarity. These line charges lie along the two opposite edges of the film, at either end of the single domain, and extend the length of the film perpendicular to the direction of magnetization.

The flux linkage of a loop coupling the film equals the internal film flux, less the closure flux that returns within the loop. The above model can be used to predict the value of this flux linkage. Fig. 2.1 is a three-dimensional sketch of the rectangular film just described, and of a rectangular coupling loop whose axis is parallel to the film magnetization direction and whose plane intersects a center-line of the film. One loop conductor lies in the plane of the film and the opposite conductor is parallel to this plane, but at a distance from it. The two end conductors of the loop are symmetrically placed with respect to the film.

The linear dimensions and coordinates used in the calculation of the film flux are indicated in Fig. 2.1. Assuming line charges of uniform strength $\pm m$ per unit length, the predicted value of the internal film flux is

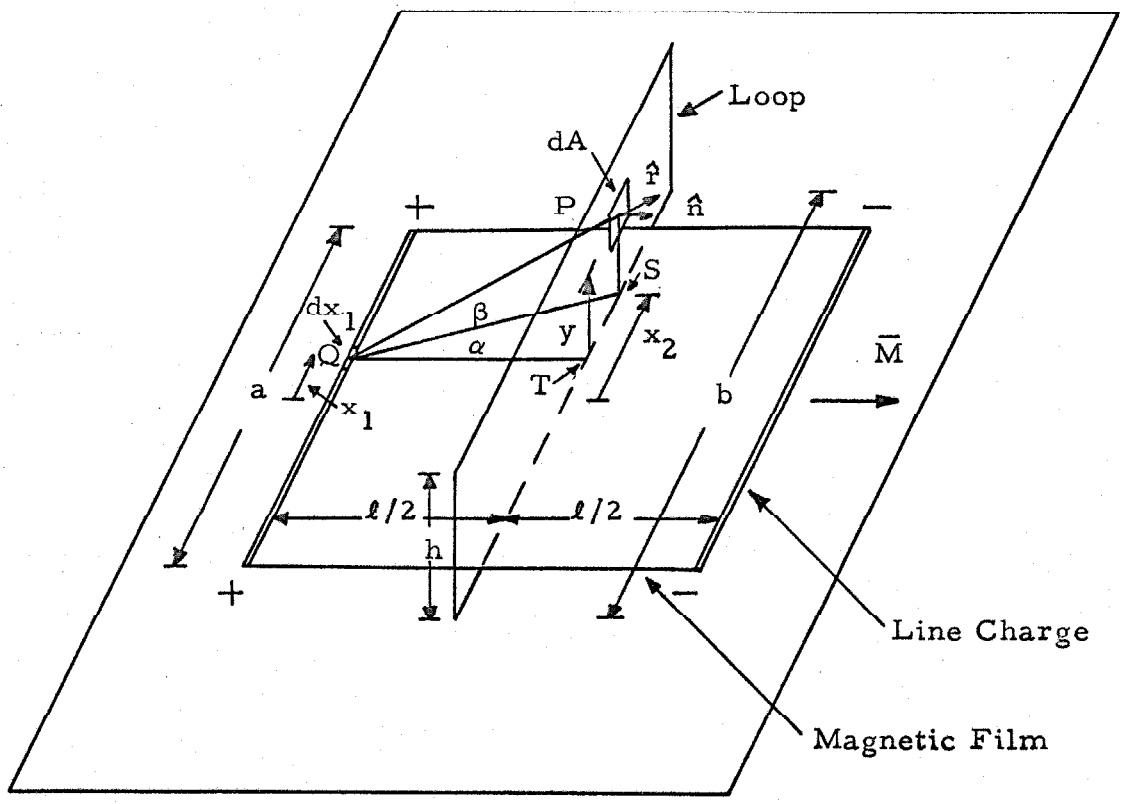

Fig. 2.1. Rectangular Magnetic Film and Coupling Loop

$$\phi_o = \mu_o m a \qquad 2.1$$

The corresponding flux density at a point P in the plane of the loop, due to an elemental length dx_1 of line charge at point Q, is expressed by

$$\overline{\Delta B} = \mu_o \frac{m\, dx_1}{4\pi\, r^2}\, \hat{r}$$

where $\hat{r}$ is a unit vector in the direction of $\overline{r}$ and $r^2 = (\ell/2)^2 + (x_2-x_1)^2 + y^2$. The component of $\overline{\Delta B}$ along the axis of the loop is

$$\overline{\Delta B} \cdot \hat{n} = \mu_o \frac{m\, dx_1}{4\pi\, r^2} \cos\beta \cos\alpha$$

where $\hat{n}$ is a unit vector along the loop axis direction and

$$\alpha = \tan^{-1} 2(x_2-x_1)/\ell \quad ; \quad \beta = \tan^{-1} y/[(\ell/2)^2 + (x_2-x_1)^2]^{1/2}$$

The normal flux contribution of the element dx_1, through an elemental area dA of the loop, is

$$\overline{\Delta B} \cdot \hat{n}\, dA = \mu_o \frac{m}{4\pi\, r^2} \cos\beta \cos\alpha\, dx_1\, dx_2\, dy$$

Due to symmetry, the total flux closure ϕ_1 within the loop is four times the flux closure due to one half of one of the line charges. Thus, integrating over half the length of one line charge, and over the complete area of the loop,

$$\phi_1 = 4\int_0^{a/2}\int_{-b/2}^{b/2}\int_0^{h} \mu_o \frac{m}{4\pi r^2} \cos\beta \cos\alpha \, dx_1 \, dx_2 \, dy \, . \qquad 2.2$$

Using the relationship $\cos\beta \cos\alpha = \frac{QT}{QP} = \ell/2r$ the above integral may be rewritten as

$$\phi_1 = \frac{\mu_o m \ell}{2\pi}\int_0^{a/2}\int_{-b/2}^{b/2}\int_0^{h} \frac{dx_1 \, dx_2 \, dy}{[(\ell/2)^2 + (x_2 - x_1)^2 + y^2]^{3/2}} = \frac{\mu_o m \ell}{2\pi} I_1 \qquad 2.3$$

The mathematical details of the evaluation of the integral I_1, together with two useful bounds I_2 and I_3, are presented in Appendix A, where the following results are derived.

The value of the triple integral I_1 is expressed by

$$I_1 = x\, I_A(x)\Big|_{(b-a)/2}^{(b+a)/2} + I_B(x)\Big|_{(b+a)/2}^{(b-a)/2} \qquad 2.4$$

where

$$I_A(x) = 2/\ell \tan^{-1} \frac{2hx}{\ell[(\ell/2)^2 + h^2 + x^2]^{1/2}}$$

$$I_B(x) = \frac{1}{2}\ln \frac{\{[(\ell/2)^2 + h^2]/h - [(\ell/2)^2 + h^2 + x^2]^{1/2}\}^2 + (\frac{\ell x}{2h})^2}{(\ell/2)^2 + x^2}$$

The integral I_1 is bounded between the two limits

$$I_2 = h\{[(\ell/2)^2 + (\tfrac{b+a}{2})^2]^{1/2} - [(\ell/2)^2 + (\tfrac{b-a}{2})^2]^{1/2}\}/(\ell/2)^2 \qquad 2.5$$

$$I_3 = h\{[(\ell/2)^2 + (\frac{b+a}{2})^2 + h^2]^{1/2} - [(\ell/2)^2 + (\frac{b-a}{2})^2 + h^2]^{1/2}\} / \{(\ell/2)^2 + h^2\} \qquad 2.6$$

The values of I_2 and I_3 are similar, when $h << \ell/2$. The average of these two values is denoted by I_4, so that

$$I_4 = (I_2 + I_3)/2 \qquad 2.7$$

This integral is a good approximation to I_1 when the limits I_2 and I_3 are close.

A useful approximation to the closure flux is obtained by assuming that the magnetic field surrounding the film is two-dimensional. This assumption corresponds to the case of a film whose domain length is negligible compared to its width. It can easily be shown that

$$\phi_5 = \mu_o \frac{ma}{\pi} \tan^{-1} \frac{2h}{\ell} = \frac{\mu_o m \ell}{2\pi} I_5 \qquad 2.8$$

where $$I_5 = \frac{2a}{\ell} \tan^{-1} \frac{2h}{\ell}$$

The flux values, corresponding to the $I_{1\ldots5}$ values can then be written as

$$\phi_i = \frac{\mu_o m \ell}{2\pi} I_i \quad : \quad i = 1, \ldots, 5 \qquad 2.9$$

and the predicted flux linkage values can be written as

$$\phi_o - \phi_i = \mu_o m a \left[1 - \frac{\ell}{2\pi a} I_i \right] \quad : \quad i = 1, \ldots, 5 \ . \qquad 2.10$$

Change in Flux Linkage During Film Switching

The flux linkage of a loop, coupling a magnetic film, can be determined by measuring the change in flux linkage which occurs when the magnetization direction is changed. Using the film flux model just presented, a study was made of some characteristics of this flux change for film and loop configurations used in later switching experiments.

The film assemblies were tested when mounted against the ground plane of the test strip line. The flux linkage was measured for a rectangular loop which has the ground plane as one conductor and whose axis is parallel to the initial magnetization direction (x-direction). In the switching experiments the film magnetization is switched through 90^o to the y-direction by an external magnetic field. The static flux pattern of the film is unaffected by the presence of the ground plane. However, when the film changes the direction of its magnetization, eddy currents are generated in the ground plane and oppose the change of flux in that region. When the magnetization is switched to the y-axis direction, the flux source (film magnetization) in the x-direction is removed, together with the accompanying air flux above the ground plane. Assuming that the change in magnetization is instantaneous (and/or ground plane material of zero resistivity), surface eddy currents appear on the ground plane to maintain the flux pattern within this conductor. It can be seen that the initial flux pattern above the ground

plane, after switching, is identical with the original flux pattern in this region except that the field directions are reversed. Thus, for fast film switching, the change in flux linkage through the coupling loop, expressed as a fraction of the change in internal film flux in the loop axis direction, is given by the equation

$$R = [(\phi_f - \phi_c) - \phi_c]/\phi_f \qquad 2.11$$

$$= 1 - 2\phi_c/\phi_f$$

where ϕ_f = internal film flux

ϕ_c = external closure flux within the loop .

Since ϕ_f is the change in flux linkage of a tightly coupled loop, situated in the plane of the rectangular loop, the quantity R can also be regarded as the ratio of the changes in flux linkages of these two loops.

Various values for ϕ_f and ϕ_c have been predicted by use of the external flux distribution model. Using ϕ_o (Eqn. 2.1) for the quantity ϕ_f, and the various ϕ_i values (Eqn. 2.9) for the quantity ϕ_c, the following R_i values are obtained as predicted values for the quantity R

$$R_i = 1 - \frac{\ell}{\pi a} I_i \quad ; \quad i = 1, \ldots, 5 \; . \qquad 2.12$$

Flux Change Within a Deposited Loop

Consider the change in flux linkage of a deposited loop coupling the rectangular magnetic film. Since the height of this loop is negligible compared to the film surface dimensions, the film may be assumed to lie in the surface plane of the strip line ground plane, even though the actual separation of these surfaces is approximately half the loop height. Thus, the values of R_i are directly applicable for this loop.

On defining R^* as the ratio of flux change in the deposited loop to the change in internal film flux, and using b^* and h^* as the deposited loop dimensions, then, since $h^* << \ell$,

$$R_5^* \approx 1 - \frac{4}{\pi} \frac{h^*}{\ell}$$

By referring to Eqns. 2.5 and 2.6, it can be seen that, in the limit of small h, I_2 and I_3 become identical and so

$$R_1^* \approx 1 - \frac{4}{\pi} \frac{h^*}{\ell} \left\{ \left[(\ell/2)^2 + \left(\frac{b^*+a}{2}\right)^2 \right]^{1/2} - \left[(\ell/2)^2 + \left(\frac{b^*-a}{2}\right)^2 \right]^{1/2} \right\} / a$$

$$= 1 - B \frac{4}{\pi} \frac{h^*}{\ell}$$

It can readily be shown that $B < 1$, and thus

$$R_1^* > R_5^* = 1 - \frac{4}{\pi} \frac{h^*}{\ell}$$

Using the expression for R_5^* which overestimates the flux closure of the deposited loop, the value of R_1^* for the standard dimensions of the film and deposited coupling loop was found to be greater than 0.99. It is assumed, therefore, that no flux closure occurs within a deposited

loop and so the change in deposited loop flux is identical with the change in internal film flux.

Comparison of Flux Ratios for External Loop

The values of $R_1, \ldots, R_5$ were first determined for the standard size film (a = 0.45" ; ℓ = 0.36") and the external loop (b = 0.722" ; h = 0.0625"), used in flux-switching experiments, and are tabulated below.

R_1	0.8177	exact model calculation
R_2	0.8097	lower bound
R_3	0.8325	upper bound
R_4	0.8211	average of bounds
R_5	0.7872	two-dimensional approximation

The variation of R_1, R_2, R_3 and R_5 as a function of each of the film dimensions, with the other dimensions held constant, is shown in Fig.2.2 and 2.3. Figure 2.2 shows the variation of these quantities with the film dimension ℓ parallel to the loop axis. As ℓ increases, R_1, R_2 and R_5 increase monotonically, tending to unity as ℓ tends to infinity. The value of R_3 also increases with ℓ, for ℓ greater than 2h, i.e., in the region where I_2 and I_3 are close limits. Figure 2.3 shows the variation of R_1, R_2, R_3 and R_5 as a function of the film dimension a perpendicular to the loop axis. Excluding R_5, which is independent of a, the values of R_i increase monotonically with a, but at a very slow rate. It can be seen that, in the limit of large a, these quantities all tend to unity. The flux closure within the loop of

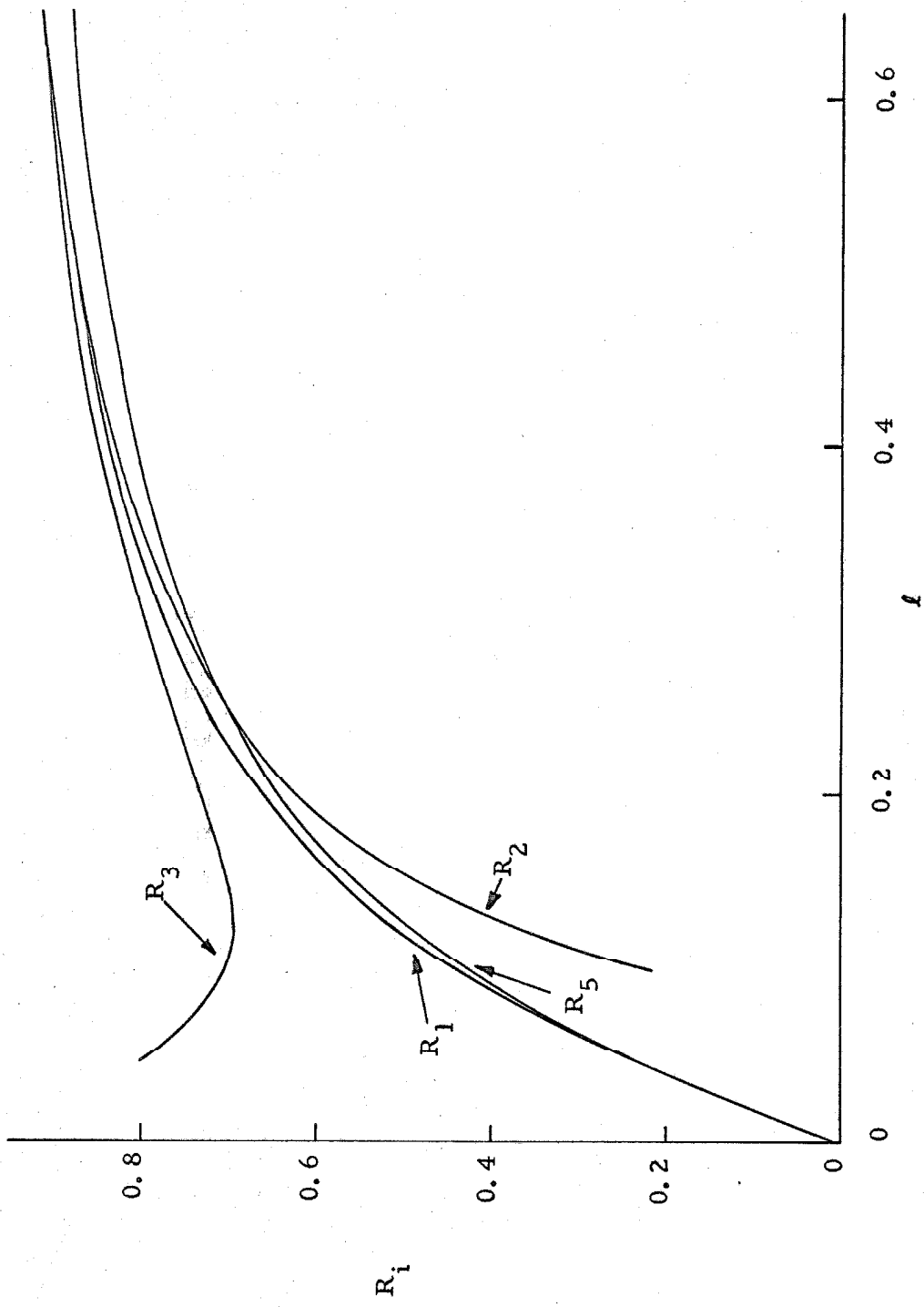

Fig. 2.2. Variation of Flux Ratios with Film Dimension Parallel to Loop Axis

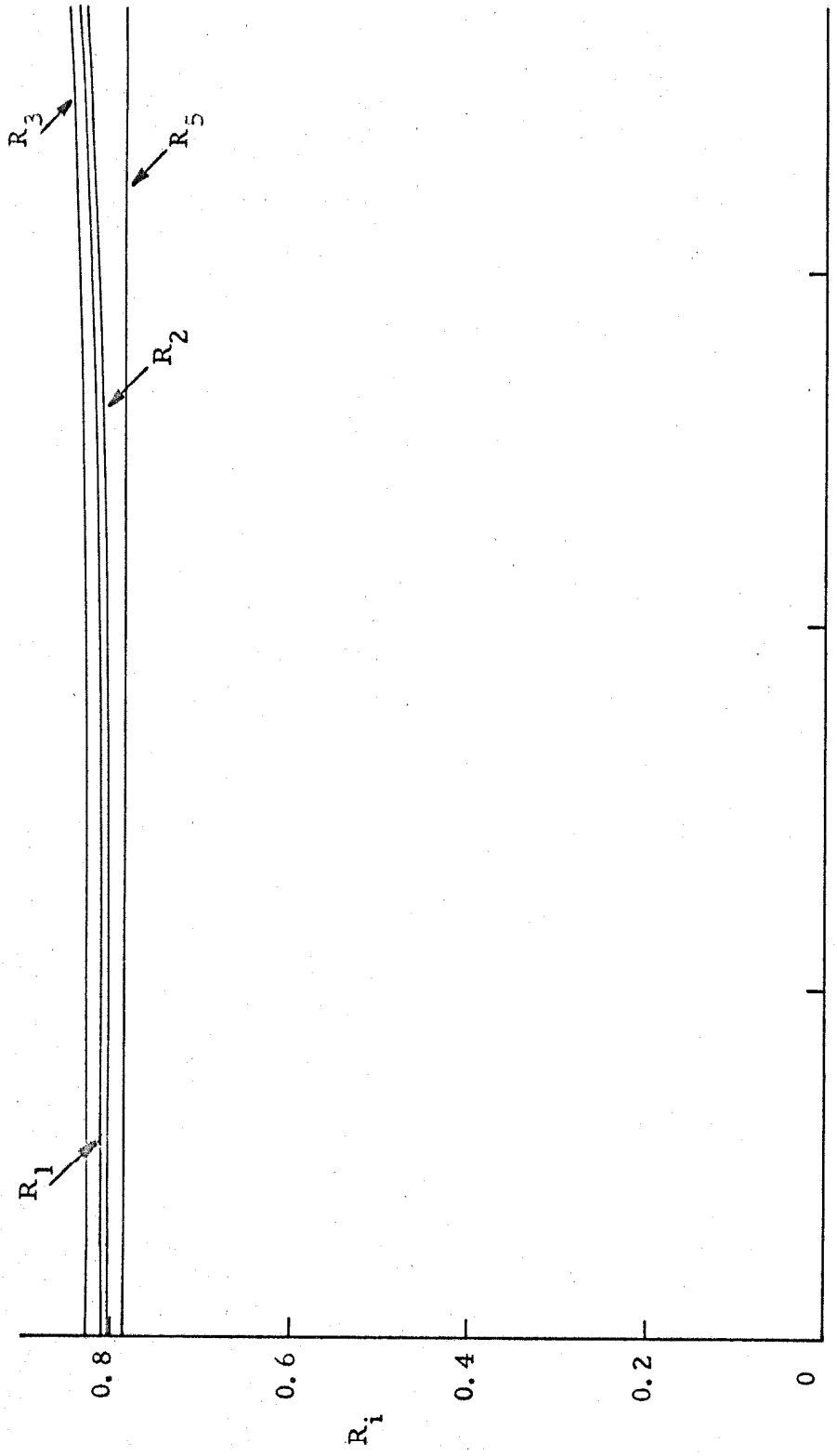

Fig. 2.3. Variation of Flux Ratios with Film Dimension Perpendicular to Loop Axis

finite length b is then negligible compared to the total flux of the film of large dimension a .

Since the field in the plane of the loop is closely two-dimensional when the film dimension a is very large, the film flux model reduces to the two-dimensional case, in the following manner.

With all other dimensions held constant,

$$R_1 = \frac{ma - mf(a)}{ma} = 1 - \frac{f(a)}{a}$$

where f(a) is a function of a . Comparing the flux change through the external loop with that occurring in a tightly coupled loop of the same length, the flux ratio is

$$R'_1 = 1 - \frac{f(a)}{b}$$

Values of R_1 , together with the corresponding values of R'_1 are shown in the following table as a function of a .

a	R_1	R'_1
0.722	0.83454	0.8345
0.800	0.84169	0.8246
1.000	0.86167	0.8084
2.000	0.92463	0.7912
5.000	0.96936	0.7878
10.000	0.98465	0.7874
25.000	0.99386	0.7874

For $a > 10$, the values of R_1' and R_5 (= 0.7872) are practically identical.

From Fig. 2.2 and 2.3 it can be seen that the two-dimensional value R_5 is always less than R_1, i.e., R_5 always overestimates the flux closure within the loop. However, it is also clear that over a wide range of parameter values R_5 is a very good approximation to R_1 and, because of its computational simplicity, is often used in later calculations.

Experimental Flux-Switching Measurements

The change in flux linkage of a loop, coupling a magnetic film, can be measured by integration of the loop output voltage with respect to time. It is shown in Appendix B that the ratio of the integrated output voltage to the integrated induced voltage depends only on the steady state attenuation of the loop and its termination impedance. When the loop has zero shunt conductance, this ratio is expressed by $r_o/[r_o + r_\ell]$ where r_o is the steady state resistance of the loop termination and r_ℓ is the total series loop resistance. The integrated output voltage is conveniently designated as the loop output flux change (usually abbreviated to loop output flux) by analogy with the integrated induced voltage, which equals the change in loop flux linkage.

The flux output of a loop depends only on the geometry of the film and the loop and on the resistive properties of the loop circuitry and its terminating impedance. When these quantities have been specified for two loops, a theoretical prediction of the output flux ratio of the two loops can be made. A number of experiments were performed using

various film and loop configurations and the flux ratios obtained were compared to the theoretical results. Reference to Fig. 2.2 and 2.3 shows that the flux linkage of an external loop, expressed as a fraction of the film flux, is very dependent on the film dimension ℓ, parallel to the loop axis, but is practically independent of the film dimension a perpendicular to the loop axis. Accordingly, flux-switching measurements were made on four sets of film assemblies having respectively, values of ℓ = 0.36"; 0.27"; 0.18" and 0.09". The corresponding values of R_1 are 0.8177, 0.7500, 0.6331 and 0.4079. Each film assembly had a narrow (0.03" wide) deposited loop, situated on the center-line of the magnetic film. This deposited loop configuration ensured linkage of the loop with the entire film flux, which must pass through the center-line of the film. If some flux emerged from the film at positions other than the film edges which coincide with the hypothetical line charges, a deposited loop placed off the center-line of the film would link a lesser amount of flux.

The flux measurements were made with the film assemblies mounted in the test strip line. The films had H_K values ranging from 3 Oe to 6 Oe and were driven to the hard axis direction by application of a transverse field of about 9 Oe. The external and deposited loops, situated on the film center-line, linked the easy axis film flux. For each film, the ratio F_r of the external loop to deposited loop output flux change was measured, together with the value of the deposited loop resistance. This resistance, determined by means of an impedance bridge, was measured before and after the

flux measurements and the mean value was used.

The results of these experiments are shown in Fig. 2.4, in which the values of F_r are plotted as a function of deposited loop resistance. The solid straight lines represent the theoretical values of this ratio, and have the equation

$$F_r = R_l\left[\frac{r_o + r_d}{r_o + r_e}\right] \qquad 2.13$$

where R_l = calculated flux linkage ratio

r_o = termination resistance = 53.5 Ω

r_d = deposited loop resistance

r_e = external loop resistance = 0.118 Ω

The agreement between the experimental and theoretical results is quite good. However, the experimental values are, in general, lower than the theoretical values. The dotted straight lines, representative of the experimental data, have almost identical slopes to the corresponding theoretical curves. The deviation of the experimental data from these lines is within the limits of accuracy attainable by the measuring equipment. Measurement of these deviations as a function of the silicon monoxide insulation thickness which varied considerably between film assemblies (at least 2/1 variation) failed to determine any correlation between these two quantities. It was concluded that the inductance and capacitance of the coupling loop had no effect on the magnitude of the observed switched flux. Thus, as already predicted, the effect of the loop circuitries on the flux outputs

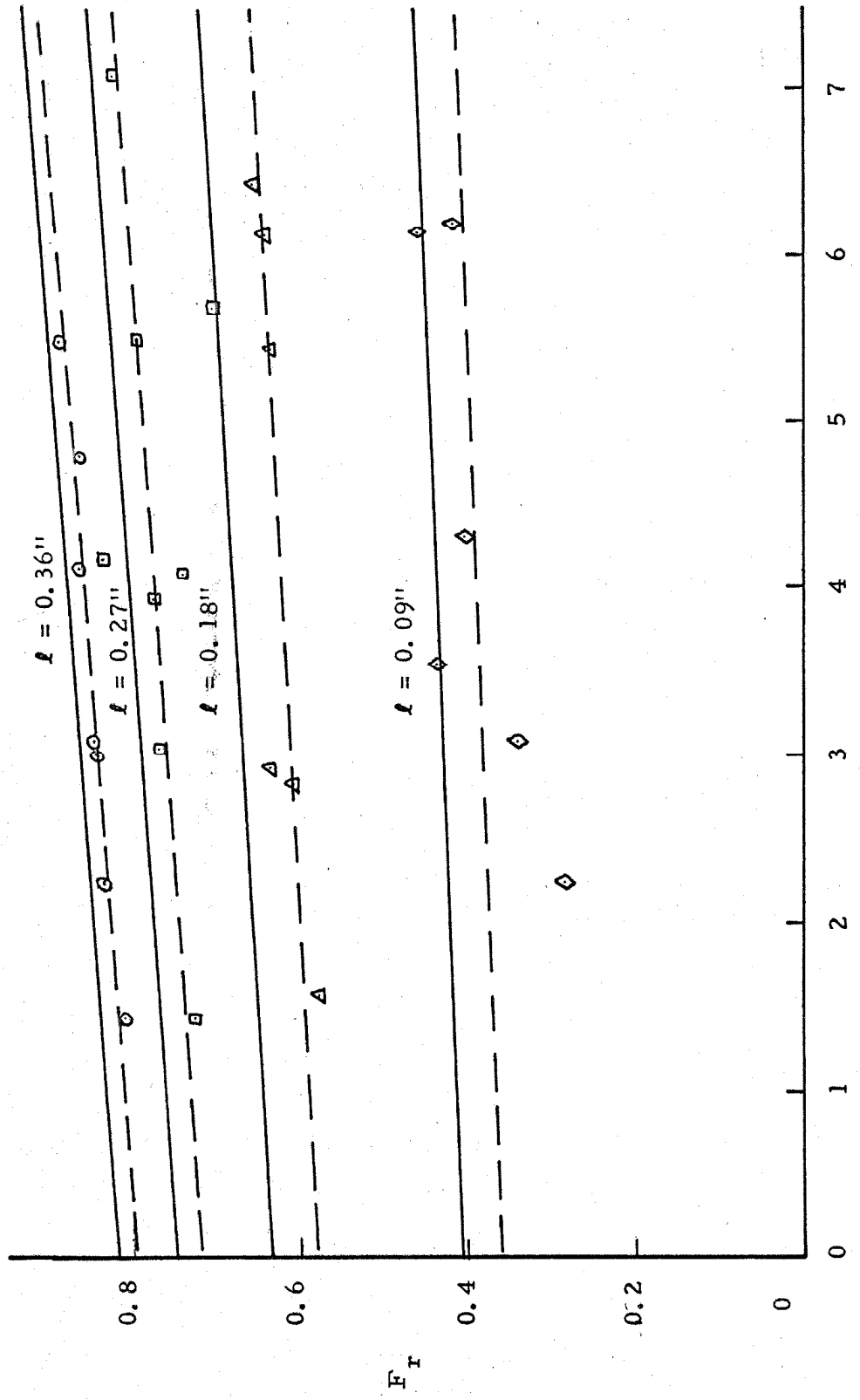

Fig. 2.4. Experimental Flux Ratios as a Function of Deposited Loop Resistance

was due solely to the resistive properties of the loops and their terminations.

The discrepancy between the corresponding experimental and theoretical values of R_1 ($F_r = R_1$ when $r_d = r_e$, see Eqn. 2.13) is seen to increase as the dimension of the film decreases from 0.36" to 0.18". (The experimental curve for $\ell = 0.09"$ is not accurately determined, due to the large scatter in the experimental results. This scatter is due to the difficulty of positioning the film assembly accurately when the dimension ℓ becomes comparable to the external loop height and the deposited loop width.) As seen in Eqn. 2.11, the quantity (1-R) is a measure of the flux closure within the external loop. The result just stated thus indicates that the line charge model for the film flux may need some modification in order to represent the actual film flux more accurately.

Measurement of flux change by means of a narrow deposited loop is assumed, after correction for the effect of loop resistance, to yield the value of flux through the region of the film directly beneath the deposited loop. Variation of the position of a narrow deposited loop, relative to the magnetic film, can be used to investigate the variation of flux through the film material. Measurement of flux change by means of a wide deposited loop, as may often be required in actual applications of thin film circuitry, can be interpreted in terms of flux change through the film material in the following way.

A wide deposited loop may be considered, in finite difference form, as a parallel circuit consisting of a large number of narrow

loops, as shown in Fig. 2.5. Each narrow loop is excited by a voltage dependent on the flux through the magnetic film directly beneath the loop and has an impedance appropriate to the width of the loop. Appendix B indicates that only the D.C. resistance of these loops are of significance in determining the output flux of the wide loop.

Let

w	=	width of wide loop
r_1	=	series resistance of wide loop
r_2	=	contact resistance between loop material and termination resistance
r_o	=	termination resistance
V	=	voltage source (D.C. voltage) at position x along width dimension of loop
V_o	=	output voltage (D.C. voltage) of loop
I	=	current per unit width of loop at position x
I_T	=	output current of loop

For a loop of width Δx, having series resistance $w r_1/\Delta x$, and situated at position x, the voltage relationship is

$$V_o = V - w r_1 I - r_2 I_T$$

Thus

$$I = (V - V_o - r_2 I_T)/w r_1$$

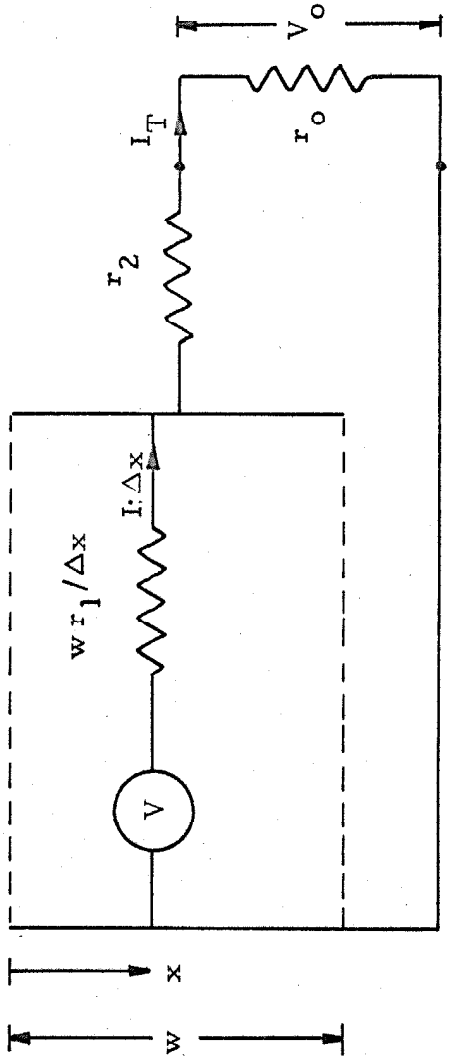

Fig. 2.5. Wide Deposited Loop with Resistive Load

Integrating across the width of the wide loop,

$$I_T = \frac{1}{wr_1} \int_o^w V\,dx - \frac{V_o}{r_1} - \frac{r_2}{r_1} I_T$$

or $$I_T \left(1 + \frac{r_2}{r_1}\right) = (V_{av} - V_o)/r_1$$

where $$V_{av} = \frac{1}{w} \int_o^w V\,dx$$

Replacing I_T by V_o/r_o, yields

$$V_o = \left[\frac{r_o}{r_o + r_1 + r_2}\right] V_{av}$$

$$= \left[\frac{r_o}{r_o + r}\right] V_{av}$$

where r = measured series resistance of loop. Thus, on correcting the output flux of a wide deposited loop for the effect of loop series resistance, the average flux linkage across the loop width is obtained.

The variation of flux through the magnetic film and the average flux linkages of some wide loops were investigated by means of flux switching experiments conducted on a number of film assembly sets. In each set, the deposited loop configuration was varied, with the magnetic film dimensions held constant at their standard values. Since the assemblies of each set were deposited at the same time, their film thicknesses were similar and flux measurements of the four films of the set were considered as having been made on the same film. The

variation of the deposited loop configurations is given below (all loop axes parallel to film easy axis).

Film Assembly 1 - Narrow (0.03" wide) loop on film center-line.

Film Assembly 2 - Narrow (0.03" wide) loop near film edge (loop center-line 0.165" from film center-line), having 100% of its width directly over magnetic film.

Film Assembly 3 - Wide (0.33" wide) loop on film center-line and covering 92% of entire magnetic film width.

Film Assembly 4 - Intermediate (0.18" wide) loop with center-line on film edge, thus having 50% of its width directly over the magnetic film.

The main quantity of interest in these experiments was the flux change, occurring within the various deposited loops. This quantity was calculated from the measured flux value by correcting for the effect of loop resistance. The external loop flux output was also measured for all the films and, due to the very small resistance of the loop, this value was taken as the flux linkage of the external loop. The position of the external loop relative to the magnetic film varied with the position of the deposited loop, since the mechanical construction of the sensing circuitry required that the external loop be directly above the deposited loop. Thus, for films 1 and 3, the external loop was situated on the magnetic film center-line, while for film 2 it was situated near the film edge and for film 4 it was situated on the film edge.

The mean of the results, obtained from flux-switching experiments on a number of sets of assemblies, are tabulated below:

Assembly	R_6	R_7
1	1.000	0.780
2	0.818	0.521
3	0.973	0.782
4	0.437	0.396

The quantity R_6 is the ratio of the deposited loop flux change for each assembly (corrected for deposited loop resistance) to the deposited loop flux change for assembly 1 (corrected for deposited loop resistance). The quantity R_7 is the ratio of external loop flux change to the deposited loop flux change for assembly 1 (corrected for deposited loop resistance). Comparison of all flux changes to the deposited loop flux change for assembly 1 resulted in expressing all flux changes as a fraction of total film flux.

The value of R_6 for assembly 2 indicates that the flux passing through the magnetic film material varied by about 18% along the easy axis direction. The decrease in the flux through the magnetic film towards the edges of the film was also evidenced by the value of R_6 for assembly 3, for which the average flux linkage through the wide loop was about 3% less than the total film flux. The value of R_6 for assembly 4 was 53.4% of the corresponding value for film 3. The deviation of this quantity from 50%, which would be obtained if the flux through the film were constant, was also attributable to the above

flux variation. The values of the quantity R_7 are also of some interest. For assembly 1, R_7 is the same quantity as the ratio R, which was measured in previous experiments. (The value obtained for R was 0.795. The difference between these two values is due to experimental error and possible small mechanical deformation of the external loop between these experiments.) The values of R_7 for assemblies 1 and 3 are seen to be similar, indicating that the presence of the wide deposited loop did not affect the flux change of the magnetic film. The progressive decrease of the values of R_7 for the assembly sequence 1, 2 and 4 was consistent with the position of the external loop, which moved from the center-line to the edge of the magnetic film. Using the two-dimensional approximation flux model for the magnetic film, a value of 0.445 was calculated for R_7, when the external loop was over the edge of the film. This value is in general agreement with the experimental results.

On the basis of the above results, the line charge model of film flux was modified to give a more accurate representation of the external flux distribution of the magnetic film. The flux distribution within the magnetic material was assumed to vary only along the easy axis dimension, with any variation along the hard axis dimension being neglected. The flux per unit length of film, perpendicular to the film easy axis, was assumed to vary from the value $\mu_o m$ on the film center-line to the value $\mu_o Km$ at either end of the easy axis. Calculations of various loop flux linkages were made for the two assumed flux distributions (linear and quadratic) shown in Fig. 2.6, and

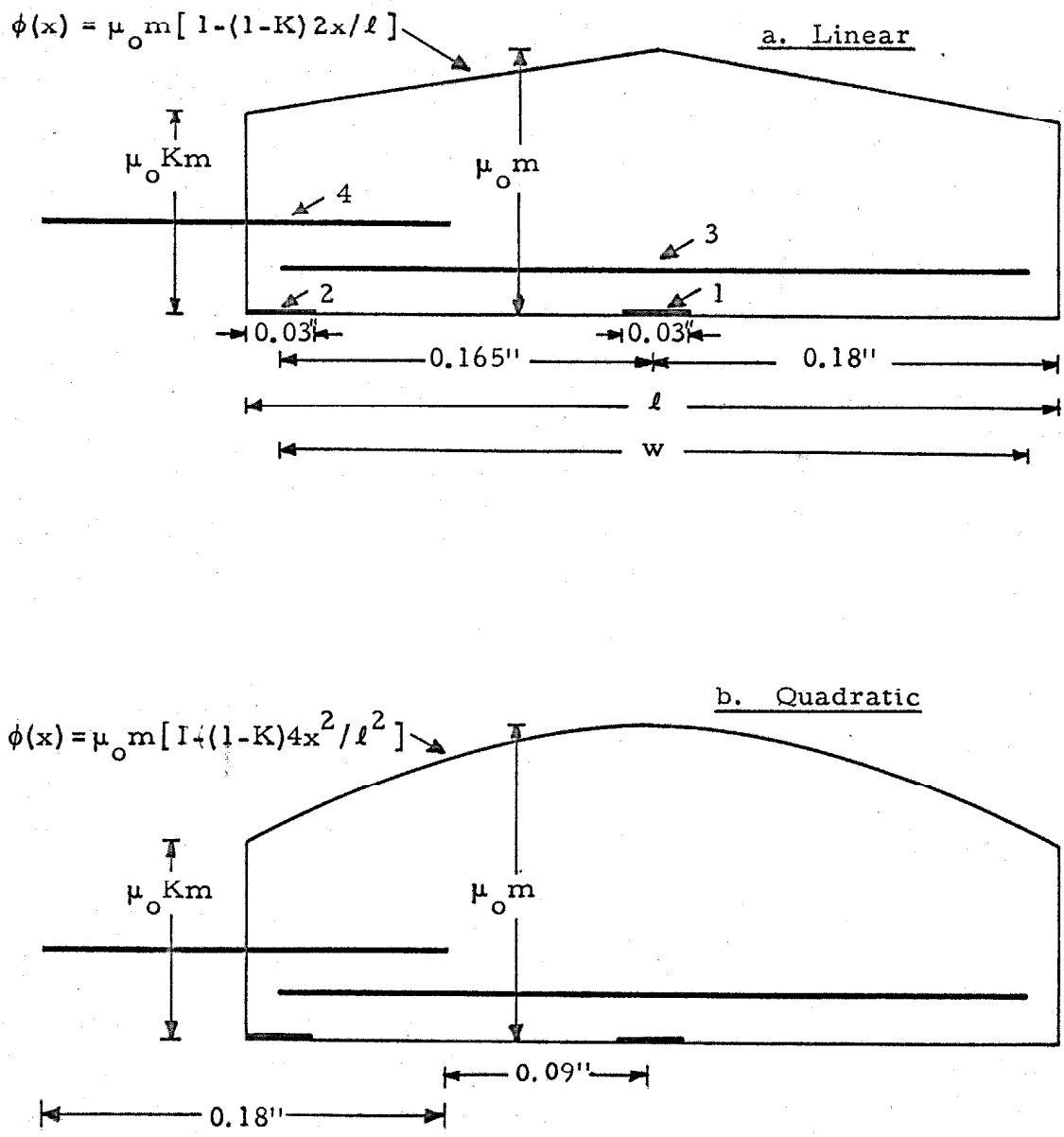

Fig. 2.6. Easy Axis Flux Distribution Models

the results obtained were compared with the experimental values. These figures also show the relative locations of the deposited loops of the four assemblies. Using the experimental value of R_6 for assembly 2, the corresponding values of R_6 for assemblies 3 and 4, and of R_7 for assembly 1, were calculated as follows.

Linear Flux Distribution Model

Let ϕ_n = average flux linkage across deposited loop of assembly n . Then

$$\phi_2/\phi_1 = \frac{1 - \frac{11}{12}(1-K)}{1 - \frac{1}{24}(1-K)} = 0.818 = R_6 \text{ (assembly 2)}$$

Solution of this equation for K yields

$$K = 0.796 \qquad 2.15$$

Thus,

$$\phi_1 = \mu_o m\,(0.9915)$$
$$\phi_2 = \mu_o m\,(0.813)$$
$$\phi_3 = \mu_o m\,(0.909)$$
$$\phi_4 = \mu_o m\,(0.423)$$

or

$$R_6 \text{ (assembly 3)} = 0.916 \qquad 2.16$$
$$R_6 \text{ (assembly 4)} = 0.427 \qquad 2.17$$

A model which is consistent with the flux distribution within the magnetic material, as shown in Fig. 2.6a, for the external flux distribution of the magnetic film when magnetized along its easy axis, consists of

two uniform magnetic line charges of strength $\pm Km$, lying at both ends of the easy axis, and uniform line charge distributions of strength $\pm 2\,(1-K)\,m/\ell$ at distance x from the film center-line, $(0 \leq x \leq \ell/2)$. The value of the flux ratio R may be evaluated by summation of the flux changes due to all the line charges, giving

$$R = K R_1(\ell/2) + (1-K)\,2/\ell \int_0^{\ell/2} R_1(x)\,dx \qquad 2.18$$

where $R_1(x)$ is the value of R_1 corresponding to line charges, separated by an axial distance $2x$. ($R_1(\ell/2) = 0.8177$, as calculated earlier.) The contribution of the line charge distribution was determined using the two dimensional approximation, since the three dimensional value R_1 leads to complicated integration processes. Inspection of Fig. 2.2 shows that, over the range of integration, $|R_1(x)-R_5(x)| \leq 0.03$ and so the resulting error ΔR in the value of R is

$$\Delta R \leq 0.03\,(1-K)\,2/\ell \int_0^{\ell/2} dx = 0.006 \qquad 2.19$$

Substitution of $R_5(x) = \frac{2}{\pi} \tan^{-1} x/h$ $(0 \leq x < \ell/2)$ for $R_1(x)$ in Eqn. 2.18, leads to

$$R = K R_1(\ell/2) + (1-K)\,\frac{2}{\pi}\left\{\tan^{-1} \ell/2h - \frac{2h}{\ell} \ln\left[\frac{h^2+(\ell/2)^2}{h^2}\right]^{1/2}\right\}$$

$$= 0.760 \qquad 2.20$$

Thus, the predicted value of R_7 for assembly 1 is

$$R_7 = 0.760/0.9915 = 0.767 \qquad 2.21$$

Quadratic Flux Distribution Model

Let

$\phi(x)$ = flux value in film material at distance x from film center-line.

ϕ_n = average flux linkage across deposited loop of assembly n .

w = width of deposited loop of assembly 3.

Then

$$\phi(x) = \mu_o m \left[1-(1-K)\, 4x^2/\ell^2 \right]$$

and

$$\phi_2/\phi_1 \approx \frac{1-(\frac{11}{12})^2 (1-K)}{1-(\frac{1}{24})^2 (1-K)} = 0.818$$

$$= R_6 \text{ (assembly 2)}$$

Solution of this equation for K yields

$$K = 0.782 \qquad 2.22$$

Then

$$\phi_1 = \mu_o m(0.999)$$

$$\phi_2 = \mu_o m(0.817)$$

$$\phi_3 = \frac{\mu_o m}{w/2} \int_o^{w/2} \phi(x)\, dx$$

$$= \mu_o m \left[1 - \frac{(1-K)}{3} (w/\ell)^2\right]$$

$$= \mu_o m [0.939]$$

$$\phi_4 = \frac{\mu_o m}{\ell/2} \int_{\ell/4}^{\ell/2} \phi(x)\, dx$$

$$= \mu_o m \left[1/2 - \frac{(1-K)}{3} (1 - 1/8)\right]$$

$$= \mu_o m [0.436]$$

or

$$R_6 \text{ (assembly 3)} = 0.940 \qquad 2.23$$

$$R_6 \text{ (assembly 4)} = 0.437 \qquad 2.24$$

A model which is consistent with the flux distribution within the magnetic material, as shown in Fig. 2.6b, for the external flux distribution of the magnetic film when magnetized along its easy axis, consists of two uniform magnetic line charges of strength $\pm Km$, lying at both ends of the easy axis and uniform line charge distributions of strength $\pm 8(1-K)\, mx/\ell^2$ $(= \pm d\phi/dx)$ at distance x from the film center-line $(0 \leq x \leq \ell/2)$. As in the linear distribution case, the flux ratio R is evaluated by summation of the flux changes due to all the line charges. Substitution of $R_5(x)$ for $R_1(x)$, $(0 \leq x \leq \ell/2)$, gives rise to a maximum error of 0.006 in the resulting value of R.

Thus

$$R = K R_1(\ell/2) + (1-K)\frac{2}{(\ell/2)^2}\int_o^{\ell/2} x R_1(x)\,dx \qquad 2.25$$

$$= K R_1(\ell/2) + (1-K)(2/\ell)^2\left[(\ell/2)^2 + h^2\right]\frac{2}{\pi}(\tan^{-1}\ell/2h) - (1-K)\frac{4}{\pi}\frac{h}{\ell}$$

$$= 0.784 \qquad 2.26$$

or

$$R_7 \text{ (assembly 1)} = 0.785 \qquad 2.27$$

The corresponding experimental and theoretical flux ratios are tabulated, as follows:

	Flux Distribution Models			
	Constant	Linear	Quadratic	Experimental
R_6 (assembly 3)	1.000	0.916	0.940	0.973
R_6 (assembly 4)	0.500	0.427	0.437	0.437
R_7 (assembly 1)	0.8177	0.767	0.785	0.780 0.795

The results indicate that the flux distribution in the film material is represented quite closely by the quadratic variance, shown in Fig.2.6b and that the corresponding line charge model gives an accurate picture of the external flux distribution of the magnetic film.

III. COUPLING LOOP CIRCUIT ANALYSIS

When the direction of magnetization in a thin film is changed, the voltage waveform induced in a conducting coupling loop is dependent on the time variance of the loop flux linkage, in the direction of the loop axis. As indicated in Fig. 1. 1, the induced voltage excites a circuit, defined by the loop electrical parameters and termination impedance. In the present study a theoretical investigation is undertaken to determine the effect of loop transfer functions on the waveform of the induced voltage. (The relative flux linkage of the two types of loops and the ratio between linked flux and observed flux have already been considered.) The electrical lengths of the loops are small but not insignificant compared to the length of the induced voltage transients. In addition, the voltages induced in the loops are distributed along the length of the loop conductors. Accordingly, a theory is developed to calculate the step response of a transmission line having a distributed EMF. Using this theory, it is shown that the rise time of the step responses of the deposited and external loops is of the order of a fraction of 1 nsec. Digital computer simulation is then used to show that the external loop has only a small effect on pulses having durations of at least 1 nsec. A similar result is obtained for the deposited loop provided that its attenuation is not excessive (< 10 db). The validity of a lumped parameter circuit approximation for the loop circuitries is also established.

Step Response of Lossless Transmission Line With Distributed EMF

Consider the pulse response of a length of lossless transmission line (characteristic impedance Z_o, electrical length T) which is shorted at one end and terminated at the other end in an impedance Z_r. A uniformly distributed voltage waveform is applied along the total length of the line and a resulting output voltage appears across the line termination.

First assume the application of an arbitrary pulse shape of total length L, to the transmission line, when the line is terminated in Z_o as illustrated schematically in Fig. 3.1. Every incremental voltage step ΔV, having the polarity shown (right end positive relative to left end), applied to an elemental length ΔS of the line, results in two voltage steps. One, $+\frac{\Delta V}{2}$, travels from the source position towards the right where it is absorbed in the Z_o termination, and the other, $-\frac{\Delta V}{2}$, travels from the source position towards the left, where it is reflected with a change in sign back along the line from the short circuit end, and is finally absorbed in the Z_o termination. The beginning of the output pulse coincides with the beginning of the input pulse, due to the voltage $+\frac{\Delta V}{2}$, originating from the element ΔS_o of the line. The output voltage continues to change until a time 2T after the end of the input pulse, due to the voltage $-\frac{\Delta V}{2}$ from the element ΔS_o. Thus the length of the output pulse is (L + 2T) and the fractional increase in the pulse length is 2T/L. The shape of the output pulse will be similar to that of the input pulse, if $L > T$, and so the rise time of the

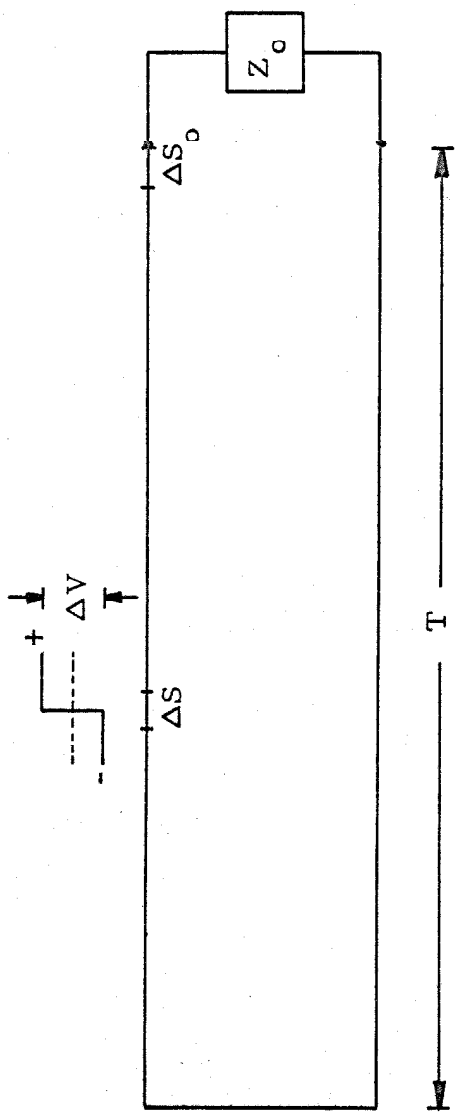

Fig. 3.1. Lossless Transmission Line with Distributed EMF

pulse also increases approximately by the fractional value $2T/L$. The lengthening of the pulse may be quite significant, even when $L >> T$ (e.g., when $L = 10T$, the increase is 20%). When the line is terminated in an impedance other than Z_o, reflections at this termination cause the pulse to be lengthened by more than $2T$. Thus, in general, the effect on the rise time of the pulse is also greater.

The response of the transmission line terminated in various Z_r, to a step input voltage, gives an upper limit to the rise time of the output waveform for all pulse inputs. Let an EMF of V per unit electrical length of line be applied as a step function at initial time. The voltage developed across Z_r at any subsequent time is determined as follows.

Consider first an infinite length of the transmission line. Initially, a step voltage $V \cdot \Delta S$, having the following polarity (right end positive relative to left end) is applied to each electrical length ΔS of the line. Each step voltage results in a step voltage $+\frac{V}{2} \cdot \Delta S$ traveling from its source position towards the right and a step voltage $-\frac{V}{2} \cdot \Delta S$ traveling from the same position towards the left. The succession of positive steps approaching any point on the line from the left produces a ramp signal with slope $+V/2$ at this point. Similarly, the negative steps approaching from the right give rise to a ramp signal with slope $-V/2$ at the same point. The sum of the two voltage waves is the voltage observed at this point. In the case of the infinite length line, this voltage clearly remains zero at all times,

although there is a linear build-up of current, determined by the series inductance of the line.

The ramp signal, which is seen to be a characteristic waveshape of a lossless transmission line with a distributed EMF, is modified by the line terminations. The voltage waves reaching the short-circuited end of the line are reflected back along the line with a change in sign, while voltage waves reaching the Z_r termination are reflected with a reflection coefficient of $(Z_r - Z_o)/(Z_r + Z_o)$. The transmission coefficient at this termination is $2Z_r/(Z_r + Z_o)$ and it is this fraction of the incoming wave that appears across Z_r . By considering the multiple reflections from the line terminations, the response to a uniformly distributed step input is obtained. Figure 3.2 shows the output voltage obtained for a number of values of Z_r . As in the case of the response to a step voltage applied at the shorted end of the transmission line, the output voltage possesses overshoot only when $Z_r > Z_o$.

This lossless line theory will be later applied to predict the step responses of the loop circuitries under investigation. Allowance will be made for the effect of line losses, which will be shown to be quite significant for the deposited loop configurations.

Circuit Parameters of Deposited Loops

The circuit parameter values for the deposited loops were calculated using the assembly dimensions shown in Fig. 6.1. Two standard loops, differing only in the width of their conductors, were chosen. One has a narrow (0.03" wide) conductor which extends 1/12th of the magnetic film width and was the narrowest conductor width used in

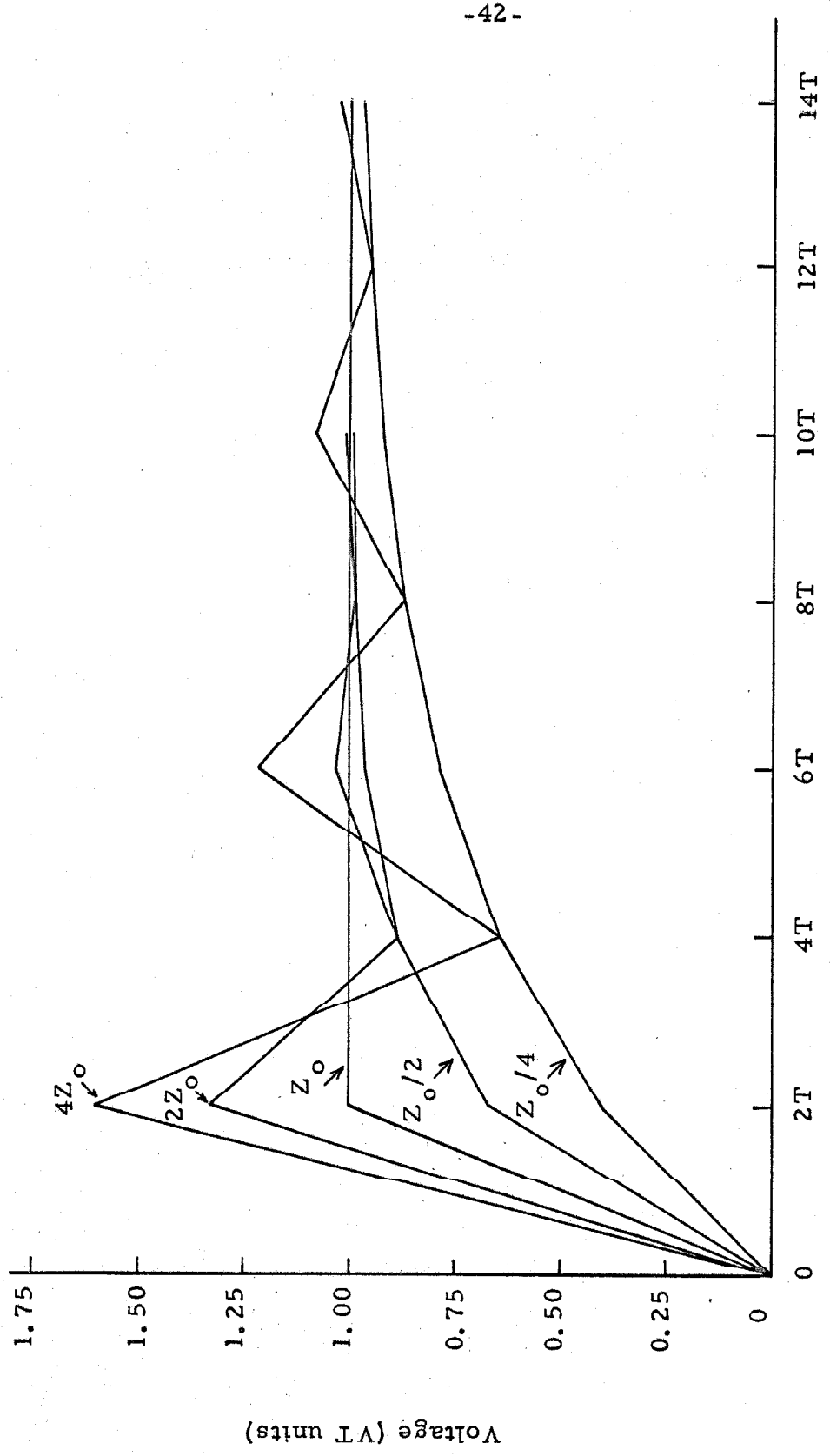

Fig. 3.2. Step Response of Lossless Transmission Line Terminated in Various Resistive Loads

this work. The other loop has a wide (0.36" wide) conductor, which extends the complete width of the magnetic film. (The ground plane conductors of each loop are 0.36" wide).

The resistivity of a 4000A thick sheet of aluminum at room temperature does not differ significantly from the bulk resistivity value:[8] ($2.82 \times 10^{-6}\ \Omega$-cm). Using this value, the skin depth δ of aluminum at a frequency representative of nanosecond speed switching, is 26,800A ($\delta > 4000$A for $f < 45$ kMc). Thus, a uniform current distribution was assumed in the conductors and the following resistance values were calculated:

narrow conductor : $R = 1.11\ \Omega$

wide conductor : $R = 0.092\ \Omega$

ground plane : $R = 0.092\ \Omega$

The resistance connection between the two loop conductors has a theoretical value of $0.2\ \mu\Omega$ and so is considered to have zero resistance.

The separation of the conductors of the loop is very small compared to their width ($< 10^{-2}$). Accordingly, the parallel plate formula is used for calculation of the loop capacitance. (The presence of the permalloy sheet, which lies along a natural equipotential of the electric field, reduces the effective separation of the conductors by the thickness of this sheet.) Using a value of 5.3 for the permittivity of the silicon monoxide dielectric[9], the following capacitance values were calculated:

narrow loop : C = 85 pF

wide loop : C = 1020 pF

The loop inductance depends on the distribution of magnetic flux within the loop and the loop conductors. As indicated in Fig. 1.1b, the time variance of film flux is regarded as a voltage which excites the passive circuit of the coupling loop. In this way, the film flux is separated from the flux due to loop circuitry and the permalloy film can then be treated in a similar way to a non-ferromagnetic material. Since the separation of the conductors of the loop is very small compared to their width, the magnetic field in the intervening space is uniform across the width of the conductors and is directed parallel to the conductor surfaces. By neglecting current spreading in the loop ground plane (this assumption is justified by the short time of the film switching process), the value of this field (in amp-turns/meter) becomes equal to the current per meter width of loop conductor. At extremely high frequencies, eddy currents prevent penetration of the magnetic field into the permalloy and loop conductors. Under these conditions magnetic flux appears only in the space between the conductors, and the inductance attains its minimum value of $\mu_o \frac{\ell}{w} [b+d]$ (for notation, see Fig. 6.1). At lower frequencies, flux penetrates the conductors and the inductance increases to $\mu_o \frac{\ell}{w} [(b+d) + c + \frac{a+e}{3}]$. Since the conductor thicknesses are small compared to the dielectric thicknesses, this increase is quite small (about 10%) and the high frequency value is chosen as the standard inductance of the loop. The following standard inductance values were calculated:

narrow loop : $L = 98$ pH

wide loop : $L = 8.2$ pH

When the film assemblies are placed in the test strip line for high speed switching experiments, the loop ground plane is mounted against a large thick brass ground plane. The penetration of flux into this ground plane increases the effective inductance of the loop. By assuming that the loop ground plane has the same conductivity as the brass ground plane, which is assumed to be infinitely thick, the additional inductance is given by the equation [10]

$$L_\delta = \frac{\tau}{\omega\delta} \cdot \frac{\ell}{w}$$

where τ = specific resistivity of brass

δ = skin depth of brass

$= (\frac{1}{2}\omega\mu/\tau)^{-1/2}$

By substitution of the value for δ into the above equation, it can be shown that

$$L_\delta = \mu_o \frac{\ell}{w} \cdot \frac{\delta}{2}$$

and so the effective loop inductance becomes

$$L_1 = \mu_o \frac{\ell}{w} \left[(b+d) + c + \frac{a}{3} + \frac{\delta}{2}\right]$$

in comparison to the standard inductance value of

$$L = \mu_o \frac{\ell}{w} \left[b+d\right] .$$

The value of L_1 increases with decreasing frequency and becomes infinite at zero frequency. However, the impedance of this inductance decreases monotonically with frequency, since the frequency dependent term of the inductance varies as $\omega^{-1/2}$. Thus, the greatest effect of the inductance on the loop properties may be expected to occur at high frequencies.

At nanosecond switching frequencies, the value of L_1 is about 50% greater than the value of L. The frequency at which L_1 attains twice the value of L was found to be 0.21 k Mc. This result indicates that the standard inductance value is quite representative of nanosecond switching speed circuit conditions and that the effect of increased inductance with decreased frequency can be examined by doubling the standard inductance value.

At nanosecond switching frequencies the loss tangent for the silicon monoxide dielectric[11] is of the order of 10^{-4}. By regarding the shunt impedance of the loop as a parallel R-C circuit, the equivalent resistive impedance is of the order of 10^4 times the capacitive impedance at these frequencies, thus indicating a minimum resistance value of about 1000 Ω. The effect of this resistance on the loop circuit properties can be neglected and so the shunt conductance of the loop is assumed to be zero.

Step Response of Deposited Loops

The loop parameter values just determined will be used to calculate the transmission line properties of the deposited loops and to estimate the step response of such configurations. The standard para-

meter values are tabulated as follows. (The resistance value is chosen to be the resistance of one loop conductor, thus assuming a zero resistance return path through the loop and strip line ground planes.)

	Narrow Loop	Wide Loop
R	1.11 Ω	0.092 Ω
L	98 pH	8.2 pH
C	85 pF	1020 pF
G	0	0

The two quantities, which specify the transmission line properties of the loop are its characteristic impedance Z_o and its propagation constant γ :

$$Z_o = \sqrt{\{(R + jL\omega)/(G + jC\omega)\}} = |Z_o| \angle\theta \qquad 3.1$$

$$\gamma = \sqrt{\{(R + jL\omega)(G + jC\omega)\}} = \alpha + j\beta \qquad 3.2$$

The real part of γ specifies the attenuation of a portion of line, 0.47" long (length of deposited loop). The quantity β/ω equals the electrical length T of this transmission line. The quantity γ is independent of the loop width w, since C is directly proportional to w and R and L are inversely proportional to w. Thus, the attenuation and electrical lengths of both narrow and wide loops are identical. The value of Z_o is inversely proportional to w, and so the wide loop has a lower characteristic impedance than the narrow loop.

The values of Z_o, α and T are shown in the following table

for the narrow loop, for a number of frequencies spanning the frequency range of interest in thin film switching signals.

f(kMc)	$\lvert Z_o \rvert$ (Ω)	$\angle\theta$	α(db)	T(nsec)
0.1	4.55	-43^o	1.45	0.285
0.2	3.23	-42^o	2.00	0.204
0.5	2.07	-37^o	2.91	0.141
1.0	1.54	-30^o	3.69	0.112
2.0	1.24	-21^o	4.16	0.099
5.0	1.12	-10^o	4.48	0.093
10.0	1.08	-5^o	4.44	0.092
∞	1.07	0^o	4.47	0.092

The characteristic impedance is seen to vary quite significantly in the frequency range of 0.1 to 10 kMc. Its magnitude varies by a ratio of about 4.5 while its phase angle varies from -43^o to -5^o. At a frequency of 1 kMc, the ratio of $\lvert Z_o \rvert$ to its infinite frequency value $\sqrt{L/C}$ is about 1.5. The attenuation and electrical length of the line both vary by a ratio of about 3.0 over the 0.1 to 10 kMc range. The ratio of α at 1 kMc to its infinite frequency value $R/2Z_o$ is about 0.85. The ratio of the electrical length at 1 kMc to its infinite frequency value $\sqrt{LC}$ is about 1.25. The results stated in this paragraph are seen to be independent of the width of the loop conductor.

The lossless line theory developed earlier is now applied to predict the response of the deposited loop circuits to a distributed input step voltage. The step response is basically determined by the

infinite frequency values of Z_o, α and T. The resulting response indicates a lower limit to the frequency range of significance in determining the step response.

The line termination Z_r is a length of 50 Ω coaxial cable and so this situation corresponds closely to the case of an infinite termination impedance. Neglecting line losses, the overshoot of the output voltage is 96% and this peak value is attained in a time $2T$, i.e., 0.184 nsec. The attenuation of the transmission line results in transmission of about 60% of a signal along the line length. The peak value of the output voltage is expected to be about 60% of the value obtained for the lossless line, giving about 18% overshoot. The time taken to attain this peak value may be expected to be somewhat greater than 0.184 nsec.

On taking the time of rise to the peak value as one quarter of an equivalent sine wave, a frequency of 1.36 kMc is obtained. This value can be taken as a lower bound for frequencies of significance in determining the step response of the line. The value of $|Z_o|$ is much less than 50 Ω for frequencies above 1 kMc and so the line termination closely approximates an open circuit, independent of the large reactive component of Z_o at the lower end of the frequency range. The predicted response is now slightly modified to have a peak value overshoot somewhat in excess of 18% (about 23%, corresponding to an average value of α for frequencies above 1 kMc) and a rise time to peak value somewhat greater than 0.184 nsec (about 0.20 nsec, corresponding to an average value of T for frequencies above 1 kMc). The wide stand-

ard loop has the same attenuation and electrical length as the narrow standard loop, but has a much lower characteristic impedance. The response of the two loops is thus expected to be quite similar, with the wide loop having a slightly greater overshoot (26%), due to its lower characteristic impedance.

It is of interest to predict the value of loop resistance R_m which produces critical damping of the step response voltage. Since the overshoot of a lossless deposited standard loop is about 100%, then no overshoot may be expected in the output voltage, if the line attenuation exceeds 6 db. Using the infinite frequency value of α, the following values of R_m were calculated:

Narrow loop : $R_m = 1.48\ \Omega$

Wide loop : $R_m = 0.123\ \Omega$

Due to variation of line attenuation with frequency, the actual values of R_m may be expected to be somewhat larger.

The inductance of the loop on the brass ground plane varies significantly with frequency, being about 50% greater than the infinite frequency value, at a frequency of 1 kMc. The effect of this inductance variation can be examined by considering a loop having twice the infinite frequency value. (As shown already, this inductance value corresponds to a frequency of 0.21 kMc, which is a very wide lower frequency limit.) The infinite frequency values of this narrow line are

$Z_o = 1.52\ \Omega$

$\alpha = 3.16$ db

$T = 0.13$ nsec

The overshoot for the lossless line terminated in 50 Ω is 94%. With an attenuation factor of 69%, the overshoot becomes 35%. The time to peak voltage is about 0.28 nsec. As in the case of the standard loop, variation of α with frequency may be expected to result in a small percentage ($\approx 5\%$) increase in the overshoot.

Digital Computer Simulation of Deposited Loop Circuitry

Computer simulation of a length of transmission line was used to determine the detailed response of the deposited loop circuitries to various input signals.

An n-section finite difference model of a loop circuit with a total voltage waveform V induced uniformly along the line length, and having a termination Z_r (= 50Ω), is shown in Fig. 3.3a. The loop output voltage is the voltage developed across terminals A-B of the circuit.

The response of the above model to various input waveforms was determined by writing the (n + 1) loop equations of the system and solving these equations on a digital computer by means of a fourth-order Runge-Kutta integration scheme[12]. The number of sections used to represent the line is a compromise between the accuracy attained by the finite difference model, and computer running time which varies approximately as the square of the number of circuit loops.

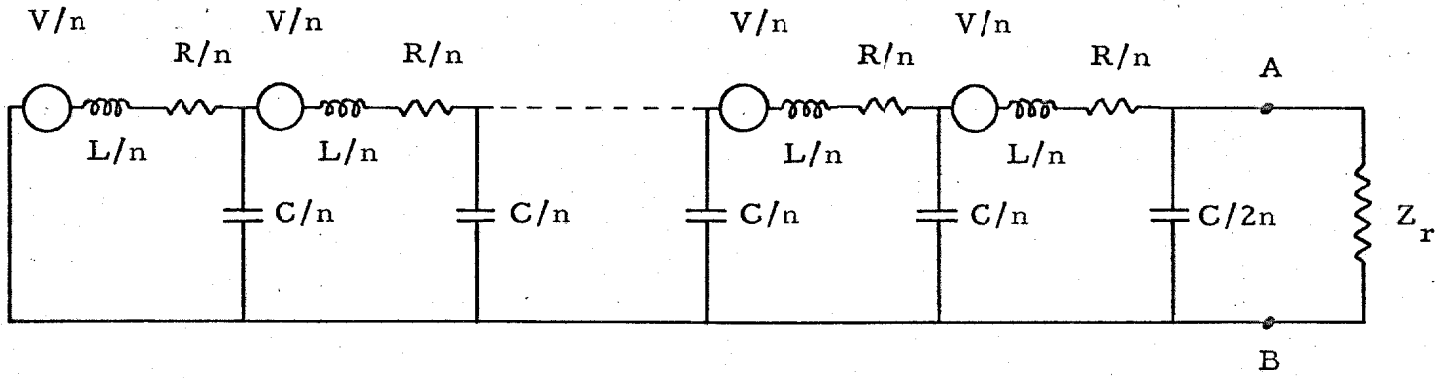

Fig. 3.3a. N-Cell Finite Difference Model for Terminated Transmission Line

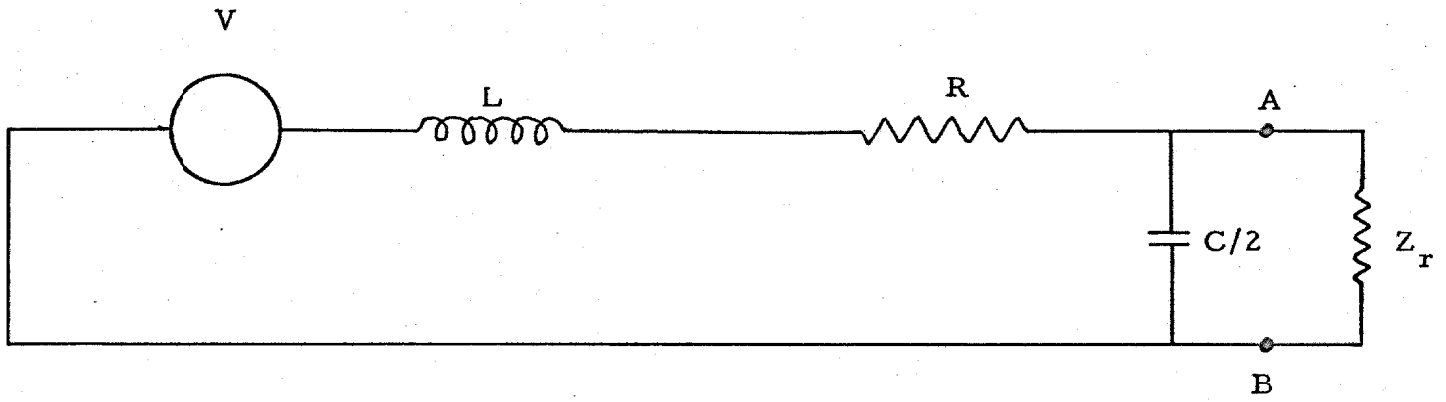

Fig. 3.3b. 1-Cell Finite Difference Model for Terminated Transmission Line

Step Response of Deposited Loop

The step responses of both 5-section and 1-section models for the narrow standard deposited loop are shown in Fig. 3.4. (The 1-section model is illustrated in Fig. 3.3b and is seen to have only half the loop capacitance.)

The good correspondence between the two results indicates that the 5-section model is a very good representation of the loop circuitry and that the 1-section model is a good lumped circuit approximation to this circuitry. Accordingly, the 5-section model was taken as being sufficiently accurate for all further calculations.

The responses of the two standard deposited loops were determined and found to be very similar. As predicted from the lower characteristic impedance of the wide loop, this loop output had more overshoot than the narrow loop output. The percentage overshoots of the two outputs were 27% and 31% and their common rise time to peak value was 0.20 nsec. These results are in good agreement with the results of the previous analysis, which predicted overshoots of 23% and 26% and a rise time to peak value of 0.20 nsec. Since the outputs of the wide and narrow deposited loops were very similar, and the difference was due solely to the lower characteristic impedance of the wide loop, only the narrow loop was considered in the subsequent analysis.

To investigate the effect of loop inductance variation with frequency, the step response of a loop having twice the standard inductance value was determined (this inductance corresponds to a frequency of

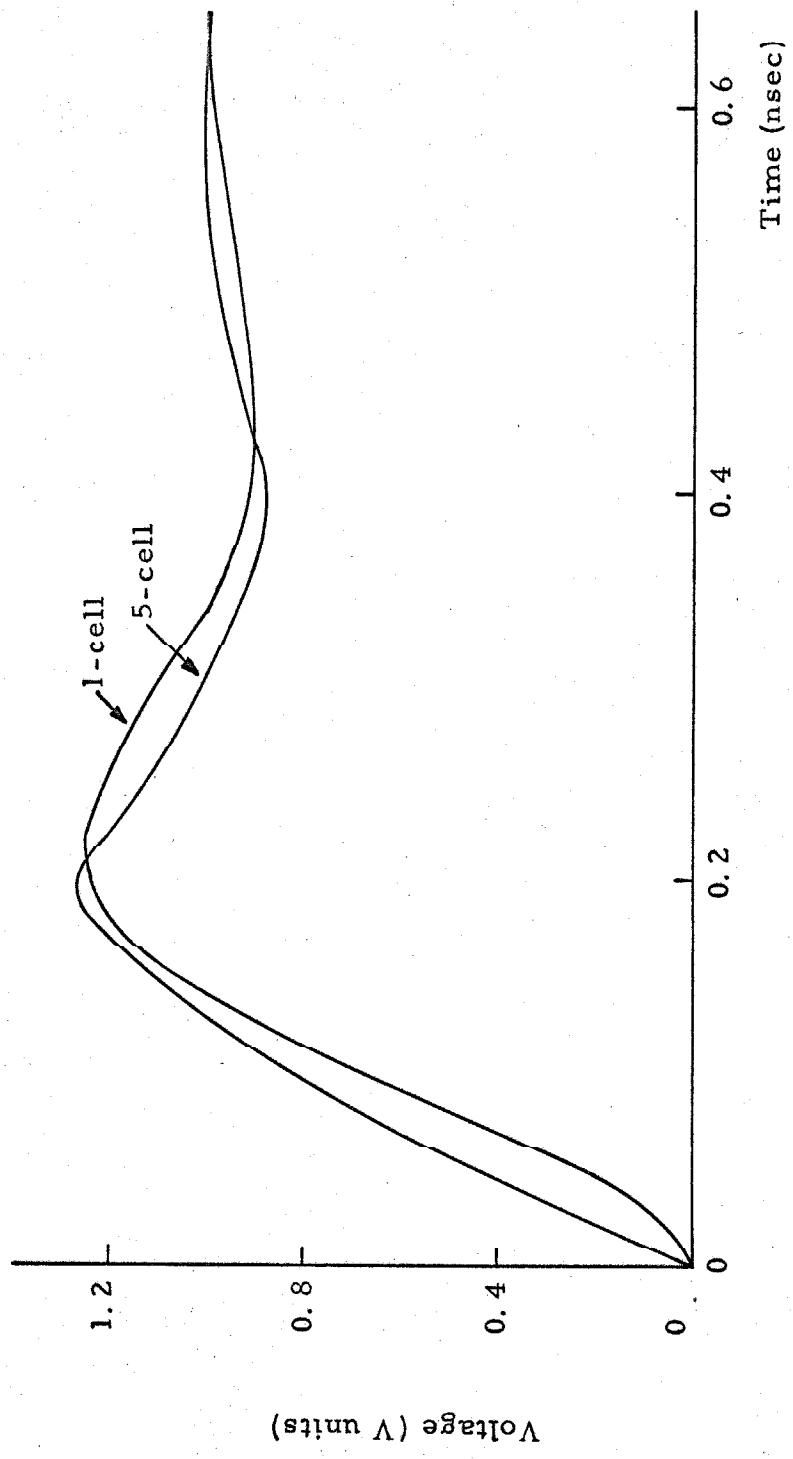

Fig. 3.4. Step Responses of 5-Cell and 1-Cell Models of Standard Deposited Loop (Narrow)

0.211 kMc, as shown earlier) and is shown in Fig. 3.5 together with the response of the standard loop. The rise time of this "twice-inductance" loop to its peak voltage is 140% of the corresponding time for the standard loop, due to its electrical length being greater by a factor of $\sqrt{2}$. The overshoot of the "twice-inductance" loop is greater than that of the standard loop, since, although it has a higher characteristic impedance, (lossless overshoot = 94%) the damping of the line is reduced by a factor of $\sqrt{2}$. For values of loop resistance greater than 5 Ω, the output voltages of the two loops are practically identical, as can be seen by inspection of the curves of Fig. 3.5. Thus, variation of line inductance with frequency becomes unimportant at high values of line resistance.

The effect of loop resistance variation was investigated for the narrow standard loop. Step responses for values of loop resistance varying from 1.11 to 20 Ω are shown in Fig. 3.6. The final value of the output voltage is determined by the ratio of the termination resistance to the total series resistance of the loop and termination. When the loop resistance is sufficiently large, no overshoot occurs in the output voltage. A curve is included, for the case where the line attenuation is 6 db (R_m = 1.48 Ω) and the previous analysis predicted critical damping of the output voltage. It is seen that the amount of overshoot present is still quite appreciable. Using the value of loop resistance corresponding to critical damping of the 1-section model ($R_{cr} = 2\sqrt{2}\sqrt{L/C}$ = 3.04 Ω) a much better approximation to a critically damped output voltage was obtained. This result is due to the close

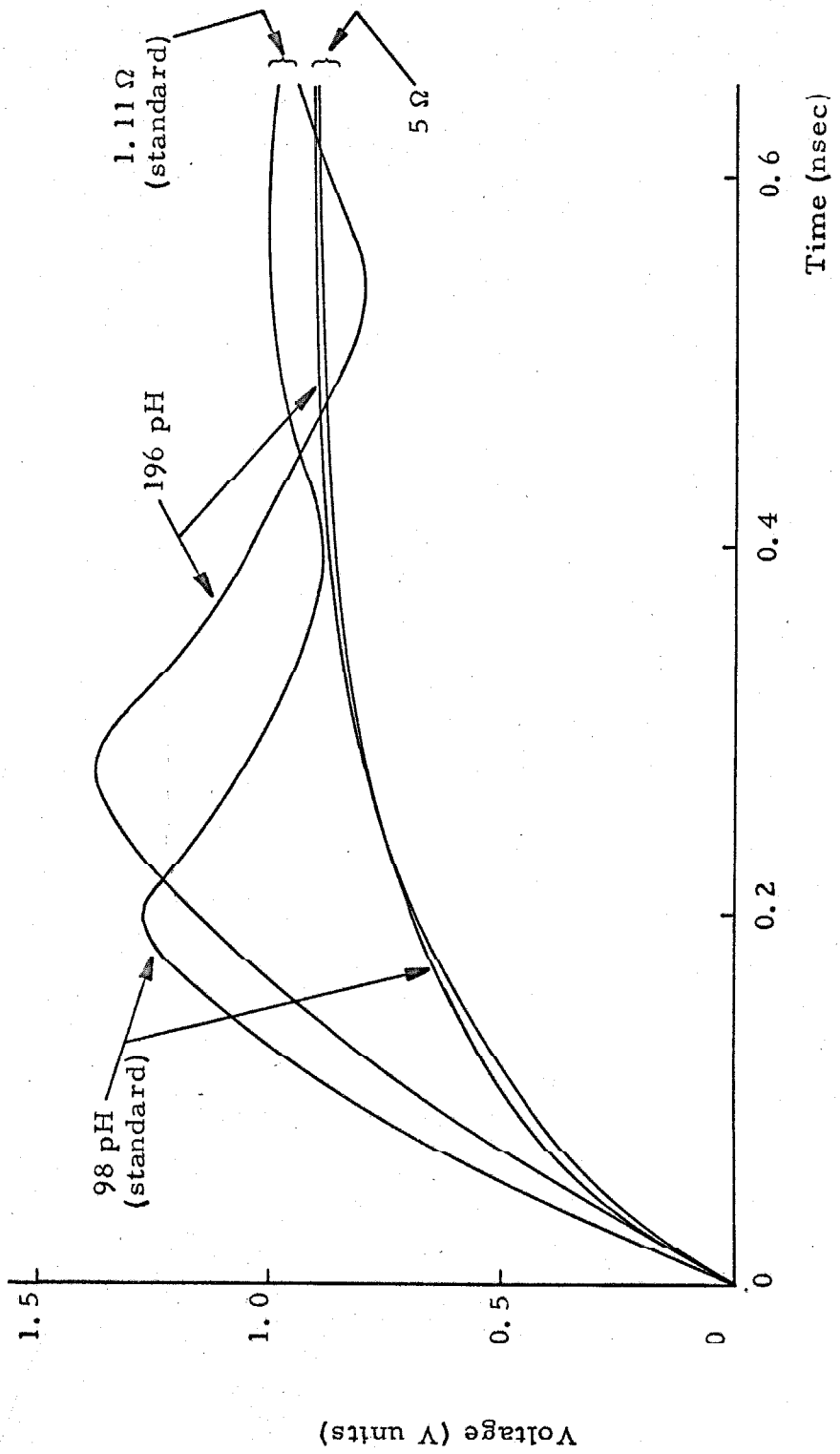

Fig. 3.5. Effect of Inductance on Narrow Loop Step Response

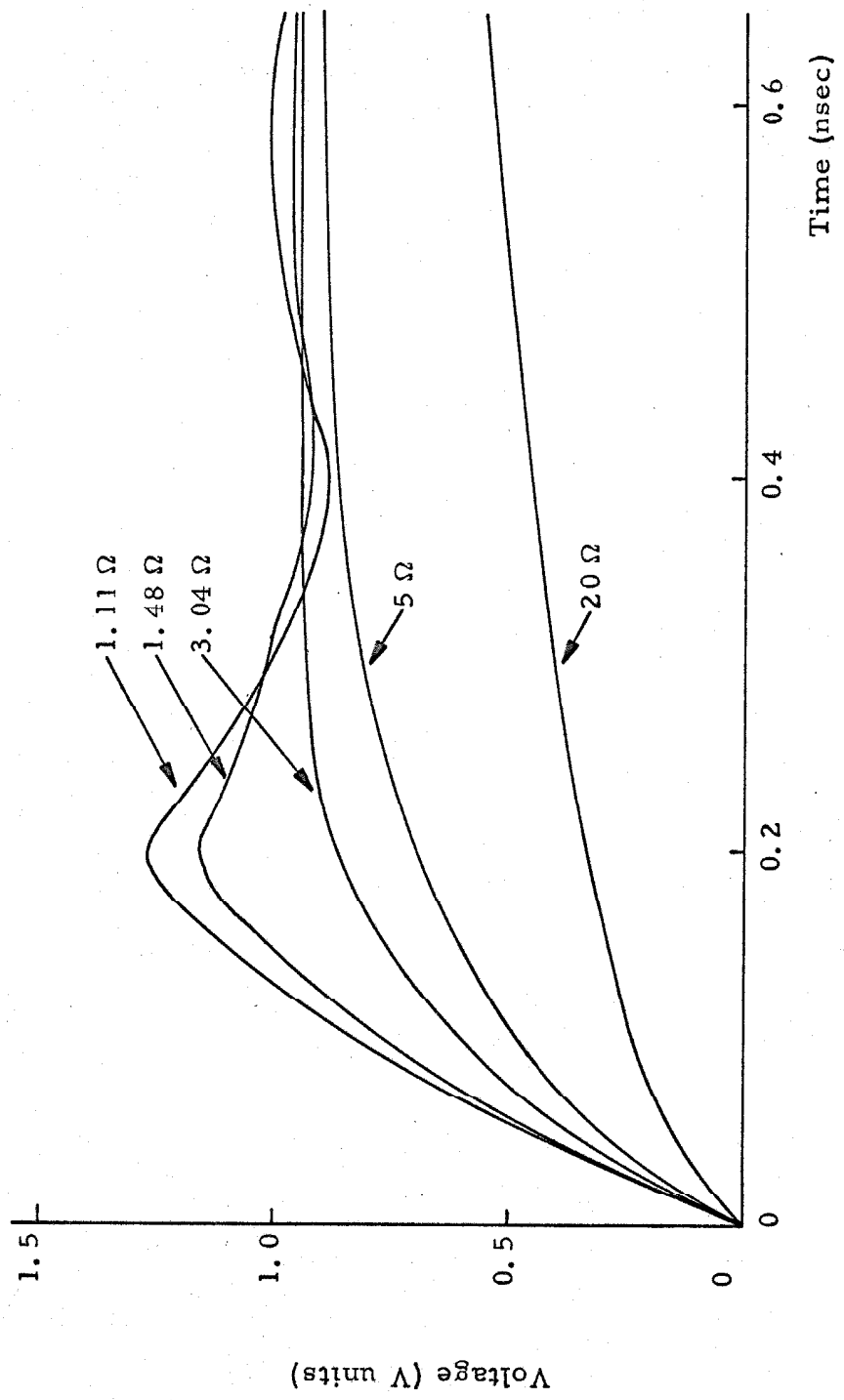

Fig. 3.6. Effect of Resistance on Narrow Loop Step Response

similarity of the responses of the 1-section and 5-section models.

The inductance and capacitance of the deposited loop depend on the separation of the loop conductors. The inductance varies directly as this distance, while the capacitance varies inversely as this same quantity. Thus, the effect of loop conductor separation can be determined by obtaining the step responses of a number of deposited loop circuits, having various L and C values but with LC products equal to that for the standard loops. In Fig. 3.7, step response curves are shown for loop circuits having inductance values varying from 0.1 to 10 times the standard inductance value, with the loop resistance held constant at its standard value. As the inductance increases the step response of the loop varies from a heavily damped to a lightly damped condition. The rise time to peak value, when overshoot is present, is practically independent of the value of L.

These results can be interpreted by observing the variation of the infinite frequency characteristic impedance Z_o ($= \sqrt{L/C}$) and attenuation constant $R/2Z_o$ with conductor separation. The value of Z_o varies from 0.1075 Ω to 10.75 Ω, as L increases through the range of values. The variation of Z_o has little effect on the response of a lossless line, when $Z_r >> Z_o$. At the higher values of Z_o, the lossless overshoot of the line is decreased somewhat (67% lossless overshoot for Z_o - 10.75 Ω). However, the decrease of attenuation as Z_o increases is the main factor which varies the response of the loop. The infinite frequency electrical length of the line $\sqrt{LC}$ is independent of the conductor separation and thus the lossless line theo-

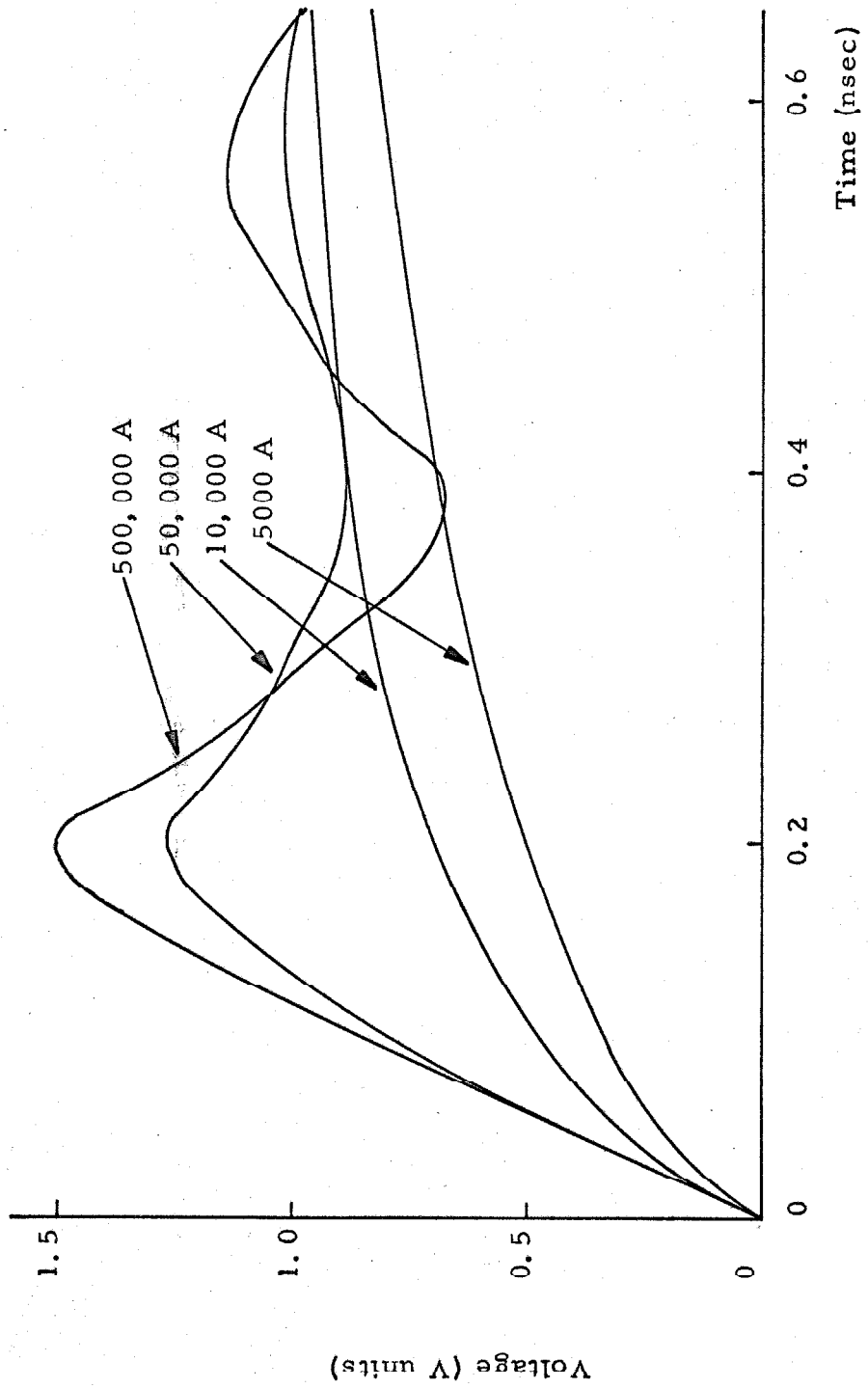

Fig. 3.7. Effect of Conductor Separation on Narrow Loop Step Response

ry predicts a constant rise time to peak value, for all values of conductor separation.

Ramp and Triangular Responses of Deposited Loop

The response of the deposited loop to the switching signals obtained from magnetic thin films was studied more fully by determining the response of the narrow standard loop to the ramp and triangular waveforms depicted in Figs. 3.8a and 3.9a, respectively.

The response of the deposited loop to various ramp inputs having a rise time τ_1 to final value varying from 0 to 1 nsec, is shown in Fig. 3.8b. For $\tau_1 = 0$ nsec, corresponding to a step input, the overshoot of the output voltage is quite large (28%) and the time to peak value is determined by the electrical length of the loop. As τ_1 increases, the overshoot decreases and the time to peak value becomes determined chiefly by the value of τ_1. For $\tau_1 > 0.5$ nsec, the output voltage has little or no overshoot and follows the input voltage quite closely.

The response of the deposited loop to various triangular inputs, varying in duration τ_2 from 1/8 nsec to 1 nsec, is shown in Fig. 3.9b. When τ_2 is small, the output waveform is characterized by a much reduced amplitude, increased width, and overshoot in its trailing edge. As τ_2 increases, the output voltage follows the input more closely, until, for $\tau_2 > 1$ nsec, the two waveforms are quite similar. It may be noted that, as τ_2 increases, the overshoot in the trailing edge first increases, reaches a maximum of about 25% when $\tau_2 \approx 1/4$ nsec, and then decreases towards zero as τ_2 increases still further.

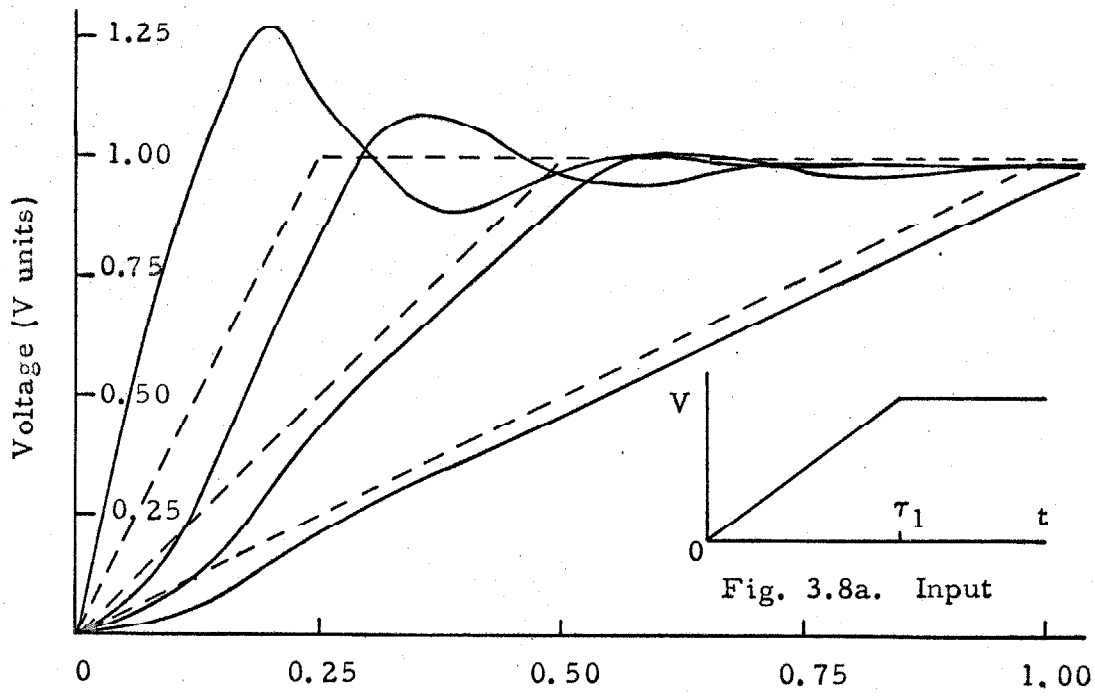

Fig. 3.8a. Input

Fig. 3.8b. Ramp Response of Standard Narrow Loop

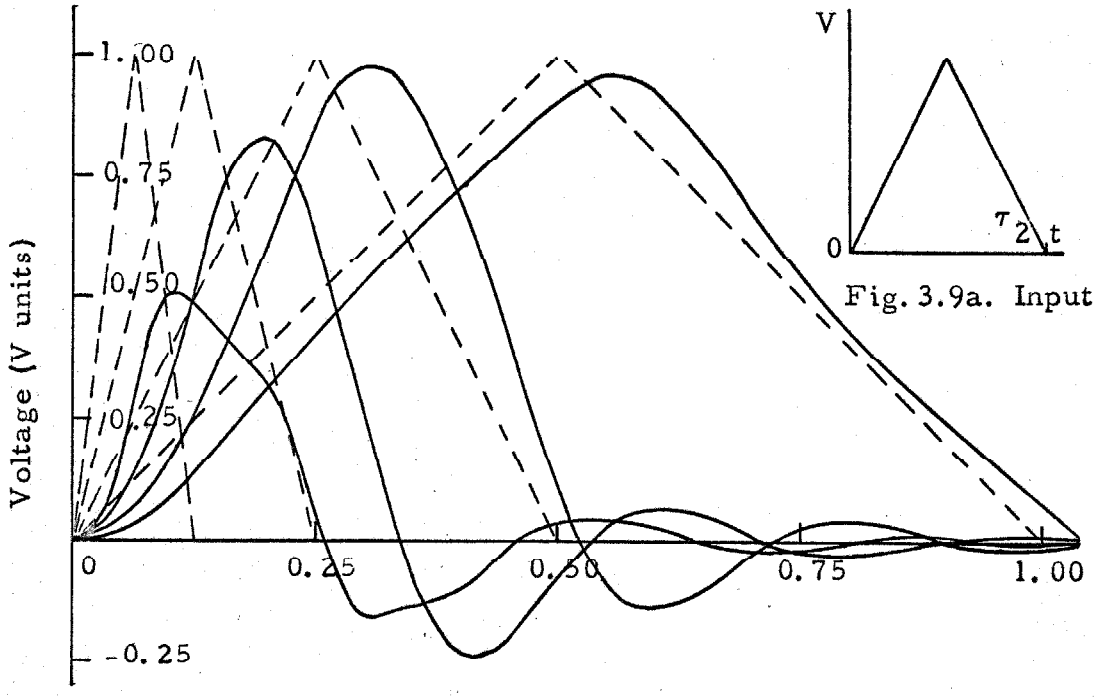

Fig. 3.9a. Input

Fig. 3.9b. Triangular Response of Standard Narrow Loop

Maximum Distortion of Film Switching Signals by Deposited Loop Circuitry

The fastest signals encountered in thin film switching have a duration of about 1 nsec. The ramp and triangular input analyses just presented indicate that the effect of the standard loop circuit transfer function on such signals is small, although not entirely negligible. However, in the film assemblies fabricated, the deviation of loop parameters from their standard values was quite large. From the calculations already made, it can be predicted that the effect of loop circuitry will be largest for the case of a low impedance line with large series resistance. In the fabricated film assemblies, the smallest loop conductor separation obtained was about 25,000 A (50% of standard separation), thus giving a line with characteristic impedance equal to about half the standard value. The largest loop resistance measured was about 10 Ω. Accordingly, the responses of a loop having L = 49 pH, C = 170 pF, and R = 10 Ω, to step, ramp and triangular inputs, were determined. These curves, shown in Fig. 3.10, indicate that such a loop circuit modifies fast switching signals quite considerably, giving output signals having much longer rise times than the input signals. The triangular response has a much longer decay time than its rise time to peak value. This long decay time may be expected to appear in the response of this circuit to all fast signals.

External Loop Analysis

The methods of analysis used to determine the response of the deposited coupling loop circuits can be applied to predict the response

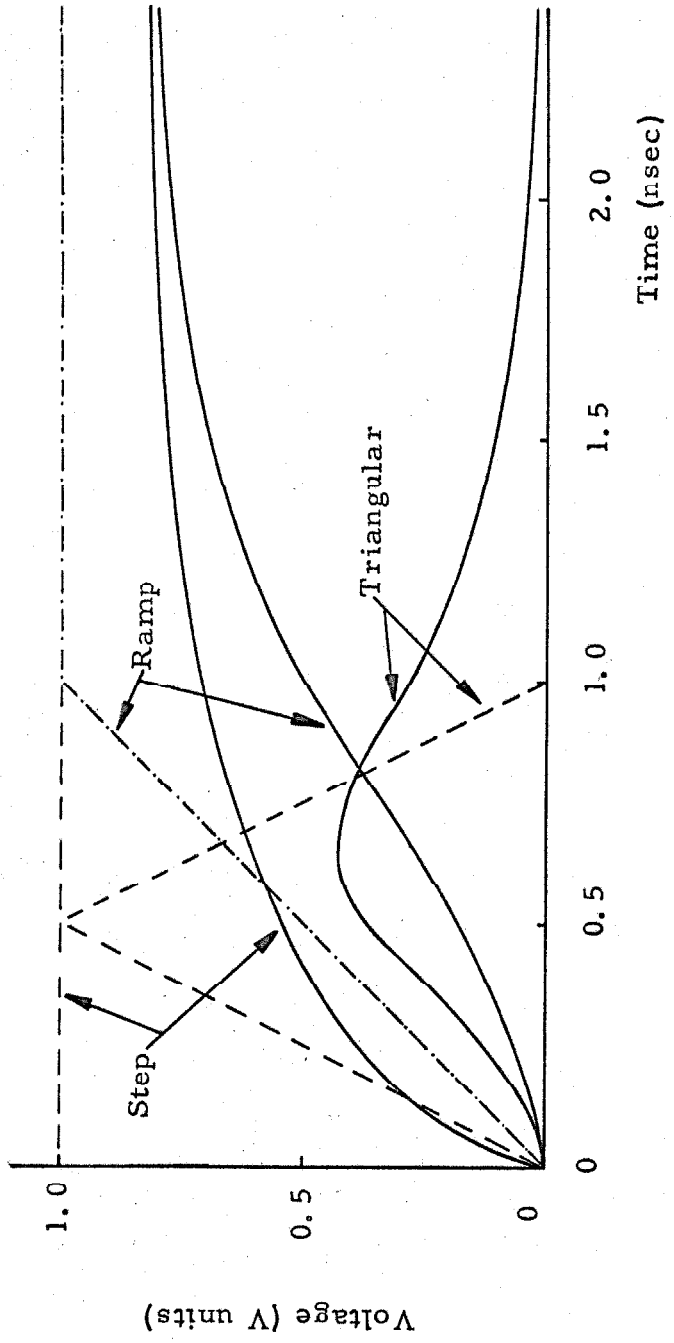

Fig. 3.10. Maximum Film Signal Distortion by Deposited Loop Circuitry

of the external loop circuit to signals induced in that loop. This loop circuit has the form of a coaxial transmission line, shorted at one end and terminated in a 50 Ω resistive load at the other end (see Fig. 6. 4). For purposes of analysis, it is assumed that the induced voltages are distributed uniformly along the entire length of the loop conductor.

The D. C. resistance of the copper loop conductor has a theoretical value of 0. 044 Ω (the measured value is 0. 119 Ω, the higher value being due to contact resistance, loop ground plane return resistance, etc.). However, at frequencies representative of high speed thin film switching, the value of the skin depth δ of copper is 1×10^{-4} cm which is about 1% of the conductor diameter and so a higher resistance is obtained. This resistance can be calculated as the resistance of a length of conductor, having width equal to the circumference of the conductor and thickness equal to the value of δ . The resistance, corresponding to a frequency of 4 kMc, is about 1 Ω and this value was chosen as the standard loop resistance.

Using the coaxial capacitor formula, the capacitance of the external loop was calculated to be 0. 97 pF. This value assumed an air dielectric for the loop,neglecting the small increase in capacitance due to a thin layer of enamel insulation on the center conductor.

At low frequencies, the loop inductance is given by the sum of the internal and external inductance of the loop conductor and has a value of 5890 pH. At high speed switching frequencies, δ is much smaller than the conductor diameter so that flux penetration into the loop conductor is negligible. Thus, at these frequencies, the loop in-

ductance is decreased to a value of 4860 pH, which is chosen as the standard loop inductance.

The standard parameter values of the external loop are tabulated as follows (assuming zero shunt conductance for the loop):

R	1 Ω
L	4860 pH
C	0.97 pF
G	0

The characteristic impedance Z_o and the propagation constant $\gamma = \alpha + j\beta$ of the coaxial line are next calculated. (The expressions for Z_o and γ are given by Eqns. 3.1 and 3.2.) Since $R << L\omega$ for frequencies above 1 kMc, then, in this range, the values of Z_o and γ reduce to

$$Z_o = \sqrt{L/C}$$

$$\gamma = R/2\, Z_o + j\omega \sqrt{LC}$$

These equations yield

$$Z_o = 50 \sqrt{2} = 70.7\ \Omega$$

$$\gamma = 0.0071 + j\, 0.069 \cdot 10^{-9} \omega$$

Thus, the line attenuation α and electrical length T are given by

$$\alpha = 0.061 \text{ db}$$

$$T = 0.069 \text{ nsec}$$

The very low value of line attenuation indicates that the line response closely follows the response of a lossless line, with the actual value of line resistance being unimportant. Since the resistive termination ($Z_r = 50\,\Omega$) has a lower value than Z_o, the step response of the line to a distributed input has no overshoot. The output voltage rises to 83% of its final value in time $2T = 0.138$ nsec and to 97% of this value in time $4T = 0.276$ nsec. The 10% - 90% rise time is thus about 0.20 nsec.

The values of loop inductance and capacitance may differ somewhat from their calculated values due to possible divergence of the loop conductor and shield inner diameters from their nominal values. This factor has no effect on the electrical length $\sqrt{LC}$ of the line and so the actual response of the line is considered to be bounded by the response of two lines, having the same LC product as the nominal line but with inductance and capacitance values varying by ratios of $\sqrt{2}$ from their nominal values. These two lines have characteristic impedances of $50\,\Omega$ and $100\,\Omega$. The step response of the $50\,\Omega$ line rises linearly to its final value in time $2T = 0.138$ nsec, giving a 10% - 90% rise time of 0.11 nsec. The step response of the 100Ω line rises to 67% of its final value in time $2T = 0.138$ nsec and to 89% of this value in time $4T = 0.276$ nsec, giving a rise time of about 0.25 nsec. Thus, the rise time of the external loop is seen to depend quite strongly on the characteristic impedance of the loop circuit but may be assumed to be less than 1/4 nsec.

The step, ramp and triangular responses of the external loop were determined by computer solution of a 5-section finite difference model for the loop. Responses were determined for the 50 Ω and 100 Ω lines, and these responses were considered to give bounds to the response of the nominal line.

The response curves are shown in Fig. 3.11. The ramp input has a total rise time to peak value of 1 nsec, while the total duration of the triangular input is also 1 nsec. The step responses are seen to be practically identical with the lossless line predictions, the slight overshoot in the 50 Ω response being due to inaccuracy of the finite difference model. The ramp and triangular responses of the two lines are quite similar, with the 100 Ω line having a slightly slower response, as may be expected from the step response curve.

Conclusions

It has been shown that the circuit parameters of the deposited and external loops are quite different. Regarded as transmission lines, the standard narrow deposited loop has a low impedance (≈1Ω) and a significant attenuation (≈ 5 db), while the external loop has a high impedance (≈ 70 Ω) and negligible attenuation (≈ 0.06 db). The pulse responses of these loops, when terminated in a 50 Ω resistive impedance are compared in Fig. 3.12. It can be seen that the response time of the deposited loop is always less than that of the external loop. In addition, the deposited loop output possesses overshoot, while the external loop output shows an overdamped characteristic. Figure 3.12 also indicates that, for film switching pulses wider than 1 nsec, the distor-

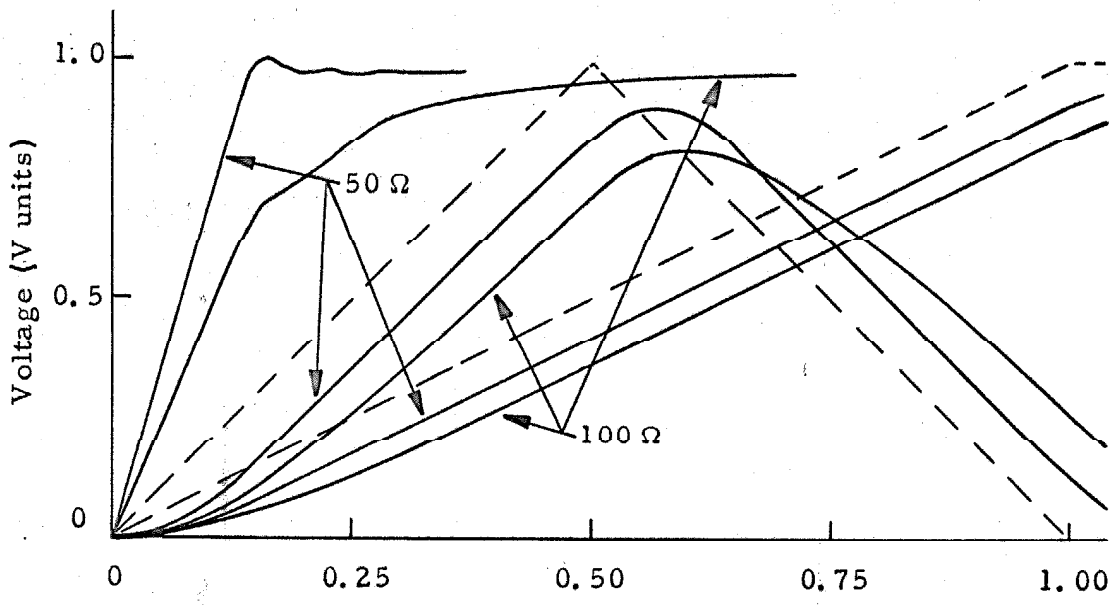

Fig. 3.11. Step, Ramp and Triangular Responses of 50 Ω and 100 Ω External Loops

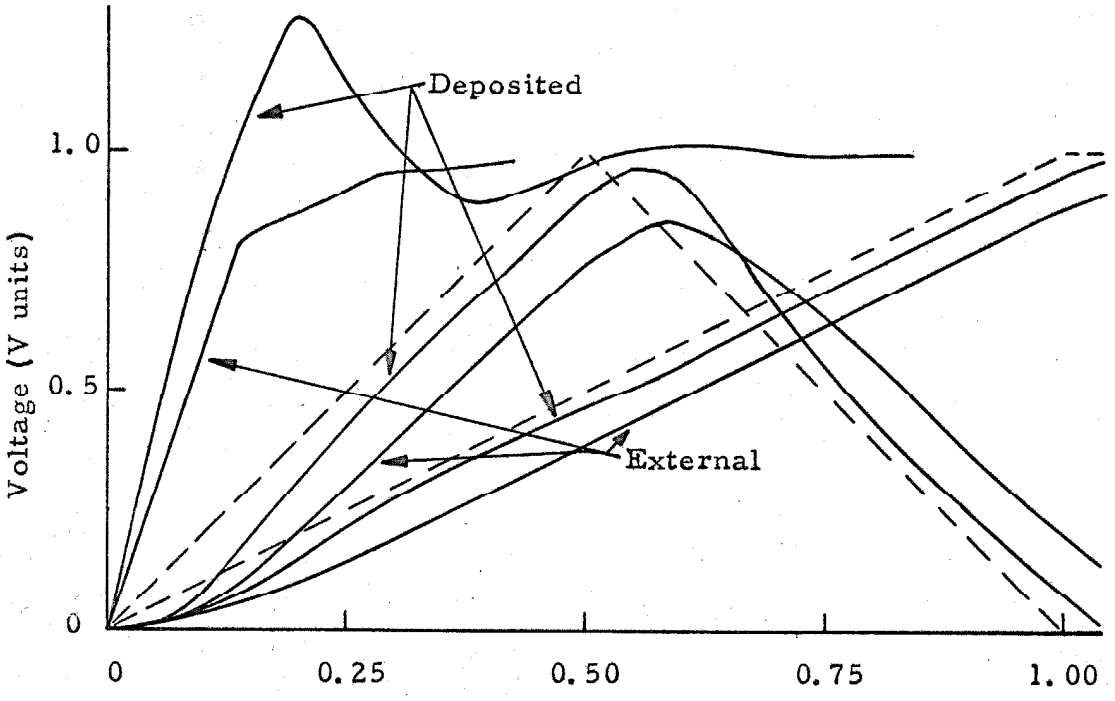

Fig. 3.12. Comparison of Deposited and External Loop Pulse Responses

tion due to the loop circuitry is quite small. However, the deposited loop study indicates that deposited loops with resistance or capacitance values significantly larger than the standard loop values will have responses which are much slower than the external loop response and possess no overshoot. The distortion of a 1 nsec wide pulse in these loops is expected to be quite large.

Experimental film switching results are in agreement with the above predictions. In general, the switching time measured at the deposited loop output was less than the corresponding time measured at the external loop output. When overshoot was present in the observed switching waveforms, it was usually much larger in the deposited loop signal than in the external loop signal (overshoot in the external loop signal was attributable to overshoot present in the film switching waveform itself). However, some cases were also observed where the deposited loop signal had less overshoot and longer rise time than the external loop signal. It is concluded that the external loop signal is always quite similar to the signal induced in its loop and that this result also holds for the deposited loop except when the loop attenuation is significantly greater than for the standard loop.

The circuit analyses have been based on transmission line representations of the loops. However, it has also been indicated that the lumped circuit of Fig. 3.3b is a good approximation to the distributed configurations. This circuit can be used, with good accuracy, to calculate the properties of a loop circuit when the loop electrical length is short compared to the width of the input pulse.

IV INTERACTION OF MAGNETIC FILM AND CONDUCTING COUPLING LOOP

A conducting loop coupling a magnetic thin film may be used as a read-out loop which senses the output of the switching film or a drive loop which applies bias or switching fields to change the state of the film. In the first case, minimal film-loop interaction is desired since interactions only tend to slow the switching of the magnetic film. In the second case, however, the inserted loop currents produce a drive field for the film so that some film-loop interaction is required. Reference to Fig. 1.1 indicates that film-loop interactions arise from eddy current fields and circulating current fields. The importance of these fields in modifying film switching was studied by calculations made with the standard film assembly dimensions, shown in Fig. 6.1, and by experiments made on film assemblies. The experiments also demonstrated the high speed read and drive properties of deposited loops.

Eddy Current Field

Consider first a magnetic film situated above a plane conducting sheet with the plane of the film parallel to the conductor surface. When the film changes the direction of its magnetization, eddy currents are set up in the conducting material. The resulting magnetic field, produced in the region of the film, opposes the motion of the film magnetization. The field of the eddy currents is maximized by assuming a semi-infinite conducting slab, occupying the entire lower half-plane and an instantaneous change of film magnetization between the two directions. Initially only surface eddy currents appear and their field

above the conductor can be represented by the net field of two image films situated as indicated in Fig. 4.1a. These two films have magnetization directions which are antiparallel to the initial direction (1) and parallel to the final direction (2) of film magnetization. Subsequently, as the eddy currents penetrate the conducting slab, the image films move away from the conductor surface in the -z direction. In the case of a very thin sheet of conducting material, the images recede with a uniform velocity[13] $2\zeta/\mu_\nu$ where ζ = area resistivity of the material.

The external field of each image film can be estimated by the use of the circular film equation[14]

$$H \approx \pi^2 (t/d) M \quad , \qquad 4.1$$

where H = average planar magnetic field (Oe) outside of the film due to its magnetization M (Oe), and t/d = film thickness-to-diameter ratio. This equation describes the average field in the space approximately defined by the film area and a distance of one-tenth the film diameter on either side of the film plane, and also gives the magnitude of the average longitudinal demagnetizing field within the film[15].

An upper bound to the magnitude of the image field produced by switching of the standard film (0.36" x 0.45" x 1500A) from the easy axis to the hard axis, can be obtained by inserting the minimum film surface dimension (0.36") into Eqn. 4.1, as the diameter of an equivalent circular film. Using the value of M for 17-83 Permalloy ($M = B_s/4\pi = 750$ Oe[16]), a field value of 0.17 Oe is obtained. This

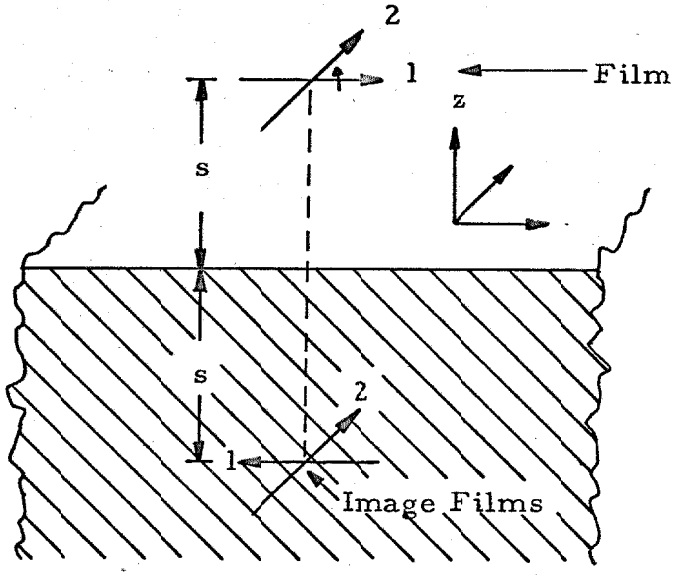

Fig. 4. 1a. Eddy Current Field Due to a Semi-Infinite Conductor

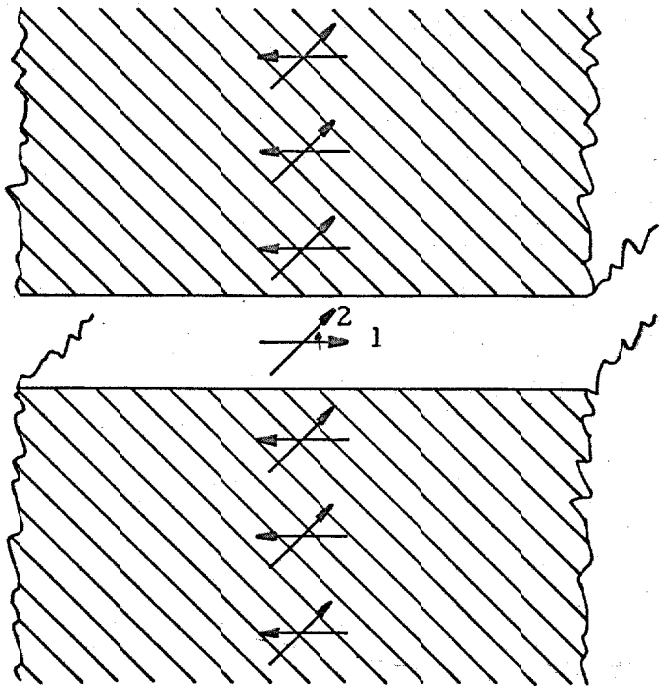

Fig. 4. 1b. Eddy Current Field Due to Two Semi-Infinite Conductors

field acts at an angle of 45° to the easy axis. It is effective out to a distance of at least 10^{7} A from the plane of the image film and so it acts on the magnetic film. The effect of this field on film switching speed is not very large, since this field is small compared to the film drive and anisotropy fields. The above result indicates that the presence of a conductor on one side of a magnetic film has a small effect on the film switching speed, provided that the film demagnetizing field, calculated by means of Eqn. 4. 1, is small compared to the film drive and anisotropy fields.

When the conducting plane is of infinite extent, the eddy current field is independent of the conductor thickness unless this dimension is very small. In this case, the image film recedes appreciably during the switching time and the eddy currents decay correspondingly. It is of interest to determine the decay rate for a 4000 A thick aluminum plane which represents a large deposited loop conductor. This plane may be considered as a very thin conducting sheet since the skin depth of aluminum at a frequency of 1 kMc, which is representative of nanosecond switching, is 26, 800 A. Application of the image recessional velocity formula gives a value of 1.12×10^{6} A/nsec. Since this field is effective out to a distance of about 10^{7} A from the image film and the initial separation of the magnetic film and its image is about 5×10^{4} A, the image field may be considered to be fairly constant for a period of about 10 nsec.

Consider next a magnetic film, situated between two plane conducting sheets, with the plane of the film parallel to both conductor

surfaces. As before, the field of the eddy currents is maximized by assuming an instantaneous change of film magnetization between the two states, and semi-infinite conducting slabs, as shown in Fig. 4.1b. In this case, the eddy current field is seen to be represented by the field of the infinite set of image films, spaced along the z-axis with separation equal to the distance between the conductor surfaces. Since the fields of the images are additive, the total eddy current field acting on the magnetic film can be quite large.

An estimate of this field was made for a film assembly with standard dimensions. With a conductor separation of 5×10^4 A and an external field, which was constant out to a distance of 10^7 A from the plane of each image, about 400 image films were effective in the calculation of the eddy current field. Since each image film had an external field of 0.17 Oe, the total was about 70 Oe. A field of this magnitude would prevent film switching in the nanosecond range, except with the use of extremely large drive fields. The eddy current decay in 4000A thick conductors in a period of 1 nsec decreases the average eddy current field by about 5% and so much thinner conductors are required before the average field becomes insignificant.

The field calculations just presented set upper bounds to the eddy current fields acting on a magnetic film situated in the vicinity of conducting planes. Since these eddy current fields have been calculated for conductors of infinite extent, the results obtained are most applicable to cases where the actual conductors are large in area compared to the magnetic film. Now consider the case where the two con-

ductors are each of smaller area than the magnetic film and are placed so that the film edges are not covered by either conductor. The conductors are situated close to the magnetic film surface and have thicknesses which are small compared to the film surface dimensions. If it is assumed that, during switching of the film, flux enters and leaves the magnetic material only at the film edges, no eddy current field results, since no flux change occurs in the two conductors. On replacing one conductor by an infinite plane, an eddy current field similar to the case of a magnetic film situated over an infinite plane, is obtained. When both conductors have areas somewhat larger than the magnetic film so that all film edges are covered, significant eddy currents may be expected to occur, since the flux through the conductors tends to change during switching. However, due to the finite extent of the conductors, the field produced will be less than that calculated for the infinite plane conductors. In general, eddy current effects may be expected to depend quite strongly on the fraction of the film perimeter covered by the adjacent conductors, i. e., on the reluctance of the various film flux closure paths during the switching process.

Circulating Current Field

Excitation of the passive network, consisting of the deposited loop circuitry and its associated termination, by the induced loop voltage results in a circulating loop current. The effect of this current on film switching was estimated by a study of the average field produced in a strip line with zero series impedance and shunt admittance which is shorted at one end and terminated at the other end in a resistive or

capacitive load.

A. Resistive Load

At any time t , the instantaneous magnetic strip line field (amp-turns/m) is

$$H = V/Rw$$

where V = induced voltage (volts)

R = loop resistance (Ω)

w = strip line width (m)

Thus,

$$H(0\text{-}T) = \frac{1}{T}\int_{o}^{T} \frac{V}{Rw}\, dt = \phi_T / T\, Rw \qquad 4.2$$

where $H(t_a\text{-}t_b)$ = average magnetic field (amp-turns/m) during time interval $t_a \leq t \leq t_b$.

$$= \frac{1}{(t_b - t_a)} \int_{t_a}^{t_b} H\, dt \ .$$

ϕ_T = total flux change (webers) of magnetic film in direction of loop axis during the switching process

T = <u>total</u> switching time (sec), i.e.,

$\phi = 0$ @ $t = 0$

$\phi = \phi_T$ @ $t = T$ with no further change in flux occurring after this time.

From Eqn. 4.2 it can be seen that the average resistive current field is inversely proportional to the switching time of the film. Since the resistor dissipates energy continuously during switching, the instantaneous field H always opposes the change in film magnetization. The value of H(0-T) gives a measure of the total slowing effect of the loop current during the switching process.

B. Capacitive Load

At any time t , the instantaneous magnetic strip line field (amp-turns/m) is

$$H = \frac{C}{w} \frac{dV}{dt}$$

where C = loop capacitance (farad) .

Thus

$$H(0\text{-}T) = \frac{C}{wT} \int_0^T \frac{dV}{dt}\, dt = \frac{C}{wT} [V(T)-V(0)] = 0 \qquad 4.3$$

The average capacitive current field is identically zero and, as a first approximation, capacitive loading should have no effect on film switching. This result is due to the lossless character of a capacitor, which slows film switching but stores up energy in the initial stages of the switching process when dV/dt is of one sign, and then speeds film switching by releasing this energy when dV/dt is of opposite sign. However, due to the nonlinear response of a magnetic film to magnetic fields, it may be expected that capacitive loading is accompanied by some net slowing of the film switching. The average value of the mag-

netic field during the period in which dV/dt is of one sign may be used as a measure of the expected slowing effect of the loop currents.

Let

$$dV/dt \geq 0 \text{ , for } 0 \leq t \leq t_1$$

$$dV/dt \leq 0 \text{ , for } t_1 \leq t \leq T \text{ ,}$$

then

$$H(0\text{-}t_1) = \frac{C}{wt_1} \int_o^{t_1} \frac{dV}{dt}\, dt$$

$$= \frac{C}{wt_1} V_m \qquad 4.4$$

and $$H(t_1\text{-}T) = - \frac{C}{w(T\text{-}t_1)} V_m \qquad 4.5$$

where V_m = maximum output voltage of the magnetic film.

Assuming an invariant waveform, then $1/V_m$, t_1 and $(T\text{-}t_1)$ are proportional to T and so $H(0\text{-}t_1)$, $H(t_1\text{-}T)$ are proportional to $1/T^2$. The above average capacitive current fields are then inversely proportional to the square of the film switching time.

The average circulating current fields corresponding to total transverse switching times of 1 nsec were estimated for the film assemblies depicted in Fig. 4.2. These assemblies, having loop conductors covering the entire film area, were assumed to have standard layer sizes and thicknesses (see Fig. 6.1). Thus the wide loop standard parameter values calculated in Section III, were used in the calculations

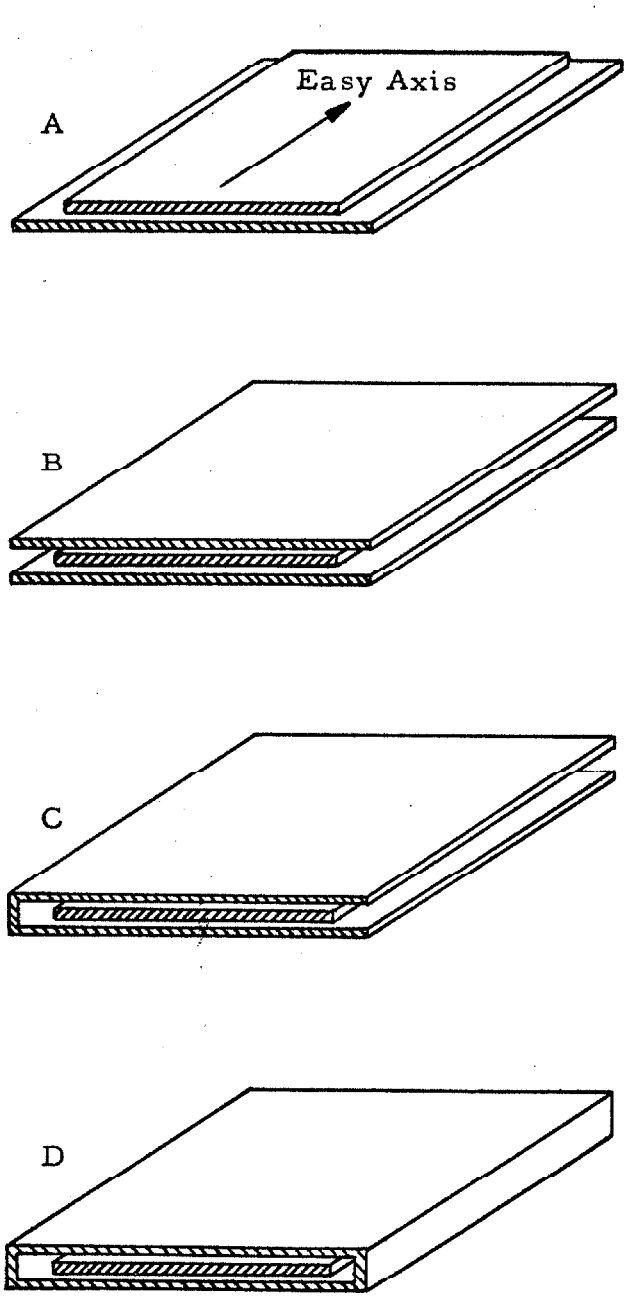

Effective Loop Fields
(1 nsec transverse
switching time)

0 Oe

0.4 Oe

1.7 Oe

12 Oe

Fig. 4.2. Film Assembly Loop Loading

(except that the resistance value was doubled to account for the two loop conductors). The effective field values, which were calculated in the following manner, are shown in Fig. 4.2.

The loop current of assembly D is independent of the loop capacitance since the voltage remains zero at all points of the line at all times. Due to the small L/R time constant (L/R = 0.045 nsec), the line was considered as a perfect voltage source loaded by the series resistance of the two loop conductors. Substituting the appropriate values of T, R, w and ϕ_T (using M = 750 Oe[16]) into Eqn. 4.2, the value of the average loop field H(0-T) was calculated as 12 Oe.

Due to the short electrical length (0.1 nsec) and small RC time constant (RC = 0.19 nsec) of the loop, the coupling loop circuit of assembly C was considered as a perfect voltage source, loaded by a capacitance C_t($C_t = C/2$, as indicated in Fig. 3.3b). Using Eqns. 4.4 and 4.5 and assuming a switching waveform having the form of a half-sine wave, the values of the average fields were obtained as $H(0\text{-}t_1) = -H(t_1\text{-}T) = H(0\text{-}T/2) = \pi C \phi_T / 2w\, T^2 = 3.5$ Oe. Since the average field during the complete switching time is zero, the effect of the capacitive current field is less than the value of H(0-T/2) indicates. The effective average field (H_e) was assumed to be of the order of 50% of this value and so $H_e \approx 1.7$ Oe.

Due to symmetry of the voltage distribution, the mid-point of the loop in assembly B remains at zero potential. Each half of assembly B can be considered in the form of assembly C, with voltage and capacitance values which are each 50% of the corresponding quantities

of assembly C. The effective average field of assembly B is thus about 0.4 Oe. For assembly A, which has no associated loop circuitry, the average field is zero.

By neglecting eddy current fields, the loop field values just calculated can be used to predict the relative effects of various loop circuits on the film switching time. The films are assumed to have an H_K of 3 Oe, and to be driven by a transverse field of 6 Oe. For assembly A, which has no loop field, this drive field results in a switching time of about 1 nsec (isolated film switching time). For assembly D, the large (12 Oe) easy axis loop field calculated for a 1 nsec switching time, indicates that the switching time with a 6 Oe drive field will be much greater than 1 nsec. Assuming that the easy axis field does not exceed the drive field, then, since this loop field varies inversely with the switching time, a switching time of at least 2 nsec may be expected. The smaller easy axis fields of assemblies B and C are expected to have correspondingly smaller effects on the switching time with the switching time of assembly B being quite close (within 10%) to the isolated film switching time.

Experimental Study of Film-Loop Interaction

Various experiments were performed to study the film-loop interaction process. In addition to verifying some of the predictions of the theoretical study just presented, these experiments also yielded some additional information about the role of the average loop fields in the switching process and about the effect of capacitive loading on film switching time.

The first experiment performed was a comparison of the switching times of a set of assemblies having the configurations shown in Fig. 4.2. The assembly ground plane (i.e., the loop conductor common to all four assemblies) faced the test strip line ground plane but was not in contact with it. The films with an H_K of 4 Oe were switched transversely by a drive field varying up to about 7 Oe. The switching waveforms were observed on the external loop.

Figure 4.3a shows the variation of switching time τ as a function of drive field (H_d) for each film assembly. (The time τ is defined as indicated in Fig 4.3b.) The experimental curves (solid line curves) are in good agreement with the general theoretical predictions. At corresponding drive field values, the switching time of assembly D was much longer than the switching time of assembly A. Assemblies C and B also showed increases in switching time from that of assembly A, but these increases were much less than that for assembly D.

The loading effect of the assemblies was further studied by a set of experiments conducted with assembly A. In these experiments the switching time of assembly A was measured as a function of drive field, with various bias fields applied along the film easy axis by external Helmholtz coils. These steady fields were used to simulate the loading effect of the assemblies which produced average loop fields along the easy axis.

The results obtained are shown in Fig. 4.3a (broken line curves). The curve for assembly D cuts across the curves of constant bias fields, indicating that the equivalent average loop field H_{av} decreases with in-

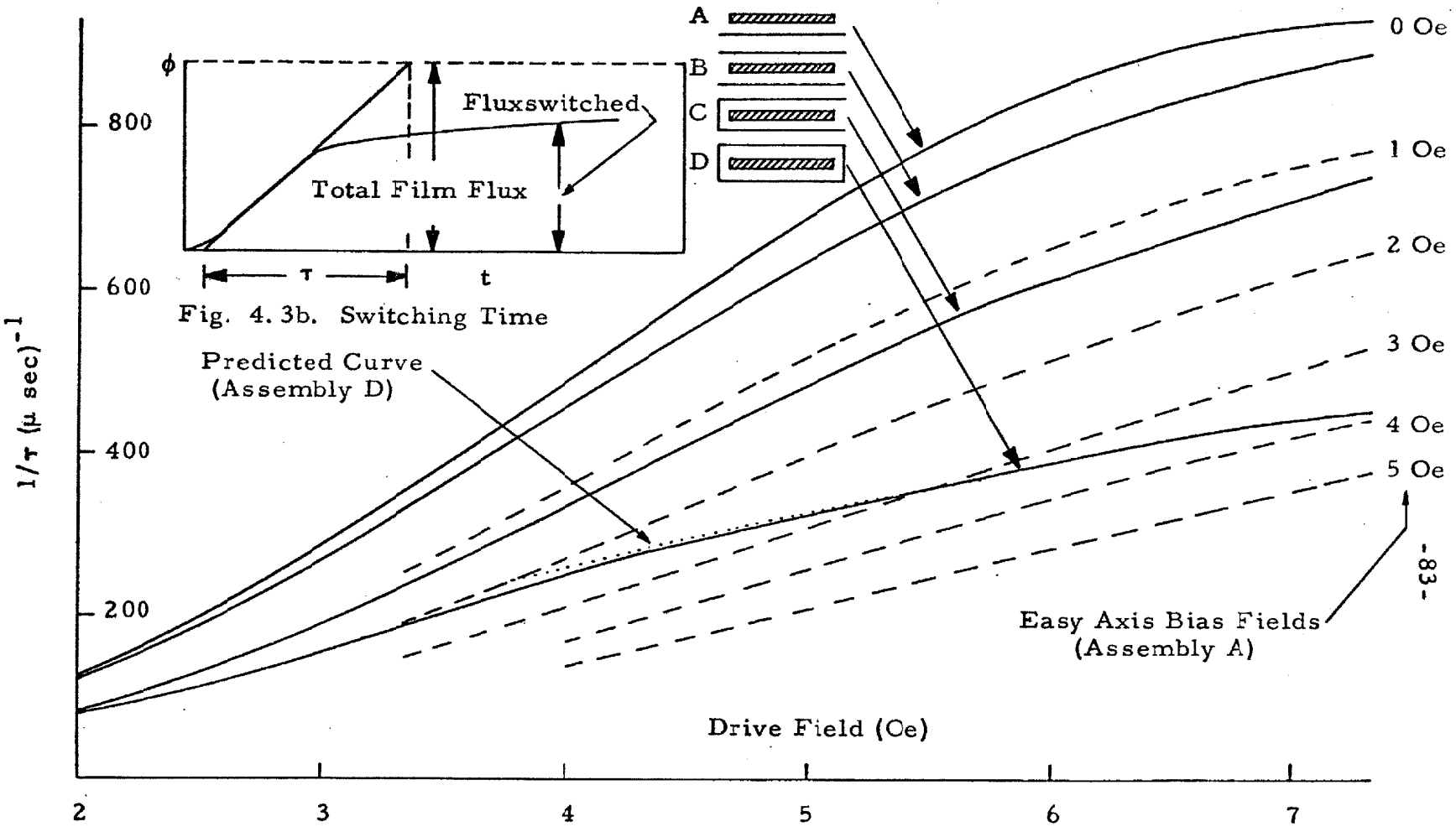

Fig. 4.3b. Switching Time

Fig. 4.3a. Variation of Film Switching Time with Loop Loading

creased switching time. According to Eqn. 4.2, the average field due to loop resistive loading is inversely proportional to the total switching time and so, neglecting eddy current fields, the value of $H_{av} \cdot T$ should remain constant as the drive field is varied. Values of H_{av}, corresponding to various $1/T$ values for assembly D, were obtained by interpolation between the bias field curves for assembly A. These field values, together with the corresponding values of $H_{av} \cdot T$, are tabulated below.

H_d(Oe)	$1/T(\mu sec)^{-1}$	H_{av}(Oe)	$H_{av} \cdot T$(Oe-nsec)
3-1/3	188	2.10	11.20
4	251	2.32	9.25
4-2/3	300	2.70	9.00
5-1/3	345	2.96	8.58
6	389	3.27	8.40
6-2/3	425	3.61	8.50
7-1/3	450	3.89	8.65

It is seen that, for drive fields greater than 4 Oe, the variation of this latter quantity is quite small. (Variation of this quantity for the lower field values is to be expected since, for drive fields less than H_K, the final positions of the magnetization are significantly different for assemblies A and D and so the loop loading simulation is not as accurate.)

The switching curve for assembly D was predicted with the aid

of the set of curves for assembly A, by assuming that $H_{av} \cdot T$ remained constant at all switching times. It was also assumed that, with an H_{av} of 3 Oe (in the middle of the range of measured values), the predicted switching time was identical with the measured value ($1/\tau = 354\ \mu sec^{-1}$). Using these values, the switching times corresponding to other field values were calculated. By interpolation between the curves for assembly A, a theoretical curve for assembly D was plotted (dotted line of Fig. 4.3a). For drive fields above 5 Oe, this curve is identical with the experimental curve for assembly D. For lower fields some divergence of the curves occurs but, over the complete range of values, the correspondence is quite good.

The loop resistance corresponding to the assumed $H_{av} \cdot T$ value was determined by substitution of the appropriate values of $H_{av} \cdot T$, w and ϕ_T (M = 750 Oe[16]; measured film thickness = 1600 A) into Eqn. 4.2. This calculation yielded $R = 0.28\ \Omega$ in comparison to a theoretical value of $0.21\ \Omega$ (measured conductor thickness = 3500 A). The agreement between these two resistance values is quite consistent with the accuracy of the layer thickness measurements and the possible presence of additional resistance due to oxide layers at the mutual contact surfaces of the two conductors.

The good agreement of the theoretical and experimental results for assembly D indicates that the additional eddy current field, introduced by the presence of the second loop conductor, did not play a major part in determining the switching time of this assembly. The variation of the quantity $H_{av} \cdot T$ over the range of drive field values from 4 Oe

to 7-1/3 Oe, may be attributed to the effect of this eddy current field. By making a number of suitable assumptions, an average value of about 1/4 Oe, acting at 135° to the drive field direction, was estimated for this field. In the theoretical discussion of eddy current fields, it was estimated that the field due to one loop conductor was less than 0.2 Oe acting in the same direction. Thus, the total eddy current field of assembly D was less than 1/2 Oe so that it was not a major factor in determining switching time.

By reference to Fig. 4.3a it is seen that the curves for assemblies B and C may be approximately simulated by application of constant fields of 1/4 Oe and 1-1/4 Oe, respectively, to assembly A. A portion of these fields may be attributed to the additional eddy current field caused by the presence of the second loop conductor. The capacitive current field must also be effective in slowing film switching since this eddy current field is limited by its value (1/4 Oe) in assembly D. However, since the value of $H(0\text{-}T/2)$ for a capacitively loaded loop varies as $1/T^2$, the constant field simulation indicates that use of this average field as a measure of the slowing effect of the capacitive loading has not as much significance as in the case of a resistively loaded loop.

The effect of loop conductor separation on film switching time was determined by switching experiments performed on various sets of film assemblies, having the standard loop configuration with 100% film coverage, and with silicon monoxide layer thicknesses of about 10,000, 20,000, 30,000 and 40,000 A in each set. By observing film switching on the external loop, it was concluded that, for any given drive field,

the film switching time decreased as the conductor separation increased. This decrease was attributed to decreased capacitive loading as the loop capacitance became smaller. Due to such factors as variation of contact resistance between the conductors and the frequent occurance of low resistance paths between the conductors and the magnetic film when the insulation layers were thin, it was not possible to obtain a set of films in which switching time decreased smoothly as the insulation thickness increased. Thus, the determination of comparative switching curves was not carried out.

When the film coverage is less than 100%, the loop currents directly affect only the region of the film covered by the loop (see Fig. 1.1). Switching curves for a set of films having film coverages varying from 8% to 100% of the magnetic film width are shown in Fig. 4.4a. The switching times τ of each film were measured on both the external and deposited loops. (The time τ is defined, as indicated in Fig. 4.4b). It is seen that, at any given drive field, both switching times increased as the fractional film coverage increased. The increase in deposited loop switching time indicates that, besides the drive field and the loop field, whose magnitude at any switching time is independent of loop width, a field dependent on loop width acted on the covered region of the film. This additional field was attributed to an interaction field which occured between the two regions of the film when the magnetization in the two regions began to switch differently (see Fig. 1.1). Then, as observed experimentally, the external loop switching time should also increase with increased film coverage as the region of the film directly

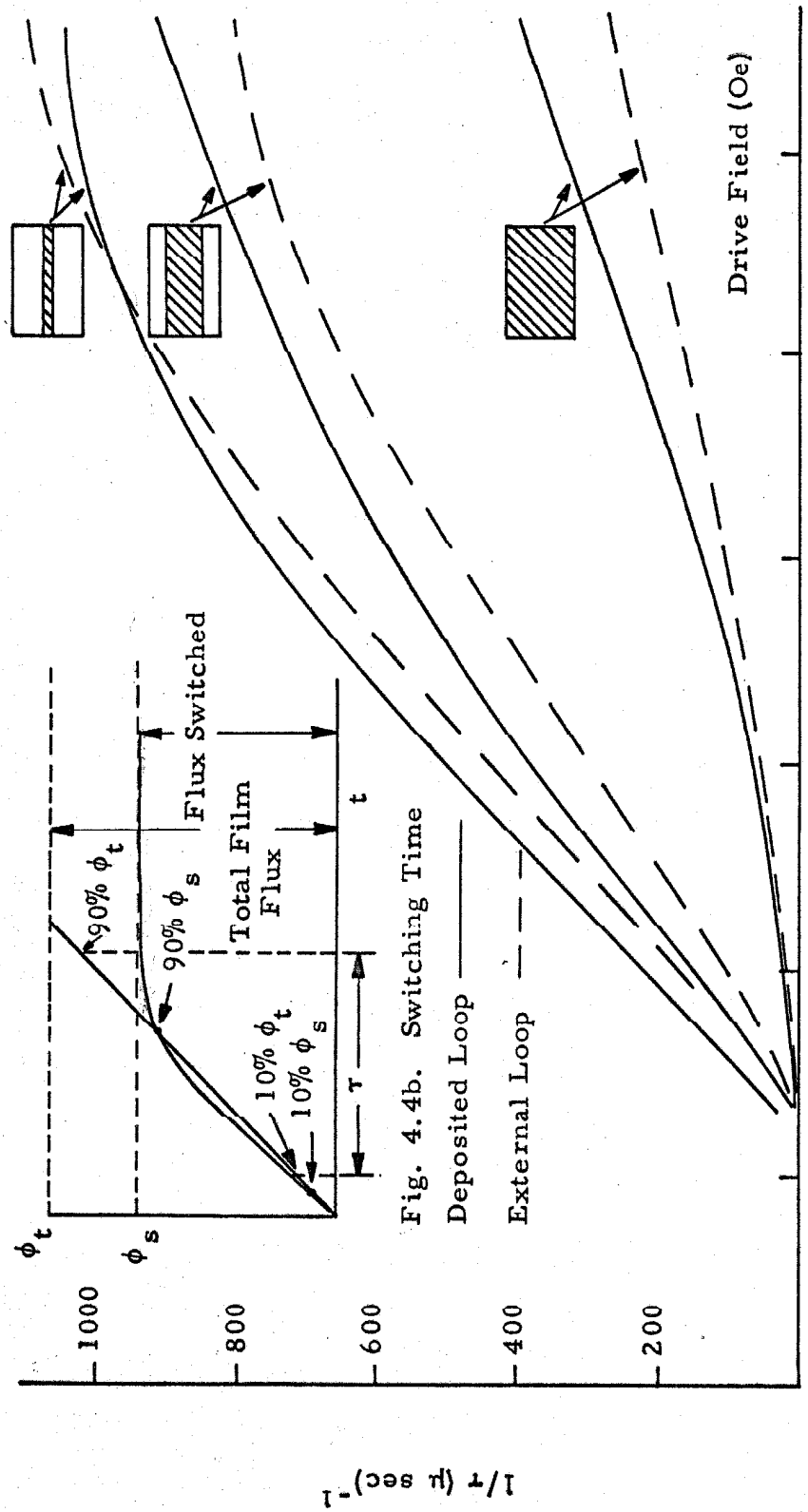

Fig. 4.4a. Variation of Film Switching Time with Film Coverage

Fig. 4.4b. Switching Time

affected by the loop currents became larger and the interaction field on the uncovered region became greater.

For all the films, the deposited loop switching time was nearly always less than the corresponding external loop switching time. This result seemed to indicate that the covered portion of the film switched faster than the rest of the film, a conclusion which was inconsistent with the already established slowing of the film switching due to the deposited loop. However, it was noted that the deposited loop signal was characterized by an appreciable amount of overshoot, while the external loop signal (which contained a large (10%-20%) slow component), reached its final value in a non-oscillatory fashion. These characteristics were in agreement with the curves of Fig. 3.12, which show the calculated responses of both deposited (standard) and external loops to various ramp signals. These curves also indicate that the external loop response is somewhat slower than the deposited loop response. Thus, the apparent shorter switching time of the deposited loop may be attributed to differences in the loop responses and to the method used to measure switching times.

The eddy current field due to the loop conductors of a film assembly was further studied by means of the following experiment. The film assembly consisted of a magnetic film (0.36" x 0.36") with a deposited aluminum ground plane (0.625" x 0.625") and an aluminum loop conductor of variable size. This conductor consisted of a square piece of 0.001" foil and was secured to the film assembly by Scotch tape. The two conductors were not in electrical contact, being separated by

silicon monoxide layers, each about 100,000 A thick. The above arrangement was chosen to keep capacitive fields small and so only the eddy current field was considered to be effective in slowing the film switching. The assembly substrate was located within the external loop of the test strip line with the film assembly facing the strip line center conductor. This orientation, which was unique to this experiment, was required so that the assembly ground plane, which was the first assembly layer deposited, would be on the same side of the magnetic film as the strip line ground plane. In this way the two ground planes effectively acted as one conductor.

Figure 4.5a shows the effect of various loop conductors on the switching time of the assembly, as observed at the external loop output. The film, which had an H_K value of 4 Oe, was driven by a transverse field of 5-1/3 Oe. Each conductor was located symmetrically relative to the film, with its edges parallel to the film edges. It is seen that the eddy current field increased rapidly when the loop conductor size exceeded the film dimensions. However, it is clear that the eddy current field, due to a conductor size of the same order as the magnetic film, was much less than the field due to an infinite extent conductor. The reduction in output flux with increased conductor size was attributed to the effect of a steady bias field, due to the eddy currents, which modified the final position of the film magnetization.

The above results are in agreement with the general predictions of the theoretical discussion of eddy currents and indicate that, by suitable design, the field effects of these currents on fast film switching can

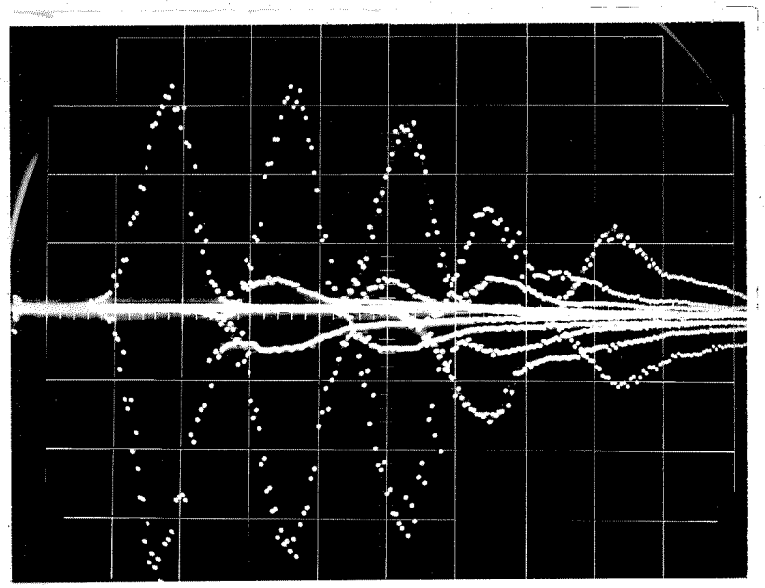

Scale

x : 1 nsec/cm

y : 400 mv/cm

	A	B	C	D	E
A	no loop conductor				
B	"	"	0.35" square		
C	"	"	0.37"	"	
D	"	"	0.45"	"	
E	"	"	0.56"	"	

Film size 0.36" square

Fig. 4.5a. Effect of Eddy Current Field on Film Switching

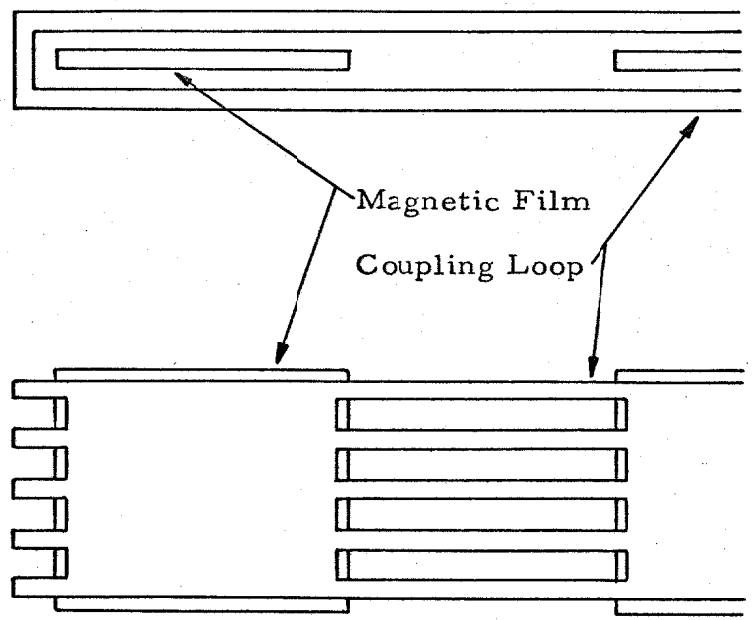

Fig. 4.5b. Low Eddy-Current Coupling Loop

be kept small. In particular, a loop conductor which covers only a small fraction of the film perimeter (such as indicated in Fig. 4.5b) should have a small eddy current field.

Bias and Drive Field Properties of Deposited Loops

In the experiments just described, the deposited loop was used as a sense conductor. In this mode of operation, the loop currents may be classed as parasitic, since they are not essential to the read-out properties of the loop and only cause an increase in the switching time. When bias or drive fields are applied to the magnetic film by means of the deposited loop, these parasitic currents still occur, but the current inserted into the loop is essential to the desired film-loop interaction. The field produced within a deposited loop of width w meters, when carrying a uniformly distributed current I is $\frac{I}{w}$ amp-turns/m i.e., $4\pi \times 10^{-3}$ I/w Oe. The field calibration for a deposited loop covering 100% of the film width (0.914 cm) was calculated as 1.375 Oe/A. Thus, in order to have an effect on the motion of the film magnetization, bias and drive currents must have magnitudes of the order of a few amps.

Bias Field

The use of a deposited loop to produce a bias field was first investigated. The biasing effect of the loop was compared experimentally with the effect of a bias field produced by an external Helmholtz coil. It was experimentally established that a steady current greater than about 1/4 A, flowing in a deposited loop with a measured resistance of about 1 Ω, resulted in destruction of the loop due to excessive resistive

losses. Thus, a current pulse with a small duty cycle, but having a constant value during the film switching process, was used to obtain large bias fields with small power dissipation.

Figure 4.6 shows the circuitry utilized to produce a bias field pulse, correctly phased relative to the strip line drive field (see also Fig. 6.2). The Rutherford pulse generator (Model B7B) was driven at a 60 pps rate by the mercury relay drive pulse. This pulse generator, having a rise time of about 20 nsec, produced pulses of either polarity, variable in width up to 10 msec and having a maximum amplitude of about 2 A into a short circuit load. The beginning of this bias pulse could be delayed relative to the trigger signal, by an amount varying up to 10 msec. The time delay between the beginning of the mercury relay drive pulse and the occurance of the strip line drive field was of the order of a few milliseconds. Thus, on triggering the pulse generator by the rise of the mercury relay drive pulse, the bias pulse could be appropriately phased to have a steady value during film switching. The bias current waveform was monitored by a P6001 Tektronix current probe clamped around the output line of the pulse generator, and the drive field was monitored by an electrostatic probe situated in the strip line. By observing these two signals on a dual-channel oscilloscope, the delay of the pulse generator was adjusted to phase the bias current pulse correctly. The width of the bias pulse was made as small as possible to minimize resistive losses in the deposited loop. Due to a relative time jitter of the two signals, attributed to a variable delay in the closure of the drive field mercury relay, the minimum width used was about 1/3 msec. Although some test assemblies were destroyed by

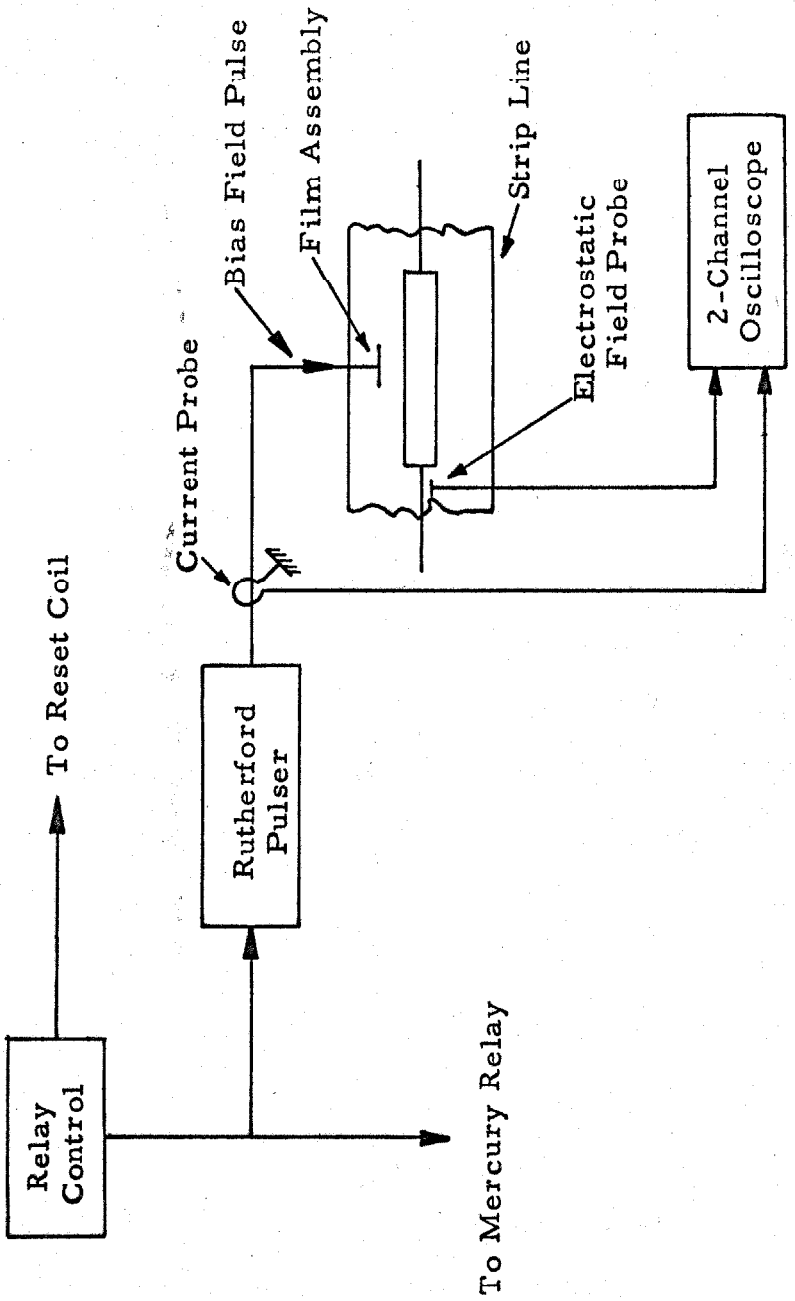

Fig. 4.6. Deposited Loop Bias Field Circuit

passage of a 2 A current pulse, use of relatively thick loop conductors and adjustment of the deposited loop probe for minimum contact resistance enabled the desired experiments to be performed.

Comparison of external and loop bias fields was carried out with a loop covering 100% of the magnetic film width, since the complete film was then directly affected by both bias fields. The deposited loop bias field (H_L) was along the film easy axis and so an easy axis external bias field (H_V) was also used. It was found that, for both sources of bias field, the switching signals observed on the external loop were very similar. With a constant value of drive field (6-2/3 Oe), the corresponding values of bias fields, which produced equal maximum amplitudes (A_m) of the film switching signal, were determined. These fields were applied in the same direction as the reset field. The following table shown a comparison of corresponding field values for one film assembly, for both directions of the reset field, up to the maximum deposited loop field. The ratio of corresponding bias fields is seen to be close to unity at all field values. The average of these results is within 1/4% of unity and so the deposited loop bias field calibration was verified.

In view of the similar effects of the two bias fields on film switching, it was expected that application of two equal and opposite bias fields (one an external field, the other a loop field) would result in the same waveform as obtained when no bias fields were applied. Figure 4.7 shows that this expected result did not occur. Figure 4.7a shows the zero-bias output waveform and the two reduced amplitude

A_m	H_L(Oe)	H_v(Oe)	H_v/H_L
-7.3	0	0	-
-6.5	0.45	0.51	1.13
-6.0	0.83	0.76	0.92
-5.5	1.17	1.20	1.03
-5.0	1.51	1.58	1.04
-4.5	2.06	2.02	0.98
-4.0	2.54	2.49	0.98
+8.5	0	0	-
+8.0	0.24	0.25	1.04
+7.5	0.55	0.55	1.00
+7.0	0.89	0.86	0.97
+6.5	1.27	1.27	1.00
+6.0	1.72	1.73	1.00
+5.5	2.20	2.20	1.00
+5.0	2.85	2.64	0.93

$$\frac{H_v}{H_L} \quad \text{average} = 1.002$$

Drive Field = 6-2/3 Oe ; Bias Field = 2.7 Oe

Scale x : 1 nsec/cm ; y : 200 mv/cm

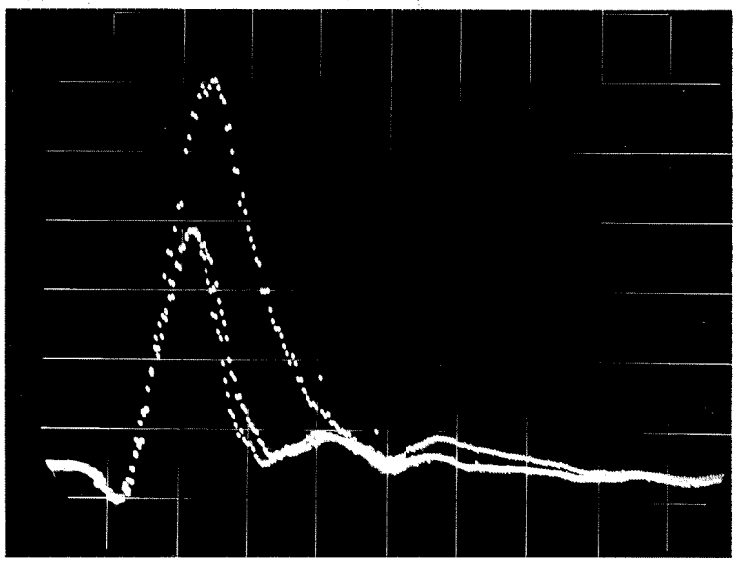

Fig. 4.7a. Zero-Bias and Single-Bias Waveforms

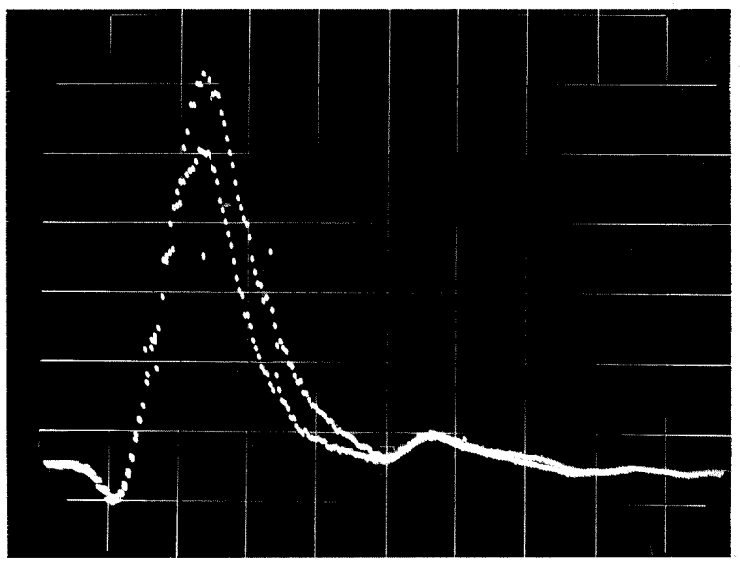

Fig. 4.7b. Zero-Bias and Opposing-Bias Waveforms

waveforms, corresponding to bias fields of 2.7 Oe applied in the reset field direction by the two bias sources. Fig. 4.7b shows the zero-bias output waveform and the reduced amplitude waveform, corresponding to an external field of 2.7 Oe in the reset field direction and a loop field of 2.7 Oe in the opposite direction. Variation of the loop field about its calculated value failed to reproduce the zero-bias output waveform and so the difference in signals could not be attributed to any errors in bias field calibration.

The discrepancy between the two signals was accounted for by consideration of the current distribution in the loop conductor. The current flow in the conductor was approximated by the current flow in a semi-infinite rectangular plate, with a symmetrically-placed point current source. The current distribution in this latter case was determined in Appendix C and the results obtained are shown in Fig. 4.8. The directions of the arrows indicate the direction of current flow at various points in the conductor. These points are situated at the tails of the arrows. The values of current density, expressed in units of average current density, are shown at the heads of the arrows. (Due to symmetry, only half the current vectors are shown.) The current density is higher than the average over one half of the conductor surface and is less than the average over the rest of the surface. It is clear that the line, corresponding to the loop conductor edge distant from the current injection point, is very close to being an equipotential line and so the approximation of the conductor by the semi-infinite plate is well justified.

The loop field was assumed to vary in a manner corresponding

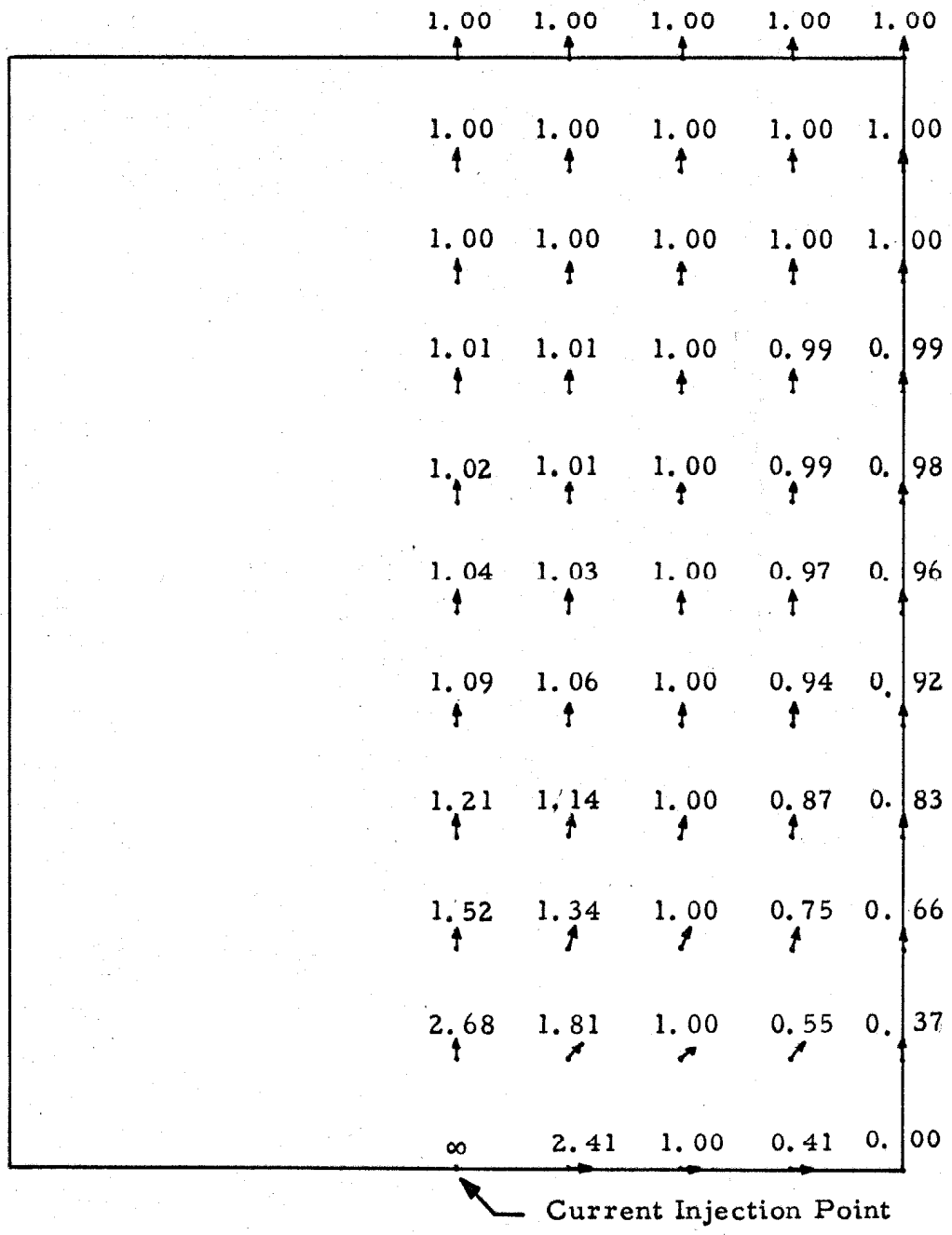

Fig. 4.8. Current Distribution in Semi-Infinite Rectangular Plate

to the current density distribution. Thus, with a uniform magnetic field acting along the positive easy axis direction and a loop field of the same average value acting in the opposite direction, the resulting bias field was non-zero over some of the film area. With the film magnetization originally set along the positive easy axis direction, application of the loop field resulted in a change of film magnetization. Reversed domains occurred where the resultant field was directed along the negative easy axis and exceeded the film coercive force. When the resultant field was of the order of the anisotropy field and was directed at a large angle to the easy axis, the magnetization was also directed away from the easy axis. On switching the film to the hard axis, the observed flux was reduced from its zero-bias value, due to the contribution of such regions as those described above. The observed loss of flux depends on the drive field, the bias field, the film coercive and anisotropy fields and the deposited and external loop geometries. Exact calculation of this loss is quite difficult. Its value was approximated to be of the same order as the experimental value.

Although the current distribution is quite non-uniform in the loop conductor, it has been shown that, when used to bias the film in the reset field direction, the loop field acts as if the current distribution were uniform. Some consideration shows that, in this case, the effect of the varying loop field, in terms of flux switched by the drive field, tends to average out over the complete film area. This result is due in particular to the absence of reversed domains, which occur in the presence of the external and loop bias fields when applied in opposite directions. The small difference in biased film waveforms, as seen in Fig. 4.7a, was attributed to the effect of the non-uniform loop current

distribution.

Drive Field

The drive field properties of the deposited loop were investigated by use of a film assembly, having two orthogonal deposited loops, placed parallel to the film magnetic axes. The hard axis loop was used to produce the drive field and so this loop conductor covered the entire film area. The narrow easy axis loop, situated on the film centerline, sensed the easy axis flux change of the film. In the fabrication of this film assembly, the hard axis loop conductor was first deposited, followed by a layer of silicon monoxide. The rest of the process followed the standard layer deposition sequence. The loop ground plane was extended to complete the hard axis loop circuit.

The circuit, illustrated in Fig. 4.9, was used to produce a deposited loop drive field, with a suitably phased reset field between pulses. Correct phasing was achieved by adjusting the Rutherford pulse generator delay until the drive field occured during the off period of the reset field. The Spencer-Kennedy Laboratory (SKL) pulse generator produced output pulses of either polarity, having a 1 nsec rise time and a length of 50 nsec determined by its 50 Ω charge cable. The magnitude of these pulses was determined by measuring the charging voltage with a digital voltmeter (0.01% accuracy ± 1 digit). The pulse generator output voltage was one half the value measured on this voltmeter. The SKL pulse generator fed a parallel combination of a 700 Ω line which supplied a trigger signal to the sampling oscilloscope and a 53.5 Ω line which carried the drive pulse to the deposited drive field

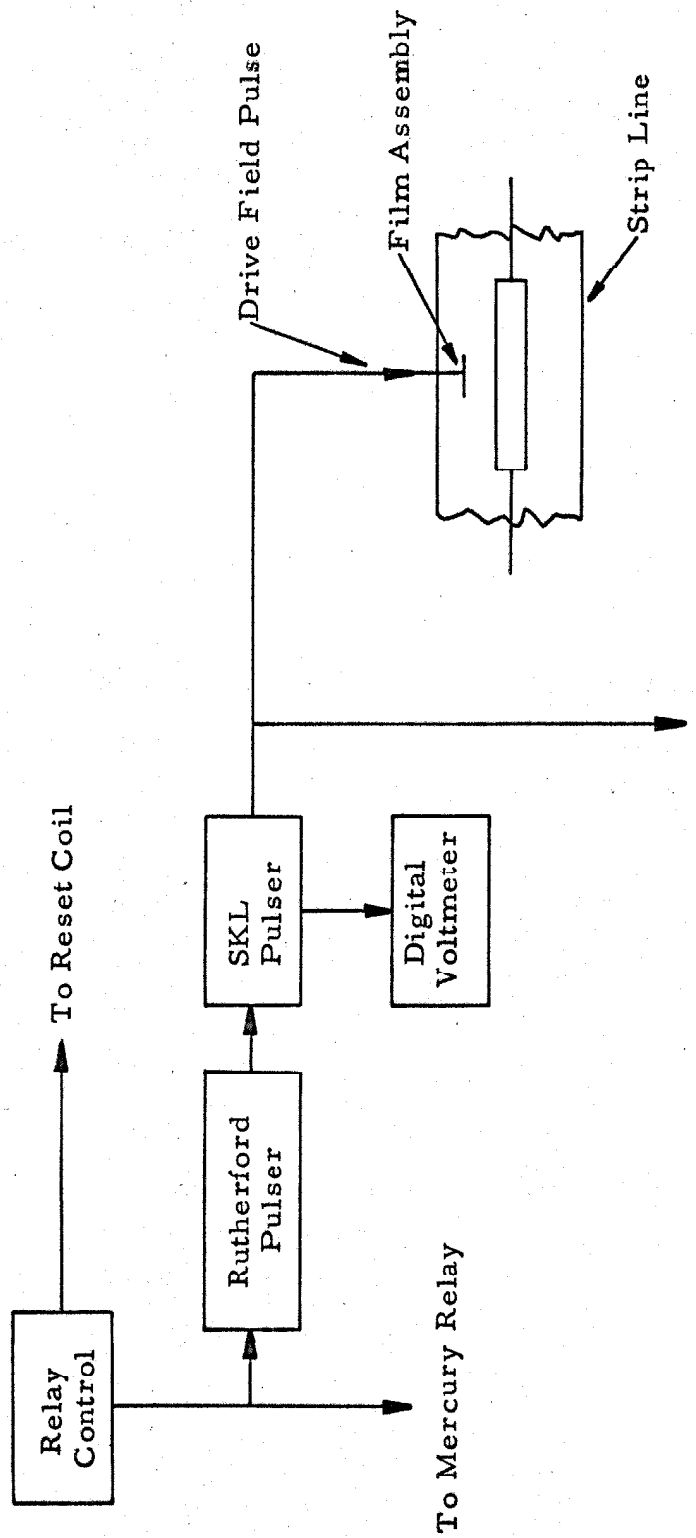

Fig. 4.9. Deposited Loop Drive Field Circuit

conductor.

The fabricated film assembly was mounted on a film holder having two deposited loop probes, one for each loop. The film holder was mounted in the test strip line so that the film easy axis was perpendicular to the direction of the strip line drive field. This arrangement facilitated alternate application of a deposited loop drive field and an external strip line drive field to the film, with the same reset field being used in both cases.

The loop field was calculated in the following manner. The impedance presented by the parallel combination of the 700 Ω trigger line and the 53.5 Ω cable was 49.7 Ω, which was an almost perfect match for the 50 Ω output impedance of the SKL pulse generator. Thus, assuming perfect matching, the output current was 1 A for a 100 V SKL charging voltage. The corresponding current pulse passing along the 53.5 Ω cable was 50/53.5 A = 0.935 A. Due to the short length of the deposited loop, the reflection coefficient at the loop termination was determined by the loop resistance rather than by its characteristic impedance. With a measured loop resistance of 2.1 Ω, the current reflection coefficient was 0.924 and so the loop current was 1.924 x 0.935 A = 1.8 A. The width of the hard axis loop was 0.45" and so its field was calculated to be 1.1 Oe/A. Thus, the drive field calibration was 1.1 x 1.8 = 1.98 Oe/100 V SKL charging voltage.

Figure 4.10 shows easy axis loop waveforms obtained on switching a film assembly by corresponding external and loop drive fields (6 Oe). Each oscillogram shows switching waveforms for reset fields

Scale

x : 1 nsec/cm

y : 200 mv/cm

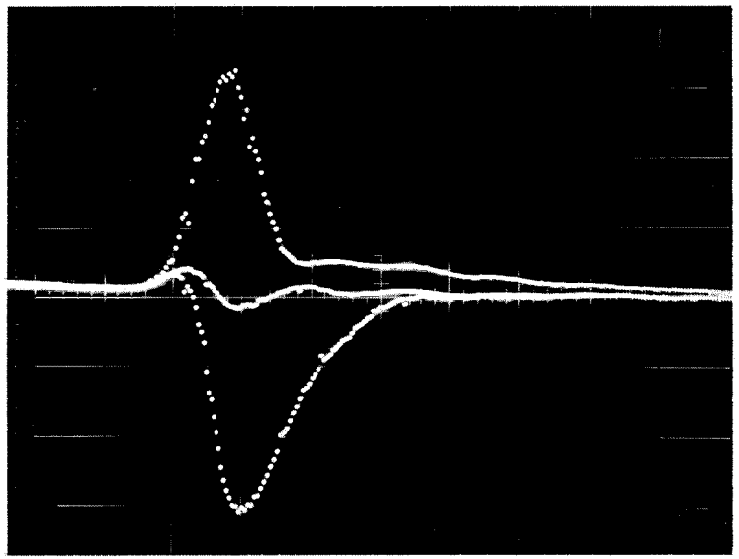

Fig. 4.10a. Deposited Loop Output Due to 6 Oe External Drive Field

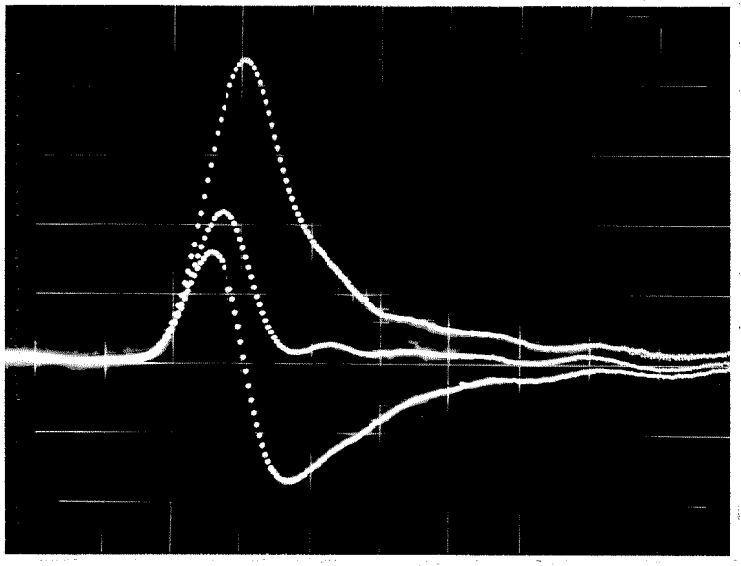

Fig. 4.10b. Deposited Loop Output Due to 6 Oe Deposited Loop Drive Field

applied along both easy axis directions. The center curve in each oscillogram represents the pickup signal in the monitored loop and was obtained by application of a 150 Oe steady blocking field prior to the drive field pulse. With an external drive field, the waveforms of Fig. 4.10a were obtained. The loop pickup signal, due mostly to the electric field of the drive pulse,was quite small. The similarity of both switching signals indicates that the film hard axis was well aligned with the external drive field. When a deposited loop drive field was applied in the same direction as the external drive field, the signals of Fig. 4.10b were obtained. The two switching signals were then quite different. This difference is due to a large pickup signal in the sense loop as seen in Fig. 4.10b. This signal was caused by capacitive coupling between the deposited drive and sense loops. Calculation of this signal amplitude, using the drive pulse and deposited loop parameters, gave a result consistent with the experimental value.

Comparison of external and loop drive fields was carried out by measurement of the film flux output when both drive fields were applied separately. A magnetic film, having an H_K value of 6 Oe was used and so, with a drive field of about 6 Oe, the flux output varied quite significantly with the drive field magnitude. The film flux was measured by integration of the various loop outputs and subtraction of the appropriate integrated pickup signals from the unblocked switching signals. As usual in flux measurements, the average flux value for both reset field directions was used as the experimental value.

According to the appropriate field calibrations, a drive field of

6 Oe is produced by an external field drive of 4.5 kv and a deposited loop field drive of 303 V. By experiment, it was found that an external drive of 4.73 kv gave the same flux output as a deposited drive of 303 V. This result indicated a 5% error in field calibration. Allowing for possible errors in external field calibration and the film flux measurements, the above experiment was considered to verify the deposited loop calibration.

The film switching waveforms due to similar magnitude drive fields were compared. Using the X-Y plotter, connected directly to the sampling oscilloscope analog output terminals, output waveforms were obtained for 6 Oe drive fields (1.50 kv external drive, 288 V deposited loop drive). The loop pickup signals were also recorded.

Figure 4.11 shows the film switching waveforms, obtained by appropriate subtraction of the pickup signals from the unblocked switching signals. The signal rise time with a deposited loop drive was about 50% longer than the rise time with an external drive. The waveforms of the strip line field and the SKL output have rise times of about 1 nsec, but the SKL pulse was slowed somewhat in the deposited loop probe circuitry. Thus, the drive pulse of the deposited loop had the longer rise time, so yielding a longer film switching time.

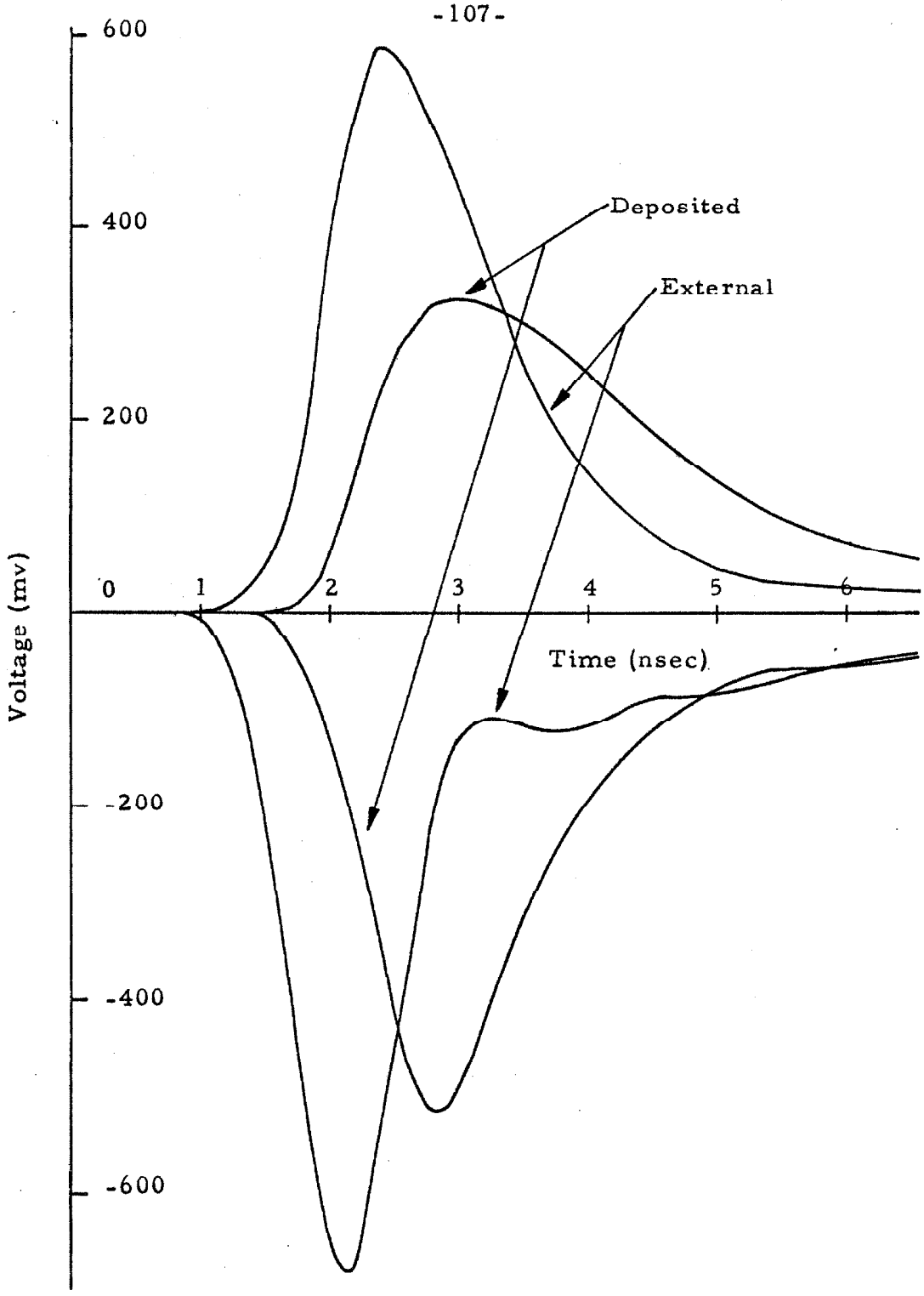

Fig. 4.11. Comparison of Film Switching Signals Due to 6 Oe Deposited Loop and External Drive Fields

V INTEGRATED DEPOSITED CIRCUITRY DESIGN

The possible future use of integrated deposited circuitry containing magnetic thin film elements, for computer circuits operating in the nanosecond range, will now be discussed. The general feasibility of such circuitry will first be established. The ultimate limit of circuit miniaturization will then be shown to be chiefly dependent on the resistivity of the coupling loops. A number of features of miniaturized circuitry, such as heat dissipation and suitable layer thicknesses will be discussed. A set of logic elements will be proposed and will be shown to have reasonable fan-in and fan-out potentialities. Finally, some general design features relating to the use of large films in deposited circuitry will be discussed.

General Feasibility

One of the main features which has made the use of magnetic thin films so attractive for computer applications has been their short switching time (in the nanosecond range) with moderate drive fields. The general feasibility of integrated deposited circuitry containing magnetic thin films, depends on maintaining this feature in such circuitry.

It has been shown in Section IV that the two main parasitic loop factors which affect the film switching time are eddy current fields and capacitive current fields. Eddy current fields can be kept quite small by use of open-structure coupling loops, such as that illustrated in Fig. 4.5b. The reduction of capacitive current fields, which were

of moderate intensity for the experimental film assemblies, can be effected by use of thicker insulation layers. Thus, it is clear that, using suitable layer design, a magnetic film coupled with a deposited conducting loop can be made to have switching properties which are very similar to those of an isolated film. This result indicates the general feasibility of using integrated deposited circuitry for future high speed computer applications.

Miniaturization

The miniaturization of computer circuitry by the use of magnetic thin films in a deposited configuration, as has been discussed by a number of authors, [2, 17, 18] can be predicated on the extremely close coupling which exists between films and coupling loops in such a configuration thus allowing utilization of the flux output of small film elements. This coupling characteristic sets no explicit limit on the amount of miniaturization possible with such circuitry. Various factors which affect this limit for film logic circuitry are discussed as follows.

An important requirement for magnetic film logic circuitry is that the switching of a magnetic film can produce a coupling loop field sufficient to bias or drive another film. This miniaturization study is based on a determination of the smallest film size which can produce the required loop field. Consider a square thin permalloy film, closely coupled by a conducting loop which covers the entire film surface. The film is assumed to switch completely from the loop axis to the transverse direction in 1 nsec. A longitudinal demagnetizing field of less than 0.1 Oe is assured by use of a film thickness-to-length ratio

of 10^{-5} (see Eqn. 4.1). With a given film size and switching time, the loop field is maximized by use of a loop with a short-circuit termination and by use of thick loop conductors of low resistivity material. The equivalent loop conductor thickness is then taken to be equal to the skin depth of the conductor material at a frequency of 1 k Mc, which is assumed to be representative of the film switching waveform.

Four film-loop cases are considered with the main requirement in each case being that the average loop field during the switching process be 1 Oe. (This field is adequate for bias field purposes.) The results of a number of calculations with these cases are shown in Fig. 5.1. In Case I, the loop conductors are thick silver sheets at room temperature. The minimum film size b is 1.36×10^{-4} m, and the corresponding film thickness is 13.6 A. Use of these film dimensions has a number of serious disadvantages. To achieve the minimum value of loop resistance, the conductor thickness c should be of the order of ten times the skin depth δ of the material, thus yielding conductor thicknesses of 203,000 A. This thickness would probably require a plating process, as well as a previous vacuum deposition process, leading to a complicated fabrication procedure. In addition, since the conductor thickness is not negligible compared to the film dimensions, use of the line charge flux model indicates that an appreciable amount of film flux cuts the conductors, leading to eddy current fields which tend to slow the film switching process.

Case II is obtained by increasing the film dimensions by an order of magnitude, allowing a decrease in conductor thickness to

	I	II	III	IV
Film size b(m)	1.36×10^{-4}	1.36×10^{-3}	1.36×10^{-5}	1.36×10^{-4}
Film thickness (A)	13.6	136	1.36	13.6
Conductor skin depth δ(A)	20,300	20,300	2030	2030
Conductor thickness c(A)	203,000	2030	20,300	203
c/b	1.51×10^{-1}	1.51×10^{-3}	1.5×10^{-1}	1.51×10^{-3}
Average voltage (mv)	0.174	17.4	1.74×10^{-3}	0.174
Noise voltage (mv)	1.63×10^{-3}	5.15×10^{-3}	0.94×10^{-4}	0.3×10^{-3}
Average power (mw)	2.35×10^{-4}	2.35×10^{-1}	2.35×10^{-7}	2.35×10^{-4}
Power Density (mw/cm^3)	94	94	94	94
Minimum Insulation Thickness (A)				
RC = 0.1 nsec	0.13	130	0.13×10^{-3}	0.13
Voltage gradient $= 10^6$ V/m	1.37	137	1.37×10^{-2}	1.37
$H_{av}(0\text{-}\tau/2)$ = 0.1 Oe	0.395	395	0.395×10^{-3}	0.395
Maximum Insulation Thickness (A)				
L/R = 0.1 nsec	-	63,000	-	6,300
1% flux loss	10,600	106,000	1,060	10,600

Fig. 5.1. Miniaturization Limits of Integrated Deposited Logic Circuitry

2030 A. This thickness is easily attainable by vacuum deposition, and is also negligible compared to the film dimensions, indicating low eddy current effects.

The minimum film size can be reduced quite significantly by operation of the circuitry at a reduced temperature. At a temperature of about 10^{o}K, the resistivity of silver is reduced by a factor of 100 over its room temperature value. (Possible variation of film switching time, due to the extremely low temperature environment, should be considered. However, recent work[19] indicates that the switching speed is not significantly different from its value at room temperature.) As shown in the results of Case III, this reduction leads to an order of magnitude decrease in minimum film size to 1.36×10^{-5} m, with a corresponding thickness of 1.36 A. In this case, a conductor thickness of 10δ yields a value of 20,300 A which can be readily obtained by vacuum deposition. However, as in Case I, the ratio of conductor thickness to film size can lead to a significant eddy current field, affecting the film switching.

Case IV is obtained by increasing the film dimensions of Case III by an order of magnitude, thus allowing a decrease in conductor thickness to 203 A. (Due to an increase in resistivity at this small thickness[8], a somewhat thicker conductor may be required.) This thickness, being small compared to the film dimensions, should result in low eddy current fields.

Further reduction in ambient temperature will result in a further decrease in minimum film size. However, since many metals become superconducting at about 5^{o}K, operation of circuitry close to

the transition region between super and normal conductivity may be inadvisable, due to the rapid change of resistivity in this region. (If the circuitry is operated with the loop in a superconducting state, a permanent loop current is set up when the film switches. This new mode of operation may have significant application in future circuitry, but is not discussed further in this work.)

Circuit miniaturization leads to the use of very thin films, with thicknesses ranging down to 1 A. Recent work[20] indicates that the anisotropy is essentially constant for film thicknesses greater than 80 A. Below about 80 A, the magnitude of K, the anisotropy constant, drops and reaches zero around 30 A. This drop matches a reduction in film magnetization M as the film thickness decreases but is slightly faster so that the value of the anisotropy field, $H_K = 2\,K/M$, drops below about 80 A. Thus, the drive field requirements of very thin films are somewhat less than for thicker films. For given film flux requirements, the decrease in M with reduced thickness can be offset by an increase in film thickness over the nominal value. It is surmised that the longitudinal demagnetizing field is not significantly increased by this procedure, since this field is also dependent on the value of M. It is concluded that films with equivalent magnetic thicknesses down to the order of 10 A can be successfully utilized.

By assuming a sinusoidal time variance of the induced voltage in the loop, the average voltage values were calculated and are indicated in Fig. 5.1. The voltage values are compared to the rms thermal noise voltages[21], generated in the frequency range from zero to 10 k Mc, which are also shown in this figure. The noise voltage is

most significant in Case III, being about 5% of the induced voltage. This result indicates that, although the problem should not be a severe one, some consideration should be given to the effect of noise voltages in this type of miniaturized circuitry.

Operation of magnetic films in the transverse switching mode, which is required for nanosecond switching with moderate drive fields, leads to little hysteresis loss in the film material. With low-loss dielectric material, the power requirements of magnetic film circuitry are chiefly dependent on the power losses in the coupling loops. Figure 5.1 shows that the power dissipation is less than 1 milliwatt (mw) per film element for all four cases considered. An upper limit to the power density is obtained by the use of film elements closely packed in parallel planes which are separated by a distance equal to the size of the film elements. (Using the line charge flux model, a separation of this order is expected to result in small interaction between adjacent films.) The power density is seen to have a constant value of about 100 mw/cm^3, independent of the film size. This upper limit to the power density indicates that heat dissipation problems in deposited circuitry will not be severe.

The range of suitable loop insulation thicknesses is determined by a number of considerations. Since the film sizes used are extremely small compared to the width of the film switching waveform, the loop passive circuit properties are accurately described by its lumped circuit values. When the loop is terminated in a short-circuit impedance its response is dependent on its L/R time constant, while, with the

loop open-circuited at one end, the RC time constant is of most significance. By restricting both of these quantities to values less than 0.1 nsec, the slowing effect of loop passive circuitry will be kept small. The resulting limits on the values of insulation thickness are shown in Fig. 5.1. Assuming dielectric material with a relative permittivity of unity, the minimum thickness is always quite small ($\leq$ 130 A), being easily attainable by a vacuum deposition process. For Cases II and IV, the upper limits to the values of insulation thickness are 63,000 A and 6,300 A, respectively, thus giving a wide range of allowable insulation thicknesses above the minimums set by the RC time constant requirement. For Cases I and III, the minimum value of L/R is 0.157 nsec. This limit is due to the contribution of the magnetic field in the conductors to the loop inductance and is an additional reason for avoiding the use of thick loop conductors.

Two other requirements also set minimum limits to the value of insulation thickness. By restricting the average voltage gradient across the insulation to 10^6 V/m (a conservative value, equal to the breakdown voltage gradient for air), a set of values of insulation thickness, shown in Fig. 5.1, were calculated. These values are seen to be somewhat greater than the limits set by the RC time constant requirement, but are still quite small. In addition, the average loop field $H_{av}(0\text{-}T/2)$ due to loop capacitance is restricted to values less than 0.1 Oe by use of values of insulation thickness greater than those shown in Fig. 5.1. In Case II, this lower limit dominates the two other limits, calculated previously, but is still quite small.

An upper limit to the value of insulation thickness is also set by the requirement of small flux closure within the deposited loop. Assuming conductors of zero thickness, maximum values of insulation thickness, corresponding to a 1% film flux closure, are shown in Fig. 5. 1. For Cases II and IV, the conductor thicknesses are seen to be small, compared to these limits and so have little effect on the amount of flux closure. For Cases I and III, since the skin depth is about twice the limiting value of insulation thickness, use of conductors with thicknesses equal to 10δ will result in appreciable flux loss. This factor indicates a further objection to the use of thick conductors in such circuitry.

The wide range of allowable insulation thicknesses enables capacitive cross-coupling between drive and sense loops to be kept to a small value, by use of a tightly coupled sense loop and a relatively loosely coupled drive loop. For Case II, a maximum attenuation factor of the order of 40 db is indicated.

Logic Elements

The transfer of information between two magnetic films is an important characteristic of integrated deposited circuitry. When two films are coupled by a deposited loop, the switching of one film can be controlled by a bias or drive field, produced in the loop by the switching of the other film. The moderate loop field requirements and the use of an external power source to energize the circuitry indicate the greater suitability of using the loop for bias rather than for drive field purposes.

An information transfer scheme, [1, 5, 22] which uses the coupling loop of two films for bias purposes, will now be discussed. Elementary computer circuits based on this scheme will then be presented. The scheme which is illustrated in Fig. 5.2a operates in the following manner.

The two film easy axes are parallel to the loop axis and initially the magnetization of film 1 is aligned along one of these directions. The drive field H_2 is first applied and, being larger than H_K, drives the magnetization of film 2 to its hard axis. The field H_2 is then removed and simultaneously, the drive field H_1 is applied to film 1. A coupling loop field, whose direction depends on the initial orientation of the magnetization of film 1, then acts on film 2. This field acts as an easy axis bias field and determines to which easy axis direction the magnetization of film 2 falls. Thus, the final orientation of this magnetization depends on the initial orientation of the magnetization of film 1 and so a transfer of information is effected.

Some characteristics of this information transfer scheme were obtained by means of the following experiment. With a magnetic film oriented with its easy axis perpendicular to an external drive field, a steady field ($\approx$ 7 Oe) was first applied along the film hard axis. A drive field of equal magnitude but of opposite direction was then applied and resulted in cancellation of the net drive field on the film. An easy axis steady bias field was used to steer the film magnetization back to one easy axis direction and the effect of varying this field was determined. The switching time of the film in this "fallback" mode was also observed.

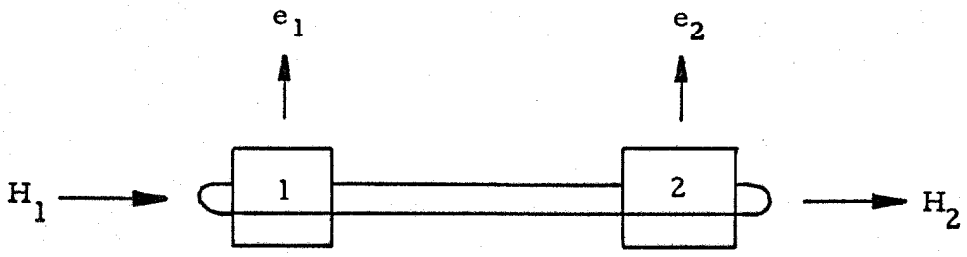

Fig. 5.2a. Information Transfer Scheme

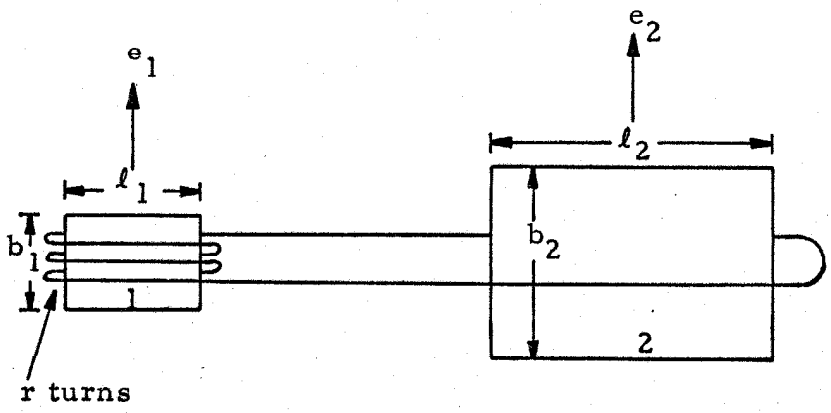

length ratio : $\ell = \ell_2/\ell_1$

breadth ratio : $b = b_2/b_1$

thickness ratio : $t = t_2/t_1$

Fig. 5.2b. Modified Information Transfer Scheme

The results of experiments, conducted with a number of films having H_K varying from 2.5 Oe to 5.5 Oe, show that effective steering occurs with a minimum bias field of 10% to 20% H_K. Above this minimum value, the flux change and switching time of the film are essentially independent of the bias field, until this field becomes large enough to affect the initial position of the film magnetization significantly. The switching time of this fallback mode is about 2 nsec and is comparable to the time obtained by application of a transverse drive field of the order of H_K (equivalent drive fields varied from 1.25 H_K to 1.50 H_K). This result is rationalized by observing that, according to the Stoner-Wolfarth model[23], with the film in its easy axis state the anisotropy effect is equivalent to application of an easy axis field H_K. With an H_K value of 3 Oe, the coupling loop field required for the information transfer scheme already described is of the order of 0.5 Oe. As already shown in a number of previous experiments, this field will have little effect on the switching time of film 1. Using a drive field of about 2 H_K, the switching time of film 1 is less than the fallback time of film 2 and so, using two equal sized films, a positive flux steering action is obtained in the initial stages of the fallback process. At a later stage, when film 1 has completed its switching process and the magnetization of film 2 is still returning to its easy axis, the bias field has reversed direction and opposes the fallback of film 2. However, if at this stage the magnetization of film 2 makes an angle of at least 30^{o}[5] with its hard axis direction, the fallback process should be completed satisfactorily. The relative phasing of the drive fields on the two films is quite important to the success of this scheme.[5]

Since the switching time of film 1 is less than the fallback time of film 2, a positive flux steering action on film 2 may be achieved even when the flux output of film 2 has a larger value than that of film 1. This situation corresponds to an increase in the thickness and/or film dimension, perpendicular to the loop axis of film 2. In addition, since a higher loop field could be tolerated for film 1 without increasing its switching time too severely, use of film 2 with an increased dimension parallel to the loop axis (and a corresponding increase in loop width over film 2) may be considered. It is concluded that successful information transfer is possible even when film 2 is larger than film 1.

An upper limit to the relative film sizes for the modified information transfer scheme, depicted in Fig. 5.2b, is now discussed. This scheme differs from the one presented previously in having a number of loops enclosing the drive film 1. These r loops can have their conductors stacked above one another so that each loop covers the entire film area, or can be placed side by side over the film so that each loop conductor width is approximately 1/r times the film dimension along the easy axis. With a given film switching time, both loop arrangements have equal induced voltages from film 1. In addition, with a given loop current, the loop field acting on film 1 is the same for both cases. Due to this equivalence, the arrangement having the conductors laid side by side is preferable, since it requires the lesser number of deposition layers and has lower eddy current losses, due to the closer spacing of the magnetic film and the loop conductors.

The bias field acting on film 2 must be sufficient to guide the

fallback of this film magnetization. At the same time, the loop field acting on film 1 must be restricted to a value which does not require an excessive drive field in order to produce fast switching of this film. These conditions limit the ratio of the two fields thus yielding the inequality $br \leq K$, where K = maximum field ratio. Another restriction is placed on the film dimensions by requiring that the maximum voltage output of film 2 does not exceed that of film 1. When the switching time τ_1 of film 1 is less than the switching time τ_2 of film 2, this condition ensures a positive flux steering action on film 2 in the initial stages of the fallback process and results in the inequality $\ell t \leq \frac{\tau_2}{\tau_1} r$. The limiting value of the relative volumes of the two films is given by the quantity $b\ell t = K \tau_2/\tau_1$, and is seen to be independent of the number of turns on film 1.

Assuming $K = 6$ (corresponding to a bias field of 0.5 Oe on film 2 and a loop field of 3 Oe on film 1) and $\tau_2/\tau_1 = 2$ (corresponding to a 1 nsec switching time for film 1 and a fallback time of 2 nsec for film 2), the limiting values of $b = 6/r$ and $\ell t = 2r$ are obtained. With $r = 1$, the easy axis flux ratio is restricted to two although the film dimension ratio b can be made quite large. With $r = 2$, a receive film of similar shape to film 1 and having four times the easy axis flux of this film, can be utilized. Thus, the use of multiple turns on the drive film is seen to allow greater choice in the shape of the magnetic films. In particular, a square drive film can be used to bias another square, but appreciably larger film. By using the values $r = 1/2$; $t = 1$ it can be seen that a film should be able to bias a film

of the same thickness, defined by $\ell = 1$; $b = 12$. This calculation indicates that, with a single turn on the drive film, a fan-out to twelve films of the same size is conceivable, when each receive film is enclosed by a two-turn loop.

It should be noted that the above fan-out ratio calculations neglect the detrimental effects of such parasitic effects as capacitive currents, eddy currents, loop circuitry, film easy axis dispersion, skew, etc. In fact, there is considerable difficulty in obtaining a fan-out ratio of unity. However, with circuit miniaturization, which alleviates some of these parasitic factors and by improved film characteristics, which will result from further research into film preparation, a fan-out ratio considerably greater than unity should be easily attainable.

The information transfer scheme just studied can be readily adapted to produce a shift register[1], as indicated in Fig. 5.3a. By use of the three-phase drive field system, supplied by other loops (not shown) from a central clock source, information is propagated in the direction indicated, in a manner similar to that described for the two-film case. Since, as already shown, a film can be used to bias an equal or larger film, there is no limit to the length of a recirculating register, which is obtained by coupling the first and final films of the string by a common loop. An open string of films in this configuration can be used as an amplifying device by progressively increasing the size of the films. This latter circuit may have application for the production of relatively large output signals for output devices.

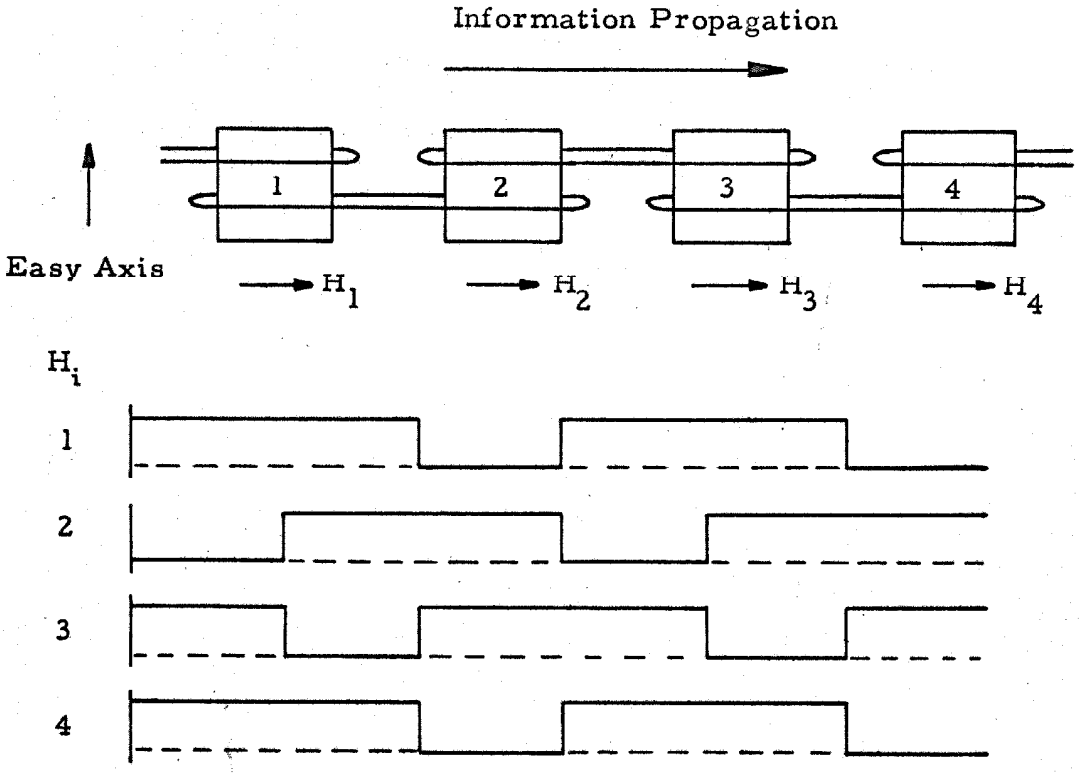

Fig. 5.3a. Shift Register

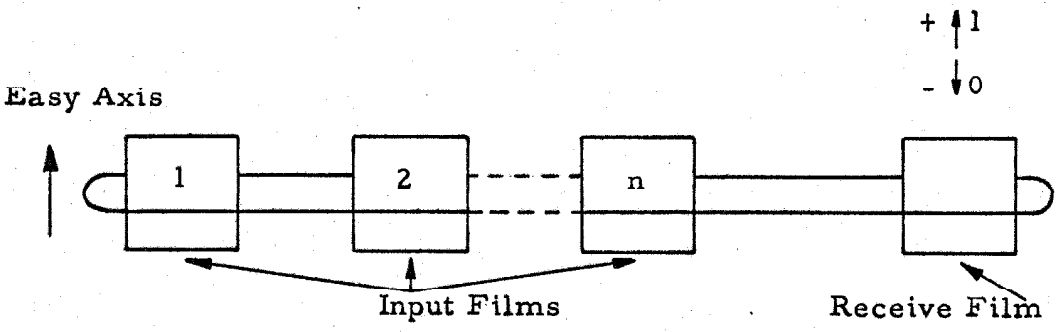

Fig. 5.3b. Logic Element

A circuit which can perform majority logic or AND or OR logic functions is illustrated in Fig. 5.3b. Initially, a number of films 1---n hold the n inputs to the logic gate. By simultaneously driving all these films to their hard axes, a loop current, whose magnitude and direction depends on the initial state of the input films, is obtained. At the same time, a hard axis drive field on the receive film is relaxed. If the loop field is the only bias field present, its direction determines the fallback direction of the receive film and so a majority logic decision is obtained. With an auxiliary bias field which is applied along the negative easy axis of the receive film and which requires positive signals from all input films to reverse the net bias field, an AND logic function is obtained. By reversing the direction of the auxiliary bias field so that a net positive bias field is obtained except when all the input films give negative output signals, an OR logic function is obtained. The complement of any logic signal can be obtained by a film pair in which the coupling loop conductors are transposed in going between the two film elements.

A limit to the fan-in ratio of the AND and OR logic circuits proposed above is set by the requirement that the change in loop field due to one film be sufficient to bias the receive film and that the auxiliary bias field be less than the film coercive force. (Possible creep[24] restricts this latter field still further.) With a minimum loop field of 0.5 Oe and an H_c of 1 Oe, the maximum fan-in ratio is about two. The use of films with a higher H_c can lead to an increase in the value of this ratio. Alternatively, this limit can be significantly increased

by replacing the steady bias field by a pulse field, which is present only during the occurrance of the loop bias field.

Large-Film Deposited Circuitry

The use of integrated deposited circuitry with magnetic films of considerably larger dimensions than the miniaturization limits already established is envisaged in future applications. These applications will arise in the initial stages of development of deposited circuitry, before extreme miniaturization is attempted and in the use of films for output devices where relatively large voltage output signals will be required.

It has been seen in Section IV that the capacitive current fields which occur during nanosecond switching of the experimental film assemblies caused an increase of the order of two in the film switching time. A study of the experimental results led to the conclusion that, for a film of the standard dimensions (0.45" x 0.36" x 1500 A), with an H_K of 3 Oe, loop insulation layers 100,000 A thick and loop conductors of the same size as the film, the effect of capacitive current on film switching should be quite small. Thus, this parasitic effect can be made negligible for films which have quite large flux outputs, and for loop configurations, which can be readily obtained by a deposition procedure.

The slowing effect of the capacitive current may be used to advantage in some applications. In a large array, an increase in switching time is required to allow for the effect of transit times on signals from distant parts of the system. When operated in the transverse switching mode, this increase may be accomplished by use of a film

drive field less than H_K . However, in this case, the flux output also decreases and so the voltage output decreases significantly. By using a drive field greater than H_K and a loop conductor spacing which causes an appreciable capacitive current field, a long switching time may be obtained without any reduction in flux output.

The switching signal observed at the output of a sense loop differs from the signal induced in the loop. For a loop with high impedance termination, two factors which affect the output waveform are the spatial distribution of the induced voltage along the loop and the transmission line attenuation of the loop. These two factors are clearly significant when large magnetic films are used. However, in the case of the standard film assemblies, it has been shown in Section III that the effect of both factors in slowing the observed switching signal is quite small. In general, the spatial voltage distribution only causes significant lengthening of a pulse, when the electrical length of the excited loop is more than 10% of the pulse width. For shorter loops, a loop attenuation of at least 10 db is required to produce a significant effect on the switching waveform. With a low-loss dielectric, such as silicon monoxide, the attenuation is due primarily to resistive losses in the loop conductors. For the standard film assembly, an attenuation of 10 db corresponds to the use of conductors, which have thicknesses less than 4000 Å. In addition to avoiding the use of very thin conductors the line attenuation can be further decreased by increasing the line impedance. This increase can be achieved by use of larger conductor separation and/or insulating material of lower capacitivity. This

latter procedure has the added advantage of decreasing the loop electrical length and so decreasing the effect of the spatial voltage distribution. The factors which affect the rise time of a pulse inserted into a deposited loop coupling a magnetic film are the loop length, determined by the film dimensions, and the loop attenuation. The effect of these factors is, in a general way, similar to their effect on the output waveform of a sense loop. Thus, loop passive circuit effects can be kept small for films with quite large dimensions.

Due to the low characteristic impedance and appreciable series resistance of a deposited transmission line, high attenuation may be obtained in quite a short length of line and may thus restrict the physical size of integrated circuit arrays. As an example, the attenuation of a line having the conductor separation and thicknesses of the standard film assembly is about 288 db/ft. However, this figure can easily be reduced to a more acceptable value by suitable design. Using silver conductors, each 20,000 A thick and separated by a distance of 200,000 A, an attenuation of about 7 db/ft is obtained. The attenuation of this line can be still further reduced by operation at a reduced temperature (e.g., at -200°C, the value is less than 2 db/ft) while operation of a line with the conductors in a superconducting state [6] reduces ohmic losses very significantly and may be advisable for pulse transmission over long distances. Under these conditions, the losses in the dielectric material become important in determining the line attenuation. Thus, the interconnection of film elements over reasonably long distances(of the order of 1 ft) is quite feasible without incurring excessive attenuation.

Conclusions

The potentialities of magnetic thin films can best be attained by the use of these elements in an integrated deposited circuit configuration. Due to the close film-loop coupling of this configuration, extreme circuit miniaturization can be achieved. This miniaturization enables the parasitic effects of loop capacitance and loop circuitry on film switching to be made quite small. In addition, the effect of signal transit time and deposited transmission line attenuation is kept small by bringing various film elements close together. However, large-film deposited circuitry is also feasible since, by suitable layer design and operation at a reduced temperature, the above parasitic effects and the line attenuation can be kept within reasonable bounds for film sizes of the order of 1 cm^2 and for circuit array sizes of the order of 1 $ft.^3$.

When deposited circuitry is operated at a temperature of about $10^{\circ}K$, the limiting film size is about 14 microns. Existing deposition procedures involving photo-etching techniques, are capable of producing line widths down to 1/2 micron and so are quite adequate for the deposition of miniaturized circuitry, including conductor widths down to 10% of the film size, as may be required for minimization of eddy current fields. The insulation layer thicknesses, corresponding to these very small film sizes, are of the order of a thousand angstroms. These small thicknesses will require the development of better insulator deposition techniques, since it has been seen that silicon monoxide (an otherwise suitable material) is liable to develop pinholes in layers less than 50, 000 A thick.

A set of logic elements, suitable for fabrication in a deposited configuration, has been shown to be capable of reasonable fan-in and fan-out ratios. The successful design of these elements is dependent on the operation of an elementary information-transfer scheme. The minimum time of operation of these elements is limited by the fallback time of film magnetization from the hard axis to the easy axis and so is of the order of 2 nsec. Attainment of this limiting operating speed is dependent on the production of films with more ideal characteristics than presently available but, with continued research along these lines, cycle times of 10 nsec or less should be possible.

VI EXPERIMENTAL EQUIPMENT AND METHODS

Film Assembly Fabrication

The film assemblies, which were made by a vacuum deposition process, consisted of permalloy films closely coupled by, but insulated from, conducting loops. Aluminum was chosen for the conducting material of the loop since it has good electrical conductivity and forms a tough film layer. (Although the oxidation rate of aluminum is high, the oxide layer formed is very thin and does not significantly affect the electrical properties of the material.) Silicon monoxide was used for the insulation material of the configuration, since it is relatively easy to deposit and has high leakage resistance.

The deposition of complete assemblies was effected without opening the vacuum of the system. This procedure minimized contamination of the various layers. The patterns deposited were determined by masks interposed between the various material sources and the substrates. The film assemblies were made four at a time. In this way various loop configurations having corresponding layers of equal thickness were associated with identical magnetic films. The assemblies were deposited on plane glass substrates, made from microscope slides. During the permalloy and silicon monoxide depositions the substrates were held at 300°C. The aluminum was deposited on a cool substrate. The pressure in the system during the assembly deposition was of the order of 10^{-4} mm. H_g.

The magnetic film was deposited from a slug of nickel-iron alloy (83% Ni, 17% Fe, by weight) contained in an alumina crucible and

heated by an induction heater. A steady 40 Oe field in the plane of the substrates was used to determine the direction of each film easy axis. This field was aligned parallel to the deposited loop axis with an accuracy of $\pm 1^{\circ}$ and had a maximum variation in direction of $\pm 0.2^{\circ}$ over the entire surface of the substrates. This field was present from the beginning of permalloy deposition until the substrates had been cooled to room temperature just prior to their removal from the deposition system.

Figure 6.1 shows a plan view and sectional elevation of a typical film assembly. The dimensions shown on the plan view are exact, while those on the elevation are nominal, varying with the deposition and the test requirements of the assembly. Each layer of material had at least one edge which was deposited directly on the glass substrate. This edge facilitated interferometric measurement of layer thickness, when needed. The tab of the permalloy layer was also used to determine the insulation between the conducting loop and the magnetic film. The output of the loop was measured between the ground plane conductor and the end tab on the loop conductor. The easy axis direction was along the loop axis so that, with the drive field applied perpendicular to the loop axis, switching occured in the transverse mode.

Static Film Assembly Measurements

A number of static measurements were made on the fabricated film assemblies to determine their suitability for the various switching experiments. Using a low frequency (20 cps) hysteresis loop tracer, the easy and hard axis loops were observed and the values of H_c and

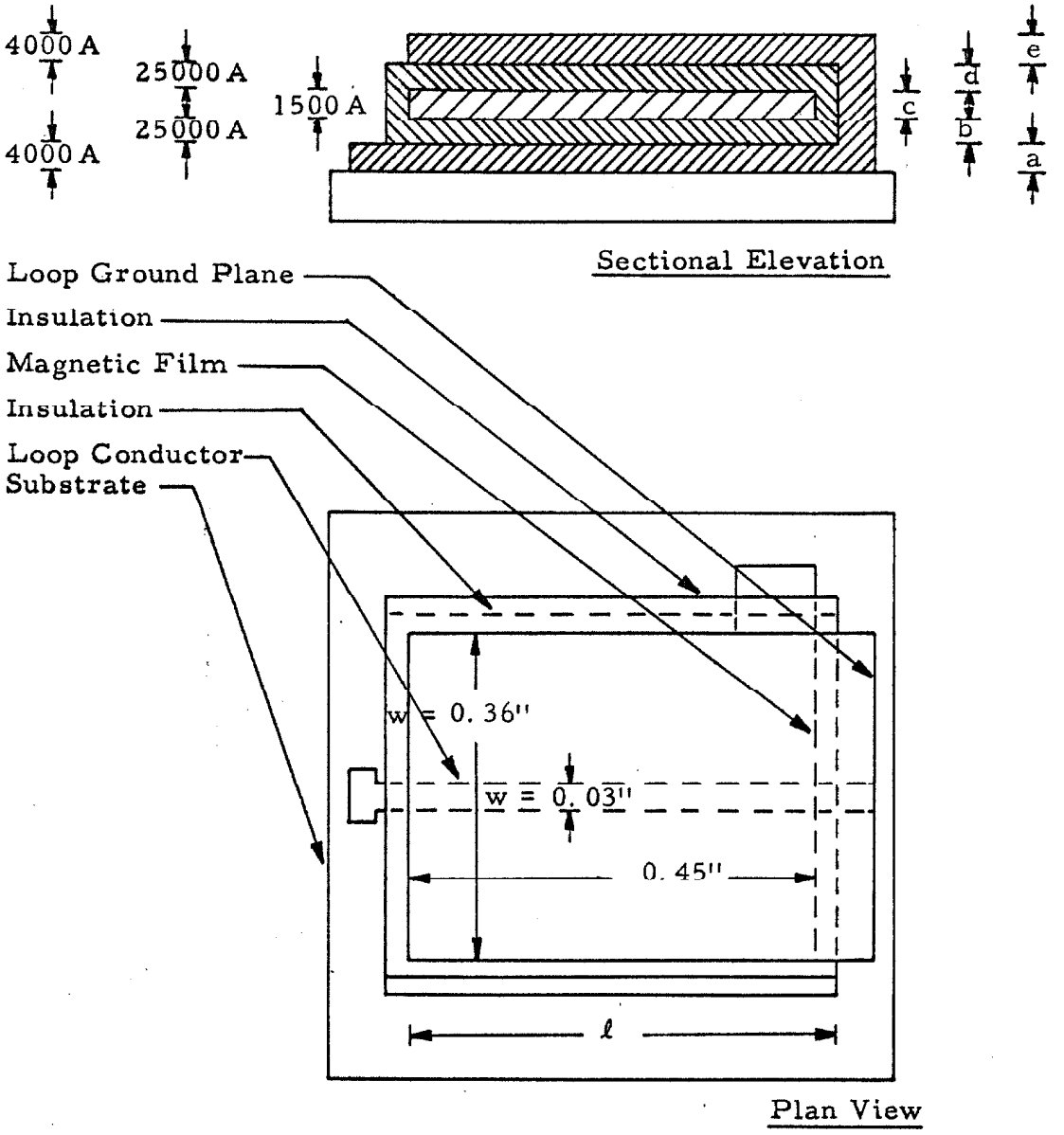

Fig. 6.1. Film Assembly Configuration

H_K were noted. (The quantity H_K was defined as the value of applied field, corresponding to the intersection of the extrapolated low drive slope and the saturation flux density.) Good magnetic films had very square easy axis loops and closed hard axis loops. In general, it was required that both B-H loops be similar to those for the other films of the set. The values of H_K obtained mostly ranged from 3 Oe to 6 Oe, although some films with considerably higher H_K values occured. In assemblies designed for switching speed experiments, a low H_K (3 Oe to 4 Oe) was preferable in order to obtain a short switching time with the maximum drive field of 7-1/3 Oe, and usable signals with drive fields down to about 2 Oe. When the assemblies were designed specifically for flux measurements, a wider range of H_K was considered acceptable but, in general, a film with $H_K > 6$ Oe was discarded, owing to excessive drive requirements. Since the films were operated in the transverse switching mode only, the value of H_c was not critical. (Measured H_c values ranged from 0.5 Oe to 2 Oe.) The relative orientation of the film axes and the deposited loop axis was also determined by means of the hysteresis loop tracer. This measurement was accomplished by rotating the assembly relative to the drive field until the hard axis loop was obtained in its most symmetrical form and then observing the angle between the deposited loop and the drive field. Assemblies having film axis deviations less than 1^o were found to be suitable for switching experiments. Film assemblies with larger deviations had very unsymmetrical output signals when switched from both directions of the easy axis.

The insulation resistance between the loop conductors and the magnetic film was measured by means of an ohm-meter, using indium test probes to avoid damage to the assembly layers. For many assemblies, the value obtained was of the order of 100 k Ω. However, frequently assemblies had an insulation resistance of a few ohms. These low values were due to pinholes in the silicon monoxide layers, thus allowing contact between the magnetic film and the other conductors. Application of about 20 V between the two conducting materials usually resulted in increasing the insulation resistance to an acceptable value (> 10 k Ω), by burning out the regions of low resistance. During this process, the pinholes were evidenced by a momentary scintillation at various parts of the assembly.

The resistance of the deposited loop was also measured. Due to oxides formed on the aluminum the measured resistance was usually greater than the calculated series resistance of the conductors. These oxides formed on the exposed surfaces of the loop conductors and at the interface of these conductors. In many cases, high interface resistance was very much reduced by exerting mechanical pressure on the assembly in this region, by a block of soft metal such as indium. Excessive oxide formation on the exposed surfaces of the conductors was removed without damage to the assembly by rubbing with 4/0 emery paper. Assemblies with measured loop resistances in the range of 1 to 5 Ω were considered most suitable for switching experiments.

Film Switching Test System

The switching properties of the film assemblies were investigated by means of a test system, in which both pulse and static magnetic fields were applied to the magnetic thin film. The resulting film output, a magnetic flux change sensed by linkage with a conducting loop, was obtained in both unintegrated and integrated form by use of a sampling oscilloscope and integrator unit. A general description of the test system is followed by a more detailed account of some of the system components.

A block diagram of the test system is shown in Fig. 6.2. The coaxial charge cable, charged by the high voltage, high output impedance D. C. power supply, was discharged by a relay with mercury-wetted contacts. This arrangement gave a fast-rising pulse (rise time < 1 nsec) which traveled along the strip line containing the test assembly and was absorbed in the matching load. This pulse produced a fast-rise magnetic field in the test region of the strip line. Cancellation of the earths magnetic field in this region was accomplished by a suitably oriented current-carrying coil while static magnetic fields were applied in the plane of the assembly by means of Helmholtz coils. The relay control circuit, which drove the mercury relay at a 60 pps rate, also drove a reset coil, which produced a suitably phased magnetic reset field for resetting the film magnetization to a definite condition before each drive pulse was applied. The repetitive film output signal was monitored on the sampling oscilloscope, which was triggered by a signal derived from the drive field pulse. The analog output of this

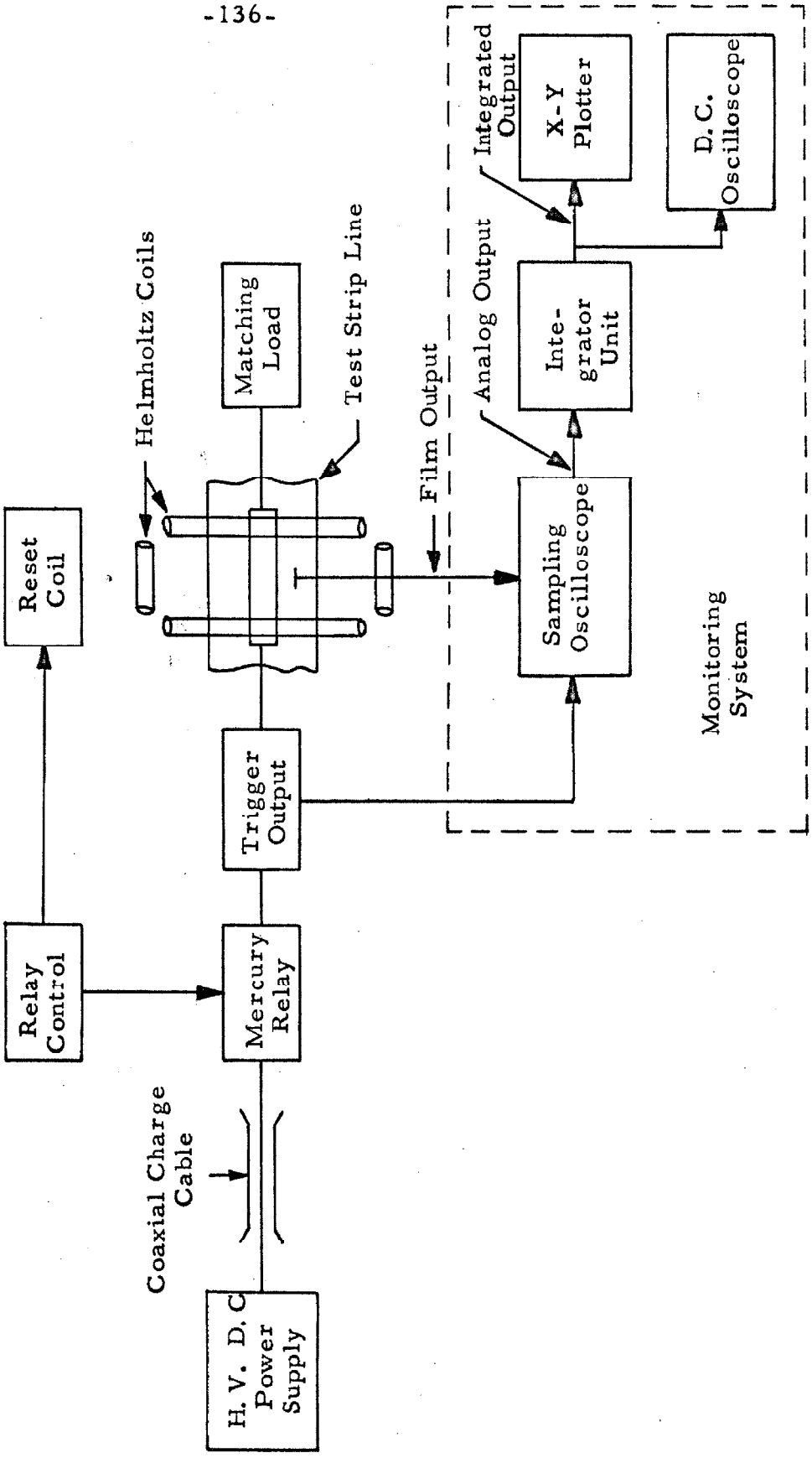

Fig. 6.2. Film Switching Test System

oscilloscope was integrated in the integrator unit and the resulting time variance of observed film flux was recorded on the X-Y plotter and the D. C. oscilloscope.

The power supply consisted of a conventional tube rectifier circuit, fed from the output of a step-up transformer, whose primary voltage was controlled by means of an auto-transformer. The open circuit voltage of the supply was continuously variable from zero to 10 kv. A voltmeter, consisting of a D. C. milliammeter and a wire-wound resistor, was used to measure the output voltage and, after calibration of the magnetic drive field, to measure the magnitude of the magnetic field in the test region of the strip line. The output impedance of the supply was required to be very large compared to the 52 Ω charge cable impedance and so a 52.5 k Ω non-inductive resistor was inserted in series with the supply output. This resistor, consisting of three 17.5 k Ω Dalohm NH resistors, each rated at 250 W, also limited the short-circuit current flow of the supply to a reasonable value.

The charge cable consisted of Belden RG-8/U 52 Ω coaxial cable. The cable length was 300 ft. and, since the output pulse had a width equal to twice the electrical length of the charge cable, a pulse width of about 1 μsec was obtained. The capacitance of the charge cable was 0.02 μf, giving an RC time constant of about 1 msec in association with the power supply output impedance. The discharge relay was open for about 10 msec in each cycle and so the cable voltage at the time of relay closure was very close to the supply voltage at that time.

The mercury relay was the glass-encapsulated portion of a

Western Electric D-168479 relay mounted in a coaxial holder fitted with a drive coil, and inserted into the coaxial line between the charge cable and the test strip line. The normally-open contact of the relay was used in the circuit, so that the charge cable was discharged when the relay was actuated. The relay drive coil was driven by a 60 pps rectangular voltage, supplied by the relay control circuit and synchronized to the utility line frequency. Use of a mercury relay resulted in an output pulse having a rise time of less than 1 nsec. The voltage applied to the relay contacts ranged up to 5.5 kv and the relay operated quite satisfactorily under these conditions, except for a tendency to close somewhat erratically at the upper end of the voltage range.

The trigger take-off consisted of an electrostatic probe which picked off a signal from the output line of the mercury relay. The electric coupling of the probe to the coaxial line was very low and so the probe did not noticeably affect the signal passing down the line.

Two views of the test strip line are shown in Fig. 6.3. The line was designed to have a characteristic impedance of 52 Ω so that the pulse from the charge cable traveled along the line with no reflection at the junctions. The transition between the coaxial and planar strip line geometries was aided by the tapering of the ground planes at both ends of the strip line. The test region of the strip line, where the magnetic film samples were placed, was centered at the mid-point of one of the ground plane walls, since this region has the maximum magnetic field uniformity in the line. The films and their associated test probes and loops were mounted on 3-3/4" diameter assembly holder

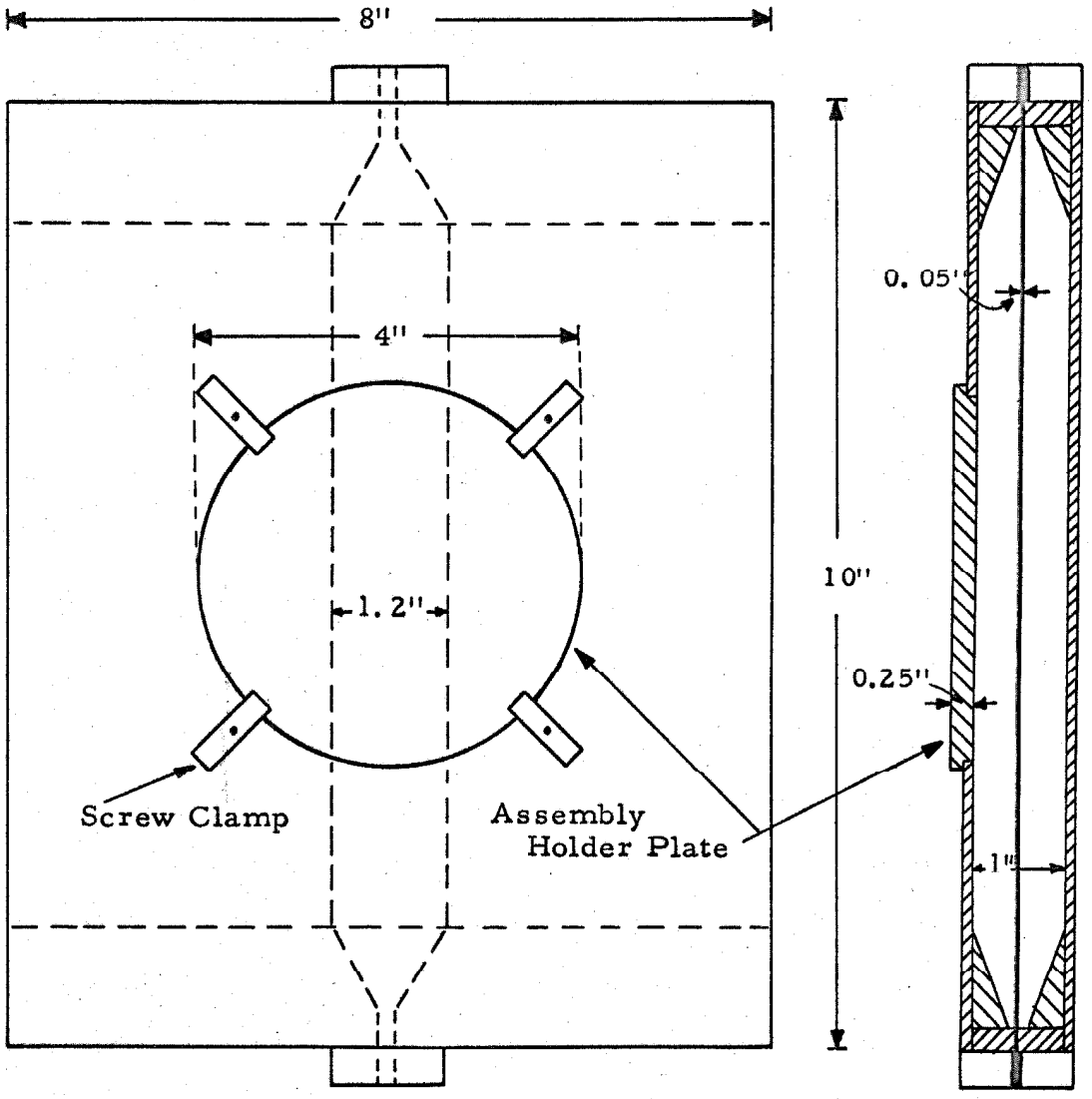

Fig. 6.3. Test Strip Line

plates, which fitted flush with the inner surface of one ground plane wall and were secured in place by four screw clamps. The diameter of the plates was made quite large in order to minimize the disturbance in the electromagnetic field, due to the discontinuity in the ground plane. The details of the test circuitry mounted on the plates are given later.

The matching termination for the strip line was a 51.5 Ω Termaline Coaxial Resistor, Model 81 BHN (Bird Electronics Corporation) with 80 W dissipation rating, and was connected to the strip line by 8 ft. of RG-8/U cable. When terminated in a matching load, the field calibration was experimentally determined to be 1.33 Oe/kv (the method of calibration is outlined later). Using a maximum charging voltage of 5.5 kv, a 7-1/3 Oe magnetic field is obtained. When it was desired to obtain higher drive fields than 7-1/3 Oe, a shorting plug was used at the end of the strip line. This termination resulted in an in-phase reflection of the current wave on the line, thus doubling the magnetic field in the test region. Since this region was not at the position of the shorting plug, the rise time of the current wave to its final value was longer than the rise time of the incident wave. For this reason the use of the matching termination was preferred, except for tests where only the final magnitude of the field was important. The charging voltage was limited to 3.5 kv, when the shorting plug was used. This charging voltage gave a field of 9-1/3 Oe in the test region of the strip line.

A reset field, having a maximum amplitude of 10 Oe, was produced in the test strip line by means of the reset coil. This coil was driven by an unsmoothed half-wave 60 cps rectified output voltage,

supplied by the relay control circuit. Correct phasing of the reset field with the drive field was achieved when the drive pulse occured in the off-period of the reset field.

Appropriate external loops and deposited loop probes were mounted on the assembly holder plates. Figure 6.4 shows a typical configuration. One end of the enamel-insulated external loop conductor was connected to the brass plate, while the other end passed through the plate and was attached to a BNC connector, situated on the opposite side of the plate. The copper tubing shielded this conductor from the electric field of the test strip line. Since, in all experiments, the magnetic drive field was applied perpendicular to the loop axis, no air-flux compensation loop was required. In this orientation, the residual pickup signal in the loop was small, being about 25 mv for a drive field of 5 Oe. The assembly substrate was placed between the external loop and the brass plate, with the assembly in contact with the plate. The substrate was held in place by a piece of plastic secured to the plate by plastic screws.

The deposited loop probe consisted of a length of ceramic-covered copper wire. Before insertion in the assembly holder, the end of the probe was ground normal to the axis of the wire to ensure maximum contact area between the probe and the deposited loop conductor and to minimize scratching of the conductor surface. A good probe end was obtained by placing the wire in a hole drilled normal to one surface of a brass block, and then lapping this surface on a flat sheet of Grit No. 360A paper. The probe was pressed into contact with the deposited

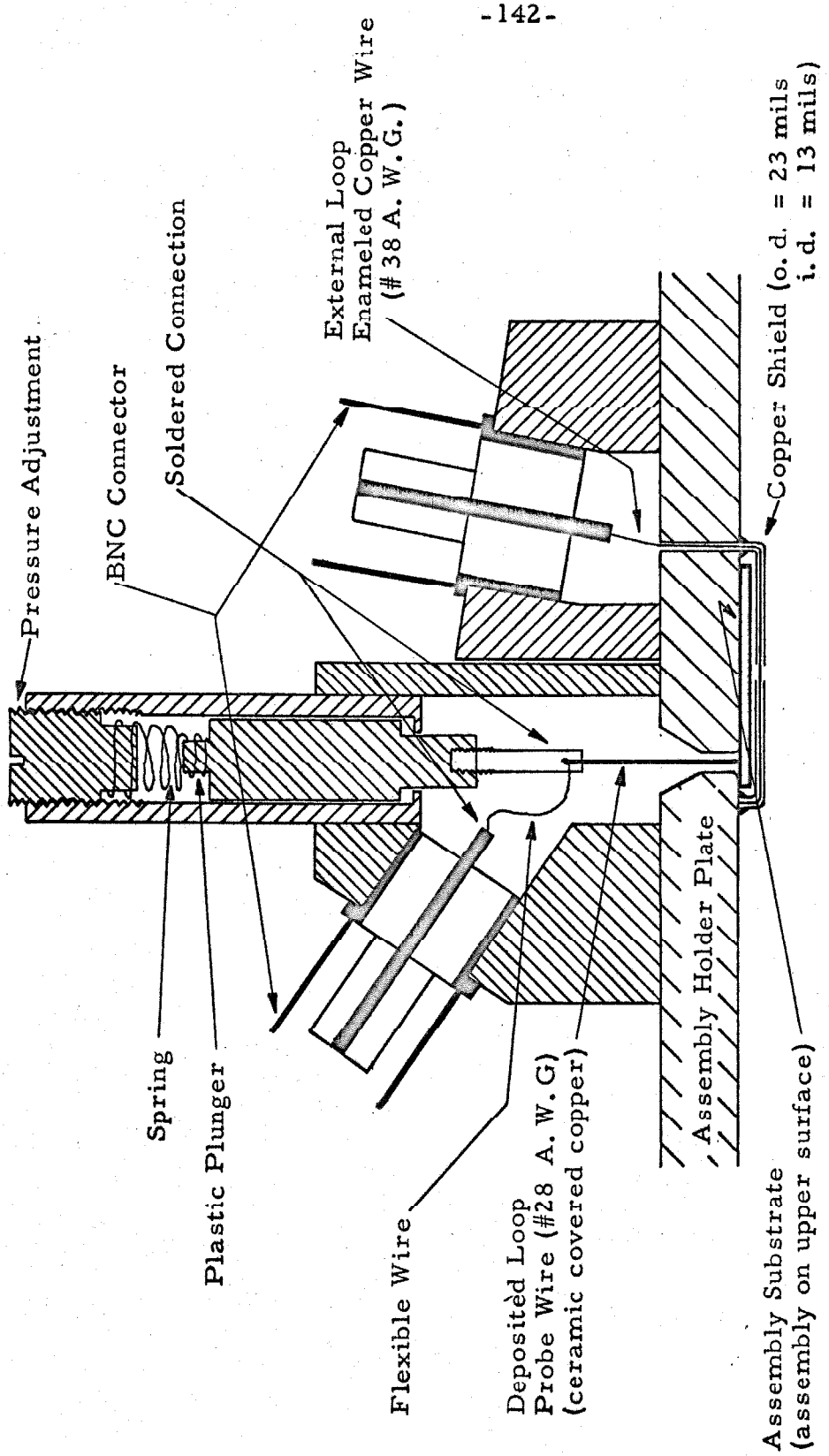

Fig. 6.4. Assembly Holder Plate with Deposited Loop Probe and External Loop

loop conductor by means of the spring and plunger arrangement, illustrated in Fig. 6.4, with pressure adjustment being controlled by the screw top of the plunger barrel. Contact between the probe and the BNC connector was made by a piece of flexible wire to avoid lateral pressure on the probe.

The drive field pickup signal of the deposited loop was measured by blocking film switching by means of a large static blocking field ($\approx$ 150 Oe). This signal, which was electrostatic in nature, varied in amplitude with the total loop resistance, being largest at high resistance values. With a drive field of 7 Oe and a loop resistance of 2 Ω, the signal amplitude was about 50 mv. This low value was due to the close proximity of the film assembly to the strip line ground plane and to the correspondingly very small protrusion of the probe into the strip line field region.

The monitoring system is discussed at length in the next subsection, since it incorporates a new method for the integration of signals having rise times in the nanosecond range. However, the sampling oscilloscope input circuitry is now described since it forms the termination impedance of the monitored loops.

Figure 6.5 is a diagram of the input circuit of one channel of the sampling oscilloscope. (The oscilloscope had two identical channels, thus allowing simultaneous monitoring of the outputs of two loops.) The delay line introduced a 120 nsec delay in the loop output signal relative to the trigger pulse for the sampling oscilloscope. This delay was required to compensate for an internal delay in the oscilloscope sweep

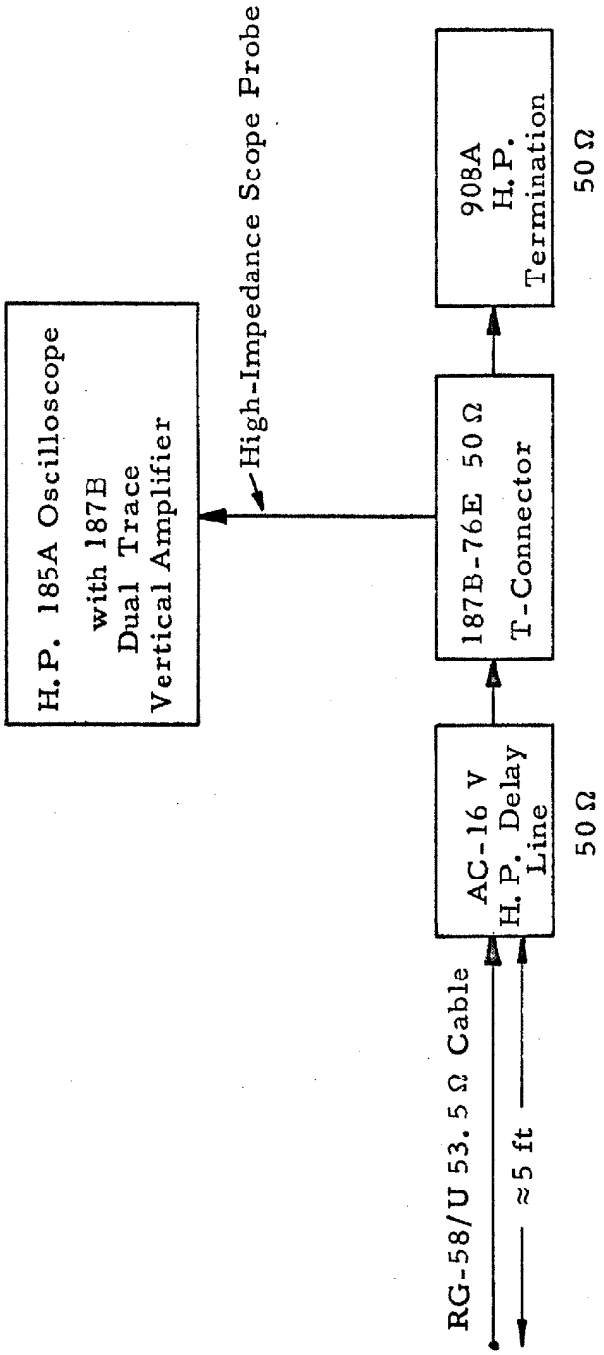

Fig. 6.5. Sampling Oscilloscope (Hewlett-Packard 185A) Input Circuitry

circuit and allowed display of the leading edge of the loop output pulse. The termination impedance of the monitored loop was 53.5 Ω, for pulses with lengths less than 15 nsec. (For longer pulses a small reflected pulse reached the loop due to the slight mismatch of the cable and the delay line.) The advertised response time of the oscilloscope with the vertical amplifier is less than 0.5 nsec. Allowing for the distorting effect of the delay line, which rounds off the upper 20% of fast-rising pulses, an effective response time of 0.8 nsec was assumed for the complete input circuit.

Monitoring System

This system, consisting of a sampling oscilloscope and integrator unit, was designed to effect integration of fast film-switching signals, thus yielding flux waveforms with switching times in the nanosecond range. In contrast to other integration systems which integrate the film output signal, this system integrated a signal similar in shape to the film output signal but having a greatly expanded time scale. This system had an effective response time of 0.8 nsec, which compares to a minimum response time of about 4 nsec for the other schemes indicated above. This system was capable of measuring, with 1% accuracy, the switching characteristics of a film with a flux of 4×10^{-10} volt-sec, when switching in a time of less than 10 nsec. The effective decay time of the system was 4 sec.

General Description - The analog output voltage of the sampling oscilloscope consisted of the superposition of two signals, (a) a stepped waveform, passing through the sample points displayed on the

oscilloscope screen and (b) an offset voltage, corresponding to the centering voltage applied to the oscilloscope deflection plates. With the offset voltage set equal to zero, the integral of the analog output voltage was similar in shape to the flux output of the magnetic film being switched. However, due to drift of the oscilloscope vertical amplifier, initial zeroing of the offset voltage became ineffective in a period of a few minutes and, if uncompensated, would have led to errors of the order of 10% in the measurement of the total flux output of the film.

The integrator unit illustrated in Fig. 6.6a incorporated a circuit which compensated for all relatively long term drift of the oscilloscope (above 8 sec). The operation of this circuit consisted in obtaining a voltage proportional to the offset voltage of the oscilloscope output, during one sweep time, and then utilizing this voltage to cancel out the effect of the offset voltage during the next sweep time while the film output signal was being integrated. The integration cycle was divided into two phases, the compensation and signal phases. These phases are indicated in Fig. 6.6b, which shows the timing diagrams of the relays of Fig. 6.6a, as well as those for two other relays, A and D, necessary for the operation of the system. At the beginning of the compensation phase, the capacitors C_1 and C_2 were discharged so that the output voltages of both integrators were initially zero. During this phase, the input to the sampling oscilloscope was grounded by means of the coaxial relay A_1 and the offset voltage of the analog output, fed through the adder (the other input being grounded) was integrated in

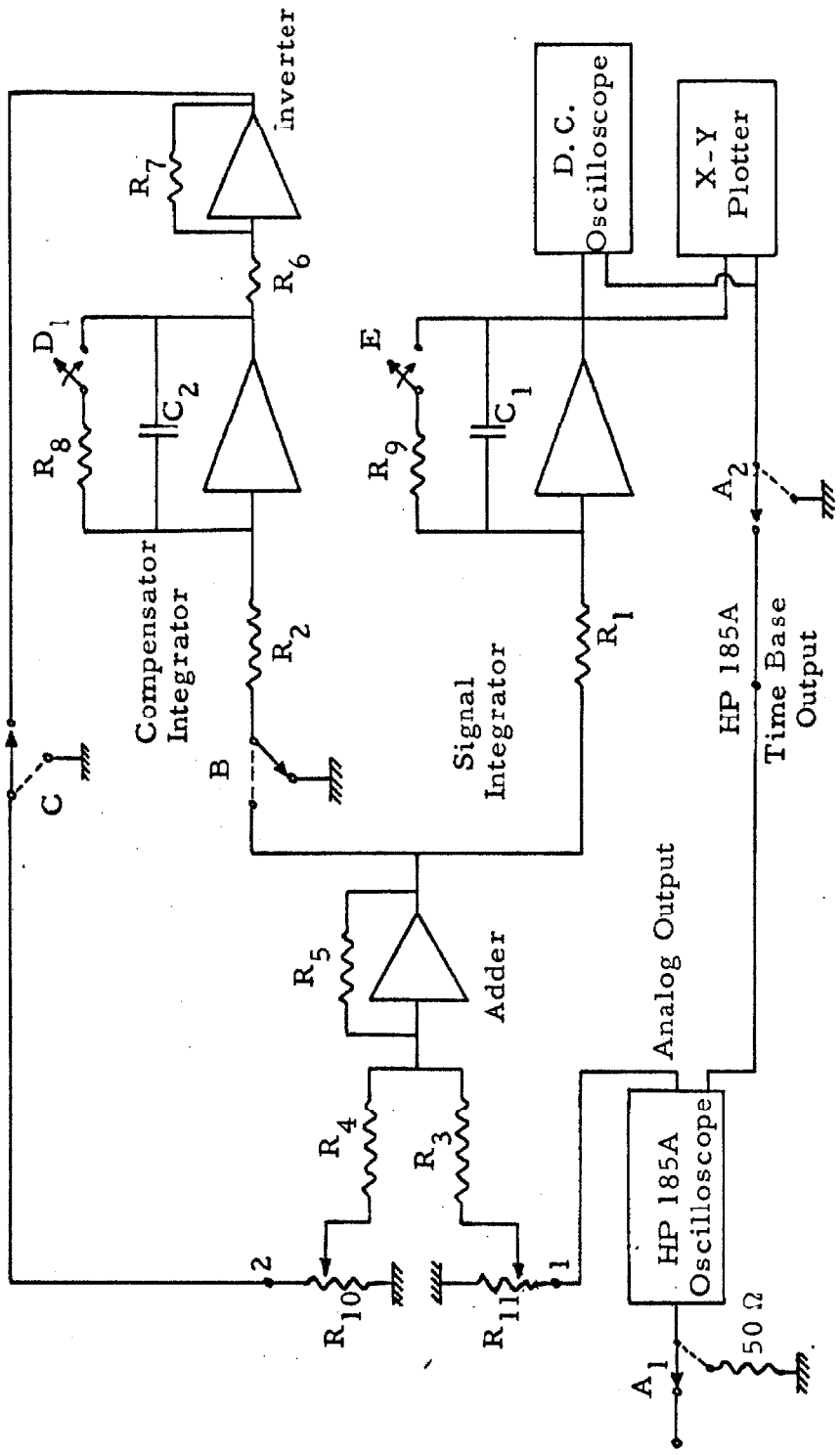

Fig. 6.6a. Monitoring System

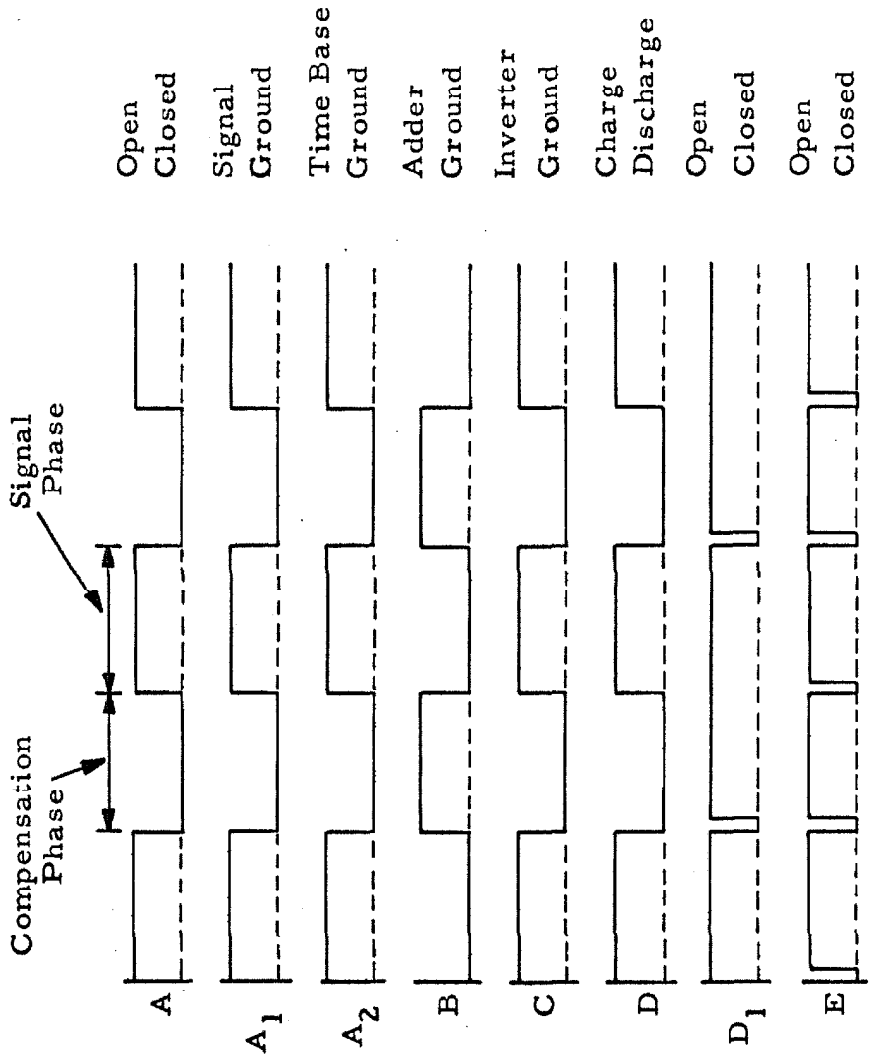

Fig. 6.6b. Timing Diagrams For Monitoring System Relays

both signal and compensator integrators. At the end of this phase, the output voltages of both integrators were proportional to the mean offset voltage of the sampling oscilloscope analog output during this phase.

At the beginning of the signal phase, the capacitor C_1 was again discharged so that the output voltage of the signal integrator was initially zero. During this phase, in which the relay A_1 connected the film output to the sampling oscilloscope, the input of the compensator integrator was grounded and the constant output voltage of this integrator was fed through the inverter to the adder, where it opposed the offset voltage contained in the oscilloscope output. To effect cancellation of this offset voltage, the adder output voltage due to the combined effect of the two above inputs must be zero, thus leading to the condition

$$k_4 = \frac{R_2 C_2}{T} \frac{R_6}{R_7} \frac{R_4}{R_5} \qquad 6.1$$

where k_4 = potentiometer gain setting on input 2 of adder

T = oscilloscope sweep time.

When the above condition was satisfied, the signal integrator output voltage during the signal phase was similar to the output flux of the magnetic film. At the beginning of the next compensation phase, both integrators were discharged and the integration cycle started over again.

The signal integrator output was observed on the D. C. oscilloscope and the X-Y plotter. The flyback time of the plotter was about 1 sec, which was comparable to the sampling oscilloscope sweep time (4 sec). To eliminate recording errors due to the flyback, the time

base output of the sampling oscilloscope was connected to the plotter through relay A_2, only during the signal phase.

Analog Circuit Design - The basic operational amplifier used was the CIT chopper-stabilized D. C. amplifier [25]. It had combined noise and hum voltages of 3 mv with 1 M Ω input and feedback resistors, a drift figure of 2.6 mv/hour with a gain of 100, and an output saturation level of about ±80 V. Wire wound resistors, and polystyrene capacitors having at least 10 M Ω leakage resistance were used in the input and feedback paths of the amplifiers.

The sampling oscilloscope had three sample densities, nominally 1000, 200 and 50 samples per time base trace, thus giving sweep periods of about 17, 3 and 1 sec with an input signal which had a repetition rate of 60 pps. The medium speed sweep having a measured sweep period of about 4 sec, was chosen for the operation of the analog circuit. With this sweep speed the integration period was minimized, while ensuring a sufficiently high scanning density to reproduce the oscilloscope input signal with good accuracy.

The sampling oscilloscope trace had a useful vertical deflection distance of ±5 cm about its mid-position with a corresponding open-circuit analog output voltage of ±1 V. Due to a slow switching component noted in the output of many films, it was found necessary to use a time base period of the order of five times longer than the fast component switching time in order to record the complete flux change. Thus, the signal displayed on the oscilloscope screen was limited to an average value of about ±1 cm deflection over the entire sweep period with a corresponding average open-circuit analog voltage of about ±0.2 V.

Consider first the response of the uncompensated analog circuit, consisting of the adder and signal integrator, to the above equivalent film output signal. Since the source impedance of the oscilloscope analog output equaled the input impedance of the adder, the corresponding signal at the adder input is 0.1 V. Using the component values indicated in Fig. 6.6a, the adder output voltage is 2.5 V and the signal integrator voltage at the end of 4 sec integration time is 50 V ($\approx$ 65% of operational amplifier saturation level).

The circuit components of the compensator loop were chosen to satisfy Eqn. 6.1 with $k_4 = 0.8$. This value allowed a wide range of adjustment for the input potentiometer to achieve correct compensation. For convenience, the compensator integrator was made identical with the signal integrator. Thus, the maximum offset voltage which could be compensated corresponded to about ± 1 cm deflection on the oscilloscope screen.

The relays indicated in Fig. 6.6a were controlled by an auxiliary control circuit (described later). These relays had operating times of less than 40 msec. This time, being about 1% of the time base period, had little effect on the theoretical operation of the analog circuit. The time constants of the discharge circuits of C_1 and C_2 were each 0.2 msec, and so these capacitors were completely discharged, as required, when these circuits were completed for a few milliseconds. The relays in the analog circuit were standard plate circuit relays and the relay A_1, which switched the input signal to the sampling oscilloscope was a coaxial relay with a bandwidth of at least 1 k Mc. This

latter relay was found to cause no observable distortion in the input signal. In operation, the sampling oscilloscope was adjusted so that the film switching analog output signal began not less than 400 msec after the initiation of the time base sweep and so the various relays completed their operation before this signal began.

Analog Circuit Operation - The analog circuit was adjusted for correct compensation in the following manner.

1) When the sampling oscilloscope and operational amplifiers had warmed up and stabilized (at least 1/2 hour), the amplifiers were balanced, observing the output voltage by means of an oscilloscope. The output voltages of the adder and inverter were limited to 1 mv and the integrated output drifts of the integrators were limited to 1 mv/sec.

2) About 0.1 V was applied to adder input 1 from a battery source. During the compensation phase, the output of the signal integrator was a ramp signal rising to a maximum amplitude of about 50 V. During the signal phase, the output of this integrator ideally remained zero, if the correct amount of compensation was used and so the input potentiometer on adder input 2 was adjusted by trial-and-error until the output voltage observed was minimized. (A voltage of about 50 mv was generally achieved.) On reversal of the input signal to the system the output should also reverse. Any failure to do this was an indication of lack of balance in the amplifiers and necessitated a recheck of step 1.

When observing the integrated signal it was noticed that the amplitude varied slightly on succeeding oscilloscope sweeps. Measurements such as amplitude and rise time were most accurately carried

out by allowing the X-Y plotter to trace out the desired signal a number of successive times. The average signal was then quite apparent from inspection of the multiple-trace pattern.

Monitoring System Characteristics - The operational amplifiers of the analog circuit caused negligible distortion of the oscilloscope output signals (amplifier open-loop gain > 10,000 up to a frequency of 500 cps). The effective response time of the system was thus equal to the response time of the sampling oscilloscope, i.e., 0.8 nsec. The 4 sec interval between the ending of one signal integration and the beginning of the next signal integration was taken as the effective decay time of the system.

The compensation loop of the analog circuit was designed to cancel the effect of a steady component in the analog output voltage. Best operation of the system was obtained when the noise and short-term drift (less than 8 sec) of this component were minimized, i.e., on the least sensitive (200 mv/cm) scale of the sampling oscilloscope. Using this scale setting with no oscilloscope input signal but with an offset analog output voltage of ± 0.1 V, it was found possible to limit the output of the signal integrator during the signal phase to ± 100 mv. The ± 100 mv error signal in the integrator output caused a 1% error in the flux measurement of a film which produced a 10 V signal at the same point. This 10 V signal would result from a steady 40 mv input signal to the oscilloscope and thus, on the 1 nsec/cm scale, from a film with a flux output of 0.4×10^{-9} volt-sec. When the oscilloscope was used on more sensitive scales it was found that the noise and short term drift of the

analog output increased. These factors resulted in larger residual output voltages from the signal integrator. It was concluded that the performance of the compensation loop deteriorated for a vertical scale sensitivity greater than 50 mv/cm.

With a repetitive film switching signal being monitored on the sampling oscilloscope the final amplitude of the signal integrator output was found to be subject to some variation. Although some of this variation resulted from noise and short term drift in the oscilloscope, the major part of this variation was attributable to a change in the time base period due to occasional mis-triggering of the sampling oscilloscope. This mis-triggering consisted of a failure to trigger when the trigger level was low or of additional triggering when the trigger level was high. The latter effect was due to a spurious trigger signal, following the normal signal by a few microseconds. This spurious signal occurred only at high values of the test strip line drive field (above 3.5 kv charging voltage). On many occasions, it was found extremely difficult to adjust the trigger level for normal operation of the oscilloscope time base.

Auxiliary Control Circuit - The auxiliary control circuit which controlled the relay contacts of the monitoring system is illustrated in Fig. 6.7. The drive for this circuit was derived from the time base output of the sampling oscilloscope. This signal had a maximum amplitude of + 12 V, starting from zero at the beginning of the oscilloscope sweep. The input RC network was chosen to effect differentiation of this signal giving a negative pulse of about 25 msec duration, when

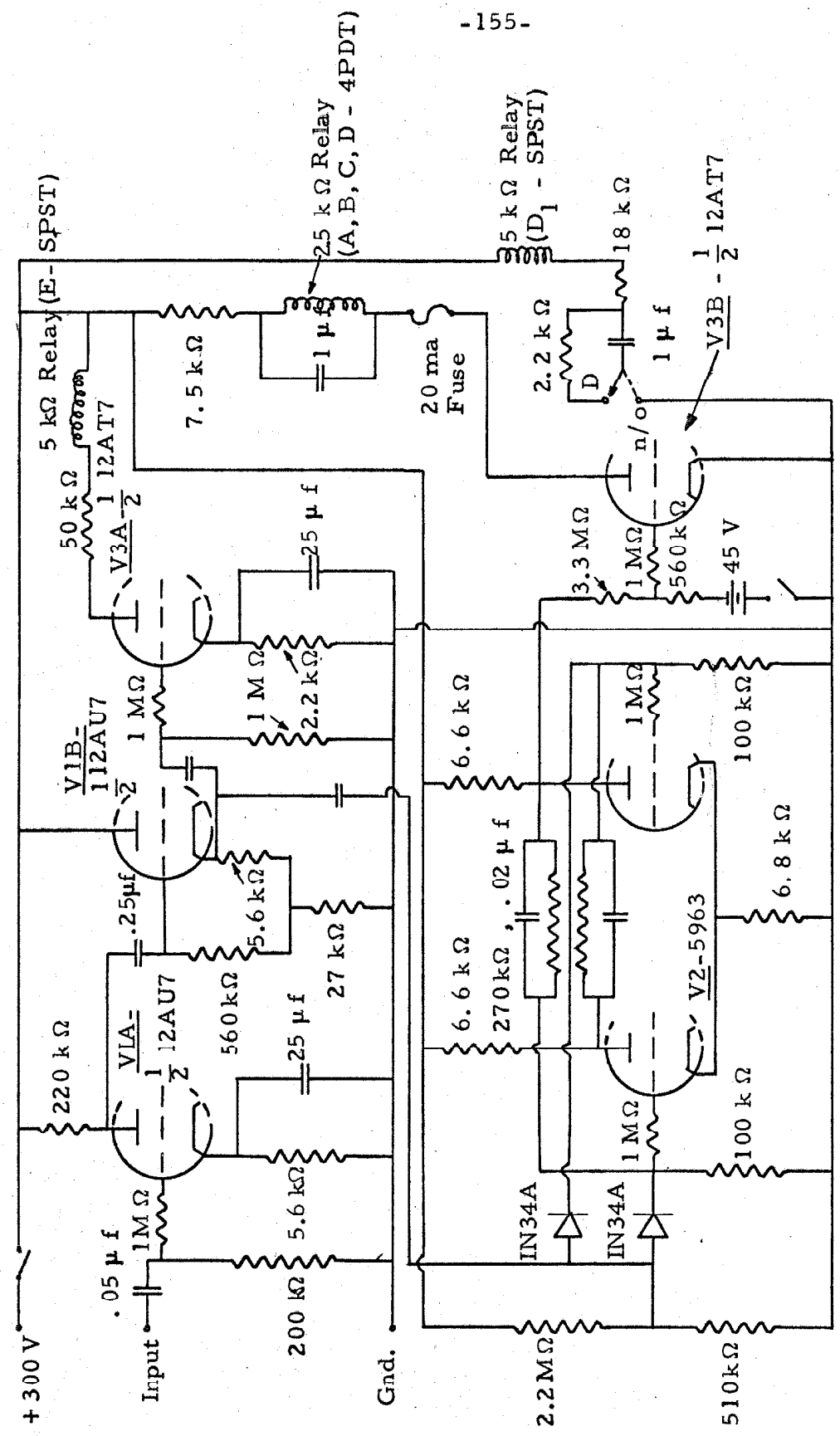

Fig. 6.7. Auxiliary Control Circuit for Monitoring System Relays

time base flyback occurred. This pulse was amplified and inverted by V1A and was fed through the cathode-follower V1B. The cathode-follower drove a single-pole relay E (see Fig. 6.6a, b) in the anode circuit of V3A, whose current was insufficient to operate the relay except during the occurrance of the positive pulse from the cathode-follower.

The cathode-follower also drive the flip-flop V2. The square-wave output of the flip-flop operated a four-pole double throw relay in the anode circuit of V3B, which swung between cutoff and full-on states as the flip-flop changed state. The four sets of contacts of this relay were designated A, B, C, D respectively (see Fig. 6.6a, b). Relay contacts A were in the drive circuit of the coaxial relay A_1, and of relay A_2. Contacts B and C were used in the analog circuit, as indicated in Fig. 6.7. By driving D_1 through the differentiating circuit, the relay closed for a short period of time each time contacts D closed (to the normal-open position).

Calibration of Drive Field Circuit of Test Strip Line

The magnitude of the magnetic drive field in the test region of the strip line depended on the charging voltage of the charge cable. With a matching termination on the strip line, a calibration value of 1.33 Oe/kv charging voltage was obtained for the drive field circuit in the following manner.

An electrostatically-shielded loop was inserted in the test region of the strip line with its axis parallel to the drive field. The output

voltage of this loop, due to the change in flux linkage of the drive field, was integrated in the monitoring system. The flux, corresponding to the final value of the monitoring system output voltage, was determined by integrating a calibration pulse of known area in the same system. (As shown in Appendix B, the ratio of the measured flux to the flux linkage of the loop depends only on the steady state attenuation of the loop and its termination impedance.) On dividing the flux linkage value by the loop cross-sectional area, the corresponding magnetic field strength was determined. The calibration value stated above was obtained from the mean of a number of measurements, taken at various magnetic field strengths and was estimated to have an accuracy of at least 5% over the entire range of drive field voltages.

Basic Procedure for Film Assembly Switching Experiments

Two different methods were used to align the external loop and the film assembly with the drive field. The choice of method depended on whether the deposited loop output was being monitored. If the outputs of both loops were required, the deposited loop was first visually aligned in the same direction as the external loop, with the deposited loop conductor tab directly over the loop probe. After clamping the substrate in position and obtaining satisfactory contact between the deposited loop and its probe, the assembly holder was inserted in the test strip line. A steady blocking field (about 150 Oe) was applied in the plane of the film by means of the horizontal Helmholtz coil to block any response of the film to the drive field. The output of the external loop was then mainly due to magnetic drive field pickup in the loop. The

assembly holder was rotated until this pickup voltage was minimized. The external loop axis was then perpendicular to the drive field and thus the film easy axis was also perpendicular to this field, if the easy axis was exactly parallel to the deposited loop axis. The magnitude of the residual output voltage of the loop, due to electrostatic pickup and other causes was of the order of 10 mv, for a drive field of 2 Oe. This voltage is small, compared to an output voltage of the order of 1 V when the magnetic film (> 1000A thickness) was switching under the influence of the same field. The output signal of the deposited loop was also observed when the film switching was blocked. This signal, which was mainly electrostatic in nature, was of the order of twice the magnitude of the external loop signal and so was small compared to the film switching signal.

When the film flux change was observed only by means of the external loop, the alignment method for the external loop and the film assembly was much simpler. With no film assembly present, the film holder was first rotated in the strip line wall until the external loop voltage was minimized. The film assembly, taped to the center of a length of 1/16" diameter glass rod, was inserted in the external loop and was visually aligned with the loop by adjustment of two supports on which the glass rod rested. This procedure facilitated a rapid change of film assemblies, but its use was somewhat limited as the exact position of the film assembly relative to the strip line ground plane was not known.

Application of either of the two above methods results in the

external loop axis being accurately aligned ($\pm 0.1^{o}$) perpendicular to the drive field. Ideally, the film easy axis and the deposited loop axis are then also perpendicular to the drive field. In this case, reversal of the reset field, which is directed along the easy axis, reverses the output voltages of the loops with the corresponding waveforms and the net flux changes remaining unchanged. When the drive field exceeds H_K, the Stoner-Wolfarth model [23] predicts that the final position of the film magnetization with the drive field still present is along the film hard axis. The net flux change during switching then attains its maximum value, being unchanged by any further increase in the magnitude of the drive field.

When the film hard axis is not aligned exactly with the drive field direction the film switching waveform and the net flux switched are dependent on the easy axis direction from which the film magnetization is switched. The effect of this misalignment on the flux switched may be predicted by means of the Stoner-Wolfarth model. The details of this calculation are given in Appendix D and the results obtained are shown in the following table. These results indicate the effect of applying a normalized field $h = H/H_K$ perpendicular to the sensing loop axis when the film hard axis makes an angle β with the direction of the drive field. The quantity θ is the angle that the final direction of the film magnetization makes with the easy axis and the quantity F is the ratio of film fluxes obtained on switching the magnetization from both directions of the easy axis. It is seen that, for fields of the order of H_K, slight misalignment of the film hard axis has a large effect on

θ^{o}

β^{o} \ h	1.0	1.5	2.0	2.5	3.0
1	71.43	87.01	88.00	88.33	88.50
2	66.69	84.08	86.01	86.67	87.00
3	63.40	81.24	84.04	85.02	85.51
4	60.79	78.54	82.09	83.37	84.02
5	58.59	75.99	80.18	81.74	82.54

F

β^{o} \ h	1.0	1.5	2.0	2.5	3.0
1	0.536	0.933	0.966	0.977	0.983
2	0.467	0.872	0.933	0.955	0.966
3	0.428	0.817	0.902	0.933	0.949
4	0.402	0.770	0.872	0.912	0.933
5	0.383	0.728	0.844	0.892	0.917

the final position of the magnetization and on the flux ratio. A misalignment of only 1^{o} results in a flux ratio of about 0.5 for a drive field h equal to unity.

Misalignment angles of a few degrees were commonly encountered in the film assemblies and so the loop output signals obtained on reversal of the reset field were often quite different. However, when $H > H_K$, Appendix D (Eqn. D-2) indicates that the mean value of the two flux changes is within 1/2% of the film flux for misalignment angles less than 5^{o} and this mean value was used as a measure of the flux

switched. In addition to compensating for the effect of misalignment of the film axis, the use of this mean value canceled out integrated signals caused by loop pickup, since such signals added to one flux value and subtracted from the other value. When the total film flux was the only quantity of interest, a drive field of 9 Oe was used to switch the film. This field corresponded to a value of $h \geq 1.5$ for films having H_K values up to 6 Oe and resulted in flux ratio values close to unity (0.9 to 1.1 was considered an acceptable range of values). The distortion of the drive field waveform, due to the finite distance between the film assembly and the strip line shorting plug produced complex film switching waveforms but did not affect the total flux switched.

The easy axis alignment has been shown to be a critical factor in determining the amount of film flux switched. Clearly, also, accurate measurement of film switching times required the use of films whose axes were aligned accurately with the loop axes. A $\pm 1^{\circ}$ tolerance was found to result in flux signals having reasonable symmetry at all drive fields on reversal of the reset field direction. The switching time was measured for both reset field directions and the average value was taken as the experimental switching time.

APPENDIX A

EVALUATION OF THE TRIPLE INTEGRAL OF EQN. 2.3

$$I_1 = \int_o^{a/2} \int_{-b/2}^{b/2} \int_o^h \frac{dx_1 dx_2 \, dy}{[(\ell/2)^2 + (x_2 - x_1)^2 + y^2]^{3/2}} \qquad A\text{-}1$$

Integrating first with respect to y , by the use of integral tables [26]

$$I_1 = h \int_o^{a/2} \int_{-b/2}^{b/2} \frac{dx_1 \, dx_2}{[(\ell/2)^2 + (x_2 - x_1)^2][(\ell/2)^2 + (x_2 - x_1)^2 + h^2]^{1/2}} \qquad A\text{-}2$$

Since the kernel of this double integral is a function of $(x_2 - x_1)$ only, I_1 may be readily evaluated by introduction of the new coordinate $x_3 = (x_2 - x_1)$. As indicated in Fig. A-1, integration with respect to x_1 and x_2 over the rectangle defined by $x_1 = 0, \ldots, a/2$; $x_2 = -b/2, \ldots, +b/2$, is replaced by integration with respect to x_3 over the same area defined by $x_3 = -(b+a)/2, \ldots, +b/2$ and appropriate elemental areas dA . Two cases result, dependent on whether b is greater than or less than a/2. Since the loop dimension b is greater than the film dimension a , the case $b > a/2$ is considered first and is illustrated in Fig. A-1. The integration is divided up into three regions of x_3 , as follows.

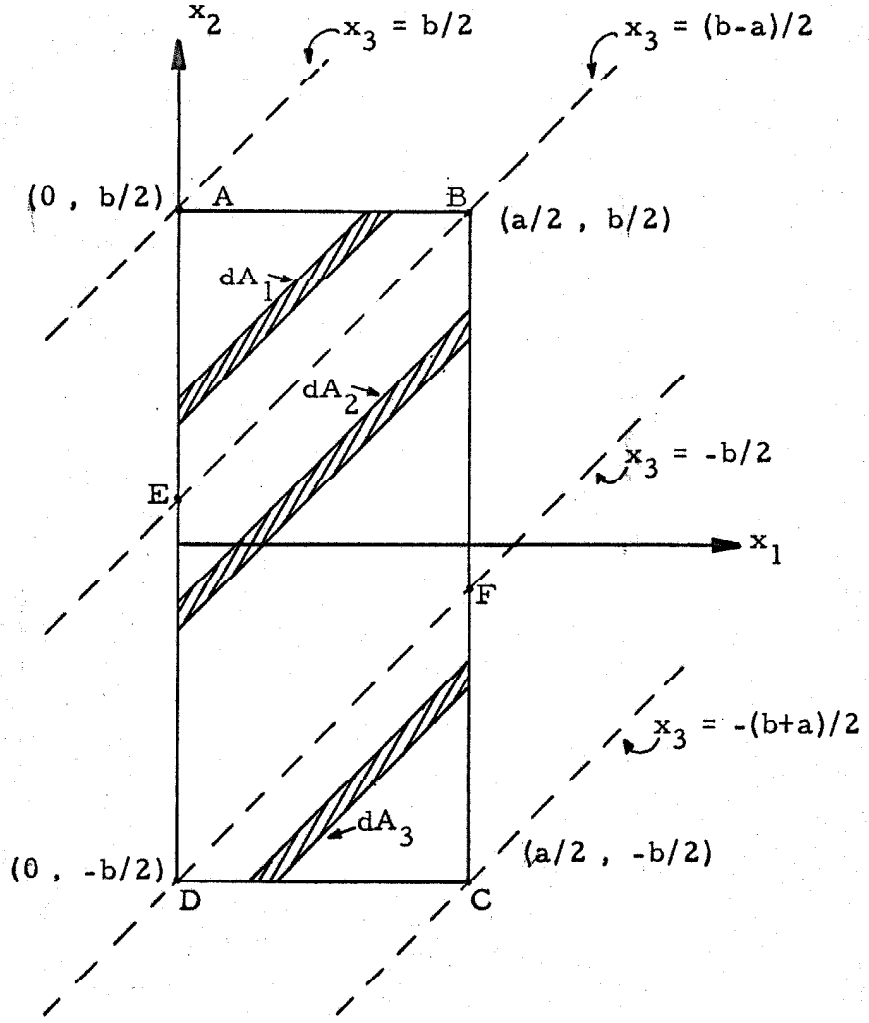

Fig. A-1. Integration Region

$$I_1 = \int_0^{a/2} \int_{-b/2}^{b/2} f(x_1, x_2)\, dx_1\, dx_2$$

$$= \iint_{ABCD} F(x_3) dA$$

$$= \iint_{EAB} F(x_3) dA_1 + \iint_{EBFD} F(x_3) dA_2 + \iint_{DFC} F(x_3) dA_3$$

where $dA_1 = [-x_3 + b/2]\, dx_3$

$dA_2 = [a/2]\, dx_3$

$dA_3 = [x_3 + (b+a)/2]\, dx_3$

Thus $$I_1 = \int_{(b-a)/2}^{b/2} F_1(x_3) dx_3 + \int_{-b/2}^{(b-a)/2} F_2(x_3) dx_3 + \int_{(b+a)/2}^{-b/2} F_3(x_3) dx_3$$

A-3

$$= \frac{b}{2} I_A(x) \Big|_{(b-a)/2}^{b/2} + \frac{a}{2} I_A(x) \Big|_{-b/2}^{(b-a)/2} + \frac{(b+a)}{2} I_A(x) \Big|_{-(b+a)/2}^{-b/2}$$

$$- I_B(x) \Big|_{(b-a)/2}^{b/2} + I_B(x) \Big|_{-(b+a)/2}^{-b/2}$$

A-4

where

$$I_A(x) = \int \frac{h\,dx}{[(\ell/2)^2 + x^2][(\ell/2)^2 + h^2 + x^2]^{1/2}}$$

$$= \frac{2}{\ell} \tan^{-1} \frac{2hx}{\ell[(\ell/2)^2 + h^2 + x^2]^{1/2}}$$

by the use of integral tables [27]

$$I_B(x) = \int \frac{h\,x\,dx}{[(\ell/2)^2 + x^2][(\ell/2)^2 + h^2 + x^2]^{1/2}}$$

$$= \frac{1}{2} \ln \frac{\{[(\ell/2)^2 + h^2]/h - [(\ell/2)^2 + h^2 + x^2]^{1/2}\}^2 + (\frac{\ell x}{2h})^2}{(\ell/2)^2 + x^2}$$

by the use of integral tables [28]

Using the relationships

$$I_A(-x) = -I_A(x) \qquad \text{A-5}$$
$$I_B(-x) = I_B(x)$$

Eqn. A-4 can be written in the following form

$$I_1 = x I_A(x) \Big|_{(b-a)/2}^{(b+a)/2} + I_B(x) \Big|_{(b+a)/2}^{(b-a)/2} \qquad \text{A-6}$$

On considering the case $b < a/2$, it can readily be shown that

$$I_1 = \frac{b}{2} I_A(x)\Big|_{-b/2}^{b/2} + b\, I_A(x)\Big|_{(b-a)/2}^{-b/2} + \frac{(b+a)}{2} I_A(x)\Big|_{-(b+a)/2}^{(b-a)/2}$$

$$-I_B(x)\Big|_{-b/2}^{b/2} + I_B(x)\Big|_{-(b+a)/2}^{(b-a)/2} \qquad \text{A-7}$$

This can be reduced to Eqn. A-6 by use of the relationships A-5. Thus, Eqn. A-6 is valid for all values of b/a .

Numerical evaluation of the integral I_1 by means of Eqn. A-6 was used to determine the variation of I_1 with the four parameters a, b, ℓ, h . Two bounds, which are somewhat simpler to evaluate, can be obtained for I_1 in the following manner.

Since the integrand of I_1 (Eqn. A-1) is always positive, this integral is bounded between upper and lower limits, I_2 and I_3 respectively, expressed by

$$I_{2,3} = h \int_0^{a/2} \int_{-b/2}^{b/2} \frac{dx_1\, dx_2}{[(c_{2,3})^2 + (x_2 - x_1)^2]^{3/2}} \qquad \text{A-8}$$

where $c_2 = \ell/2$:

$$c_3 = [(\ell/2)^2 + h^2]^{1/2}$$

When $h << \ell/2$, it can be seen that the values of I_2 and I_3 are close to each other and their average value $I_4 = (I_2 + I_3)/2$ is then a good approximation to I_1 .

Integrating Eqn. A-8 by introduction of the coordinate $x_3 = (x_2 - x_1)$, leads to the expression

$$I_{2,3} = x\, I_C^{2,3}(x) \Big|_{(b-a)/2}^{(b+a)/2} + I_D^{2,3}(x) \Big|_{(b+a)/2}^{(b-a)/2} \qquad \text{A-9}$$

where

$$I_C^{2,3}(x) = h \int \frac{dx}{[(c_{2,3})^2 + x^2]^{3/2}} = \frac{h}{(c_{2,3})^2} \frac{x}{[(c_{2,3})^2 + x^2]^{1/2}};$$

by the use of integral tables [26]

$$I_D^{2,3}(x) = h \int \frac{x\, dx}{[(c_{2,3})^2 + x^2]^{3/2}} = \frac{-h}{[(c_{2,3})^2 + x^2]^{1/2}}$$

By suitable manipulation, it can be shown that

$$I_{2,3} = h \left\{ \frac{[(c_{2,3})^2 + (\frac{b+a}{2})^2]^{1/2} - [(c_{2,3})^2 + (\frac{b-a}{2})^2]^{1/2}}{(c_{2,3})^2} \right\}$$

Thus,

$$I_2 = h \left\{ \frac{\left[(\ell/2)^2 + \left(\frac{b+a}{2}\right)^2 \right]^{1/2} - \left[(\ell/2)^2 + \left(\frac{b-a}{2}\right)^2 \right]^{1/2}}{(\ell/2)^2} \right\}$$

$$I_3 = h \left\{ \frac{\left[(\ell/2)^2 + \left(\frac{b+a}{2}\right)^2 + h^2 \right]^{1/2} - \left[(\ell/2)^2 + \left(\frac{b-a}{2}\right)^2 + h^2 \right]^{1/2}}{(\ell/2)^2 + h^2} \right\}$$

A-10

APPENDIX B

PASSIVE NETWORK ATTENUATION OF THE TOTAL TIME INTEGRAL OF AN INPUT PULSE

Consider a linear, passive, lumped parameter, 2-port network. The ratio of the output voltage V_2 to the input voltage V_1 is expressed, in Laplace transform notation, as:

$$\overline{V}_2(s)/\overline{V}_1(s) = P(s)/Q(s) \qquad \text{B-1}$$

where $\overline{V}_2(s)$ is the transformed output voltage, $\overline{V}_1(s)$ is the transformed input voltage and $P(s)$, $Q(s)$ are polynomial functions of the variable s. Assuming that all the time derivatives of V_2 and V_1 exist and that the values of the voltages and all their time derivatives vanish at initial and final time, Eqn. B-1 yields:

$$[\,1 + C_1 d/dt + C_2 d^2/dt^2 + ---\,]V_2 = \frac{P(0)}{Q(0)}[\,1 + K_1 d/dt + K_2 d^2/dt^2 + --\,]V_1 \qquad \text{B-2}$$

where C_1, C_2---, K_1, K_2---, are constants.

Integrating Eqn. B-2 timewise between the limits $t = 0$ and $t = \infty$ gives:

$$\int_0^\infty V_2 \, dt = \frac{P(0)}{Q(0)} \int_0^\infty V_1 \, dt \qquad \text{B-3}$$

Thus, the ratio of the time integrals of the two voltages is identical with the steady state attenuation of the network, and so is determined by the resistive properties of the circuit.

APPENDIX C

CURRENT DISTRIBUTION IN A SEMI-INFINITE THIN RECTANGULAR PLATE, WITH A SYMMETRICALLY-PLACED POINT CURRENT SOURCE

Figure C-1a shows a sketch of the rectangular plate and its associated point current source. Assuming material of uniform resistivity ρ, the voltage and current density distributions (U and i respectively) are given by the equations

$$\nabla^2 U = 0$$
$$i = -\frac{1}{\rho} \nabla U \qquad \text{C-1}$$

with the boundary condition that the normal component of i be zero at the edges of the plate (except at the current injection point). This two-dimensional problem can be solved by mapping the rectangular plate in the z-plane into the upper half of the z_1-plane, as indicated in Fig. C-1b. The following mapping function[29] effects the desired transformation, with corresponding points $\pm a$ of both planes being images of each other. This mapping function is

$$z_1 = a \sin\left(\frac{\pi}{2} \cdot \frac{z}{a}\right) \qquad \text{C-2}$$

The field solution W of the z_1-plane problem is

$$W = U + i V = -K \ln z_1 \qquad \text{C-3}$$

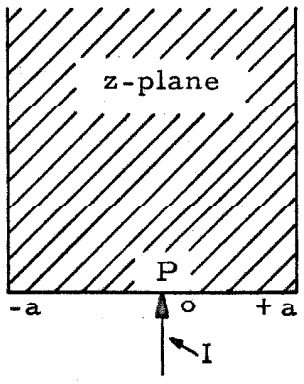

Fig. C-1a. Semi-Infinite Rectangular Plate and Point Current Source

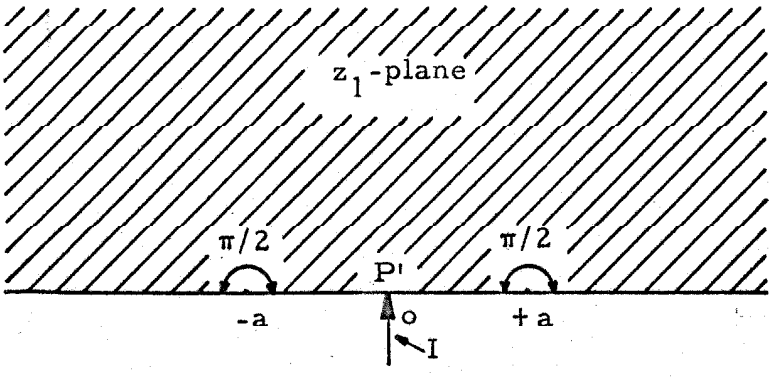

Fig. C-1b. Upper Half-Plane Plate and Point Current Source

where U = potential function

V = stream function

By evaluating $\frac{\delta U}{\delta r} = \left|\frac{dW}{dz}\right|$ on a semicircle of radius r, centered at P', and equating the total current flowing across this boundary to the injected current I, it can be shown that $K = \frac{I\rho}{\pi}$. On substituting Eqn. C-2 into Eqn. C-3, the solution of the z-plane problem is obtained as

$$W = -\frac{I\rho}{\pi} \ln \left[a \sin \left(\frac{\pi}{2} \cdot \frac{z}{a}\right)\right] .$$

The derivative $\frac{dW}{dz}$, whose absolute value at any point gives the magnitude of the electric field at that point, is expressed by

$$\frac{dW}{dz} = -E_x + j E_y$$

$$= -\frac{I\rho}{2a} \cot \left(\frac{\pi}{2} \cdot \frac{z}{a}\right) \qquad \text{C-4}$$

where E_x = x-component of electric field

E_y = y-component of electric field

The absolute value of the current density is expressed by

$$|i| = \frac{1}{\rho} \left|\frac{dW}{dz}\right| = \frac{I}{2a} \left|\cot \left(\frac{\pi}{2} \cdot \frac{z}{a}\right)\right| . \qquad \text{C-5}$$

The quantity $I/2a$ is the average current density in the plate at a point far distant from the current injection point and so the ratio of the absolute value of the current density to the average density is

given by

$$N = \left| \cot \left(\frac{\pi}{2} \cdot \frac{z}{a} \right) \right| \quad . \qquad \text{C-6}$$

The direction of current flow at any point of the plate makes an angle α with the x-axis, where (using Eqn. C-4)

$$\alpha = \tan^{-1} \left(\frac{E_y}{E_x} \right) = \tan^{-1} \left[\frac{\text{Im} \left(\frac{dW}{dz} \right)}{-\text{Re} \left(\frac{dW}{dz} \right)} \right] \qquad \text{C-7}$$

The current distribution over the plate is shown in Fig. 4.8. The directions of the arrows indicate the direction of current flow at various points which are situated at the tails of the arrows. (Due to symmetry only half the current vectors are shown.) The values of N are shown at the heads of the arrows.

The current density is higher than the average over one half of the conductor surface and is less than the average over the rest of the surface. On the lines $z = \pm a/2 + iy$, the current density is identical with the average value.

APPENDIX D

EFFECT OF MISALIGNMENT OF FILM HARD AXIS AND DRIVE FIELD ON FLUX SWITCHED IN TRANSVERSE MODE

Figure D-1 shows a representation of a magnetic film having an easy axis defined by $\bar{e}_1$ and $\bar{e}_2$. The drive field H is applied at an angle β to the film hard axis and the resulting flux change is measured by means of a closely coupled loop, whose axis makes an angle α with the film easy axis. According to the Stoner-Wolfarth model[23], when $H \geq H_K$ there is only one stable equilibrium direction for the film magnetization M and this direction makes an angle θ with the film easy axis, where θ satisfies the equation

$$MH \cos(\theta + \beta) = K \sin 2\theta \qquad \text{D-1}$$

which can be written as

$$2h \cos(\theta + \beta) = \sin 2\theta \qquad \text{D-2}$$

where $h\ (= H/(2K/M) = H/H_K)$ is the normalized drive field. For given values of h and β, this equation may be solved iteratively for θ.

When the magnetization is switched from the direction of $\bar{e}_1$, the magnitude of the flux change in the direction of the loop axis is given by

$$\left|\Delta\phi_1\right| = M\,[\cos\alpha - \cos(\alpha + \theta)]$$

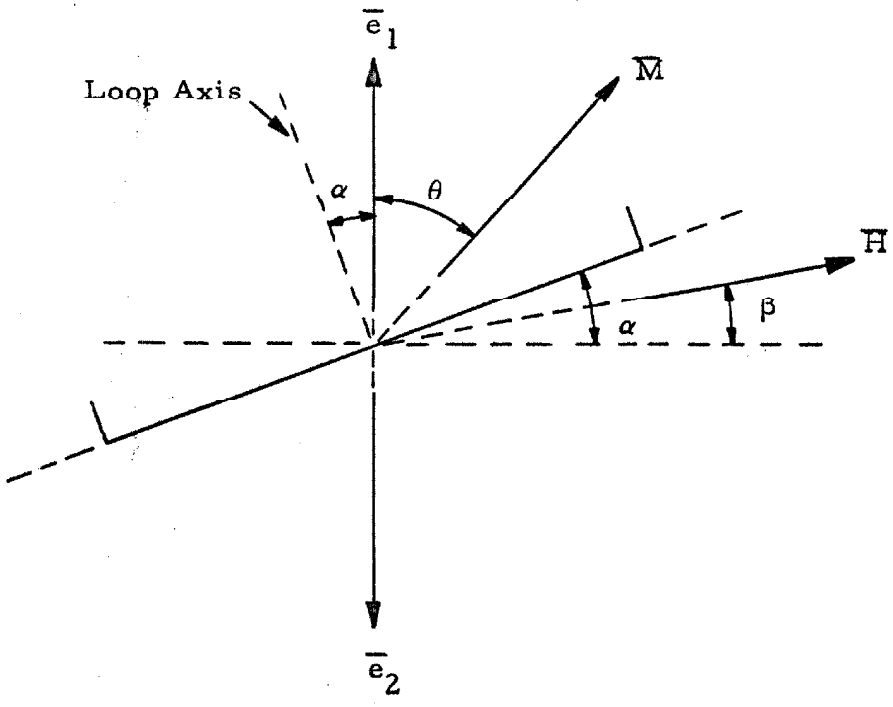

Fig. D-1. Orientation of Magnetic Film, Drive Field and Loop Axis

The corresponding flux change magnitude obtained in switching from the direction of $\bar{e}_2$ is given by

$$\left|\Delta\phi_2\right| = M\ [\cos\alpha + \cos(\alpha + \theta)]$$

The mean value of these flux change magnitudes is

$$\left|\Delta\phi\right| = M\cos\alpha \qquad \text{D-3}$$

which is within 1/2% of the value of M for $\alpha < 5^{\circ}$. The ratio of $\left|\Delta\phi_1\right|$ to $\left|\Delta\phi_2\right|$ is denoted by

$$F = \frac{\cos\alpha - \cos(\alpha + \theta)}{\cos\alpha + \cos(\alpha + \theta)} \qquad \text{D-4}$$

The effect of easy axis misalignment was determined for the case of a film, whose loop axis was aligned exactly perpendicular to the drive field (i.e., $\alpha = \beta$). The variation of θ and F with the quantities β and h was obtained by means of a computer program which solved Eqn. D-2 iteratively for θ, and then calculated the corresponding value of F. The results obtained are tabulated in the final subsection of Section VI.

REFERENCES

1. W. E. Proebster, S. Methfessel, C. O. Kinberg, "Thin Magnetic Films", International Conference on Information Processing, 1959.

2. J. I. Raffel, T. S. Crowther, A. H. Anderson, T. O. Herndon, "Magnetic Film Memory Design", Proc. IRE, Vol. 49, No. 1, January 1961.

3. E. E. Bittman, "Thin Film Memories", IRE Trans. on Electronic Computers, Vol. EC-8, No. 2, June 1959.

4. E. M. Bradley, "A Computer Storage Matrix Using Ferromagnetic Thin Films", Journal Brit. IRE, pp. 765-784, October 1960.

5. M. W. Green, "Research on Thin Magnetic Film Logic Devices", (Stanford Research Institute, October 1961).

6. H. J. Harloff, "Operating Speed of Thin-Film Memories", International Solid-State Circuits Conference 1963.

7. G. Piefke, "Dampfung und Verzerrung eines Impulses auf einer bandleitung mit magnetischer Zwischenschicht", Archiv elektr. Uberth, June 1963.

8. F. W. Reynolds, G. R. Stilwell, "Mean Free Paths of Electrons in Evaporated Metal Films", Phys. Rev. 88, p. 418 (1952).

9. G. F. Hughes, Private Communication, California Institute of Technology, Pasadena, California.

10. W. R. Smythe, "Static and Dynamic Electricity", (Mc Graw - Hill Book Company, Inc., New York, 1950), 2nd ed., Chap. 11, p. 393.

11. The loss tangent of siliconmonoxide is not readily available in the literature. Accordingly, the value stated in the text was based on the value for quartz (tan $\delta = 0.6 \times 10^{-4}$ at 3 k Mc, A. von Hippel "Dielectric Materials and Applications", The Technology Press of M. I. T. and John Wiley and Sons, Inc., New York, 1954) since, under certain conditions, evaporation of silicon monoxide can lead to a deposited layer of silicon dioxide.

12. J. Todd, Ed., "Survey of Numerical Analysis", (McGraw-Hill Book Company, Inc., New York, 1962), pp. 80-81.

13. Smythe, op. cit., p. 403.

14. R. M. Bozorth, "Ferromagnetism", (Van Nostrand Company, Inc., Princeton, New Jersey, 1951), pp. 845-849.

15. H. Chang, "Analysis of Static and Quasidynamic Behavior of Magnetostatically Coupled Thin Magnetic Films", IBM J. Research Develop., Vol. 6, No. 4, October 1962.

16. Bozorth, op. cit., p. 109.

17. J. I. Raffel, D. O. Smith, "A Computer Memory Using Magnetic Films", International Conference on Information Processing, 1959.

18. C. J. Kriessman, T. J. Matcovich, W. E. Flannery, "Low Power Thin Film Memory", International Conference on Non-linear Magnetics 1963.

19. F. B. Humphrey, "Flux Reversal at Low Temperatures", J. Appl. Physics, Suppl. March 1964.

20. F. B. Humphrey, "Magnetic Character of Very Thin Permalloy Films", J. Appl. Phys., Vol. 34, No. 4 (Part 2), pp. 1067-1068, April 1963.

21. G. E. Valley and H. Wallman, Eds., "Vacuum Tube Amplifiers", (McGraw-Hill Book Company, Inc., New York 1948), p. 505.

22. W. E. Proebster, H. J. Oguey, "High-Speed Magnetic-Film Logic", Solid-State Circuits Conference 1960.

23. E. D. Stoner and E. P. Wolfarth, Phil. Trans. Roy. Soc. London 240A, p. 599 (1948). [See also D. O. Smith, Conference on Magnetism and Magnetic Materials, AIEE, Spec. Pub., February 1957, p. 625.]

24. S. Middelhoek, "Domain Wall Creeping in Thin Permalloy Films", IBM J. Research Develop., Vol. 6, No. 1, January 1962.

25. G. D. McCann, Unpublished Course Notes for Course in Analog Computation , Electrical Engineering Department, California Institute of Technology, Pasadena, California.

26. H. B. Dwight, "Tables of Integrals and Other Mathematical Data", (Macmillan Company, New York), 4th Ed., p. 50. eq. 200.03.

27. W. Gröbner and N. Hofreiter, "Integraltafel", (Springer-Verlag, Wien und Innsbruck 1957), Vol. 1 p. 49, eq. 19a.

28. Ibid, eq. 20b.

29. Smythe, op. cit., p. 90.